UNIVERSITA' DEGLI STUDI DI PARMA

PhD Course in Molecular Medicine

XXIX CYCLE

Functional and molecular analysis of Organic Cation Transporters (OCTs and OCTNs) in human airway epithelial cells and macrophages

PhD Coordinator:
Prof. Luciano Polonelli

Tutor:
Prof. Valeria Dall'Asta

Candidate:
Filippo Ingoglia

CONTENTS

Chapter I – INTRODUCTION

1. The Cell Membrane

The cell membrane (plasma membrane) is a thin semi-permeable membrane that surrounds the cytoplasm of a cell. Its function is to protect the integrity of the interior of the cell by allowing certain substances into the cell, while keeping other substances out. It also serves as a base of attachment for the cytoskeleton in some organisms and the cell wall in others. Thus the cell membrane also serves to help support the cell and help maintain its shape. Plasma membranes enclose the borders of cells, but rather than being a static bag, they are dynamic and constantly in flux [1]. The plasma membrane must be sufficiently flexible to allow certain cells, such as red and white white blood cells, to change shape as they pass through narrow capillaries.

The cell membrane is primarily composed of a mix of proteins and lipids (Figure 1). Depending on the membrane's location and role in the body, lipids can make up anywhere from 20 to 80 percent of the membrane, with the remainder being proteins. While lipids help to give membranes their flexibility, proteins monitor and maintain the cells chemical environment and assist in the transfer of molecules across the membrane.

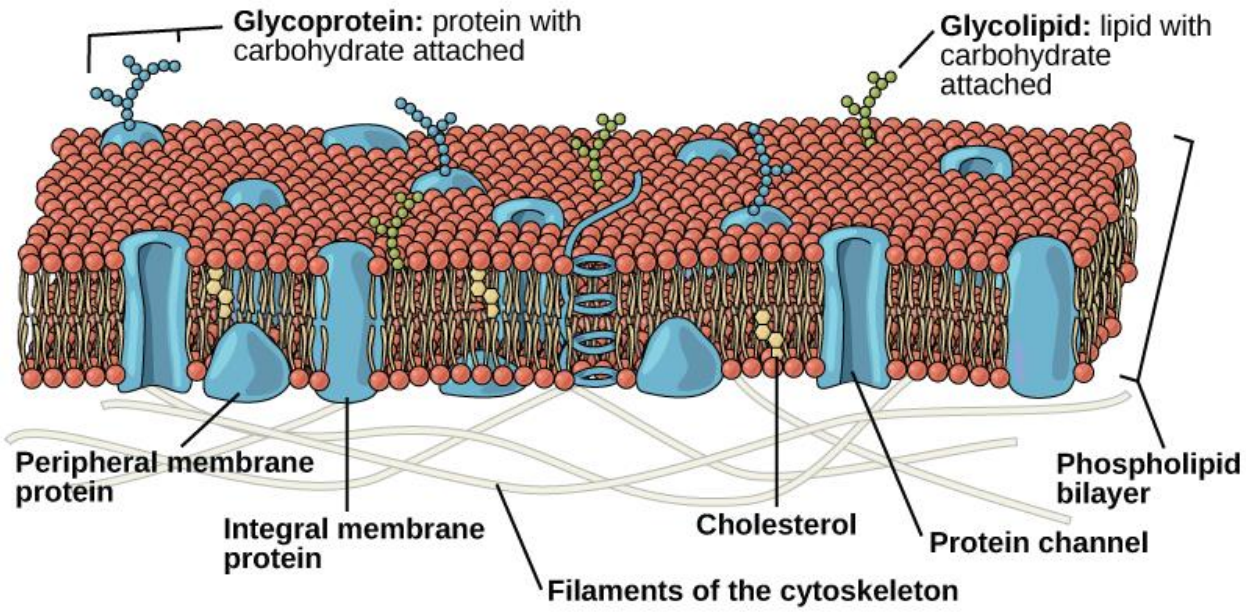

Figure 1: The fluid mosaic model of the plasma membrane structure describes the plasma membrane as a fluid combination of phospholipids, cholesterol, proteins, and carbohydrates. Taken from http://philschatz.com/biology-concepts-book/contents/m45433.html

1.1 Cell Membrane Lipids

Phospholipids are the major component of cell membranes. Phospholipids form a lipid bilayer in which their hydrophilic heads spontaneously arrange to face the aqueous cytosol and the extracellular fluid, while their hydrophobic tails face away from the cytosol and extracellular fluid. The lipid bilayer is semi-permeable, allowing only certain molecules to diffuse across the membrane [2].

Cholesterol is another lipid component of animal cell membranes, not found in the membranes of plant cells. Cholesterol molecules are selectively dispersed between membrane phospholipids. This helps to keep cell membranes from becoming stiff by preventing phospholipids from being too closely packed together [2].

Glycolipids are located on cell membrane surfaces and have a carbohydrate sugar chain attached to them. They help the cell to recognize other cells of the body [2].

1.2 Cell Membrane Proteins

Cell membrane proteins have a number of different functions. Structural proteins help to give the cell support and shape. Cell membrane receptor proteins help cells communicate with their external environment through the use of hormones, neurotransmitters, and other signaling molecules. Transport proteins, such as globular proteins, transport molecules across cell membranes through facilitated diffusion. Glycoproteins have a carbohydrate chain attached to them. They are embedded in the cell membrane and help in cell–to-cell communications and molecule transport across the membrane [3].

2. The transport function of cell membrane

The cell membrane is a selective barrier that compounds need to cross [4], in this way the cell membrane controls the entrance of various nutrients, organic and inorganic ions, as well as various drugs that will enter the cell to be further metabolized through a series of interconnected processes, and in the end be extruded out of the cells and finally out of the organism.

Essential elements of the cell membrane are proteins embedded in its lipid bilayer through hydrophobic interactions[5]. They play important role in all cellular processes, from receiving the signal molecules and passing on the signaling messages to transporting of physiological compounds in order to be modified or processed by the receiving cells.

The crucial membrane proteins mainly responsible for the absorption and excretion of endo- and xenobiotics are membrane transporters. They are key regulators of bioavailability of all endo- and xenobiotic compounds [6, 7] . Based on their specificities and transport mechanism,

membrane transporters regulate both the cell uptake and extrusion of various substrates. Transporter proteins are expressed in all tissues throughout the body, which implies their important role in the maintenance of physiological homeostasis and defensive functions of cells.

2.1 Membrane transport proteins

Membrane transport proteins can be either passive or active (Figure 2). Passive transporters (also called uni-porters or facilitative transporters) transport substrates down a concentration gradient. By contrast, active transporters (or cotransporters) couple the movement of one type of ion or molecule against its concentration gradient, to the movement of another ion or molecule down its concentration gradient. Like ATP pumps, cotransporters mediate coupled reactions in which an energetically unfavourable reaction is coupled to an energetically favourable reaction.

When the transported molecule and cotransported ion move in the same direction across a membrane, the transporter is called a symporter; when they move in opposite directions, the transporter is called an antiporter (or exchanger). If the intracellular net charge following transport becomes more negative, the process is termed electronegative; if the intracellular net charge becomes more positive, the process is called electropositive; if the resulting intracellular net charge remains unchanged, the process is termed electroneutral.

Up until recently, it has been considered that lipophilic organic and inorganic molecules pass the membrane by passive diffusion, due to specific hydrophobic nature of the membrane lipid bilayer.

However, discoveries in the relatively young field of membrane transporters gave a new insight in transport across not only cell membranes, but all membranes in the cell [8].

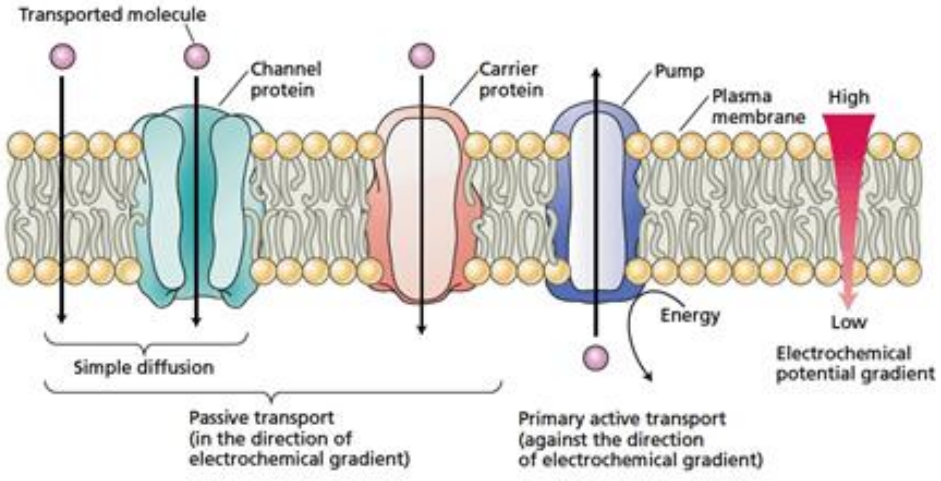

Figure 2 : Transport pathway through cell membrane and basic mechanism of transport. Taken from Taiz L., Zeiger E., 2010

2.2 Ion channels

Ion channels are pore-forming membrane proteins that help to establish and maintain small-voltage gradients across plasma membrane surfaces of all living cells. As such, they regulate the cell's electric potential by allowing the flow of ions down their electrochemical gradient. Ion channels usually occur in the closed state but different factors can open them: voltage changing, proteins and ligands [9-11]. Cationic and anionic substrates are transferred down their electrochemical gradients at extremely high efficiencies (as much as 108 sec^{-1}). More than 400 genes are known to encode ion channel subunits [12].

2.3 Aquaporins

Aquaporins are a unique class of transporters. These proteins are bi-directional membrane channels which transport water, but they are not ion channels because the H2O is transported as an uncharged molecule and not as an ion. The driving force for aquaporins is the presence of osmotic gradients across membranes [13].

2.4 Transporters

Transporters facilitate the movement of a specific substrate, either with or against its concentration gradient, and the conformational change in the transporter protein is important in this transfer process. Transporters move molecules at only about 102-104 sec-1, a rate much slower than that associated with channel proteins.

The body is equipped with broad-specificity transporters for the excretion and distribution of endogeneous organic cations and for the uptake, elimination and distribution of cationic drugs, toxins and environmental waste products.

Due to their essential role, especially in absorption and excretion of pharmaceutical compounds, efforts have been made to identify new transporters and to determine detailed transport mechanisms and substrate preferences of individual transporters.

Two superfamilies of membrane transporters have been identified as relevant ones for these processes: ATP-binding Cassette (ABC) and solute carrier family (SLC) [14].

2.4.1 ABC transporters family

One of the largest transporter gene families is the ATP-binding cassette (ABC) transporter superfamily [15]. These proteins translocate a wide variety of substrates including sugars,

amino acids, metal ions, peptides, and proteins, and a large number of hydrophobic compounds and metabolites across extra- and intracellular membranes. ABC genes are essential for many processes in the cell, and mutations in these genes cause or contribute to several human genetic disorders including cystic fibrosis, neurological disease, retinal degeneration, cholesterol and bile transport defects, anemia, and drug response.

To date, there are 48 characterized human ABC genes. The genes can be divided into seven distinct subfamilies, based on organization of domains and amino acid homology. Many ABC genes play a role in the maintenance of the lipid bilayer and in the transport of fatty acids and sterols within the body.

2.4.1 SLC transporter family

The largest group of transporters are the Solute Link Carrier (SLC) proteins that comprises 55 gene families, having at least 362 putatively functional protein-coding genes [16]. SLC transporters are often found in epithelial membranes and mediate uptake and secretion of (among many other substrates) organic cations [7]. The solute-carrier (SLC) gene superfamily, include passive transporters, sym-porters and antiporters, as well as mitochondrial and vesicular transporters.

Members of SLC family are termed polyspecific transporters: whereas most plasma membrane transporters are “oligospecific,” i.e. specialized for translocation of specific metabolic or nutritional compounds, “polyspecific” transporters accept compounds with different sizes and molecular structures. These transporters may exhibit large variations in affinity and turnover for different compounds and may have specific physiological roles (see Table 1). In addition, they serve to transfer a wide range of drugs and toxins of different size and chemical constitution [7] across plasma membranes and are involved in drug uptake and in drug excretion in liver, kidney and in many other tissues (see table 2).

Transporters involved in organic cation translocation are electrogenic cation transporters OCT1-3 (SLC22A1-3), cation and carnitine transporters OCTN1 and OCTN2 (SLC22A4-5), proton/cation antiporters of the MATE family (SLC47A1-2), monoamine neurotransmitter transporters (SLC6 family), cationic amino acid transporters (SLC7 family), nucleoside transporters (SLC28A1-3 and SLC29A1-4) and several choline transporters (SLC5A7 and SLC44A1-4) [17, 18].

3. The SLC22 family

The SLC22 family is a member of the major facilitator superfamily MFS that comprises transporters from bacteria, plants, animals and humans in 18 transporter families [19]. They include passive transporters, ion transporters and exchangers, but not the primary active transporters, ion channels and aquaporins. Transport via solute carriers is effected on the ion or proton gradient, not on the hydrolysis of ATP [20].

In addition to four organic anion transporters OAT1-4 (SLC22A6,7,8,11) and one urate transporter URAT1 (SLC22A12), the SLC22 family includes three organic cation transporters (hOCT1-3 or SLC22A1-3) and three transporters for carnitine and/or cations (OCTN1 or SLC22A4, hOCTN2 or SLC22A5, hCT2 or OCT6 or SLC22A16) [7].

The first transporter of the SLC22 family in mammals, the organic cation transporter OCT1 (SLC22A1), was cloned in 1994 [21]. Later, 16 additional human family members and many orthologs from different species were identified [22].

In humans, the genes coding for OCT1, OCT2 and OCT3 are localized within a cluster on chromosome 6.q26-7 [23-25]. Each of the three genes comprises 11 exons and 10 introns [25, 26]. OCTN1 and OCTN2 have been cloned from human, rat and mouse [27, 28], while OCTN3 from mouse [29]; the human genes coding for OCTN1 and OCTN2 are localized in a cluster on chromosome 5q31 [30, 31].

Molecular organization

Like most members of the SLC22 family, the organic cation (OCTs) and carnitine transporters (OCTNs) have a predicted membrane topology that comprises 12 α-helical transmembrane domains (TMDs), an intracellular N-terminus, a large glycosylated extracellular loop between TMDs 1 and 2, a large intracellular loop with phosphorylation sites between TMDs 6 and 7, and an intracellular C-terminus (Figure 3)

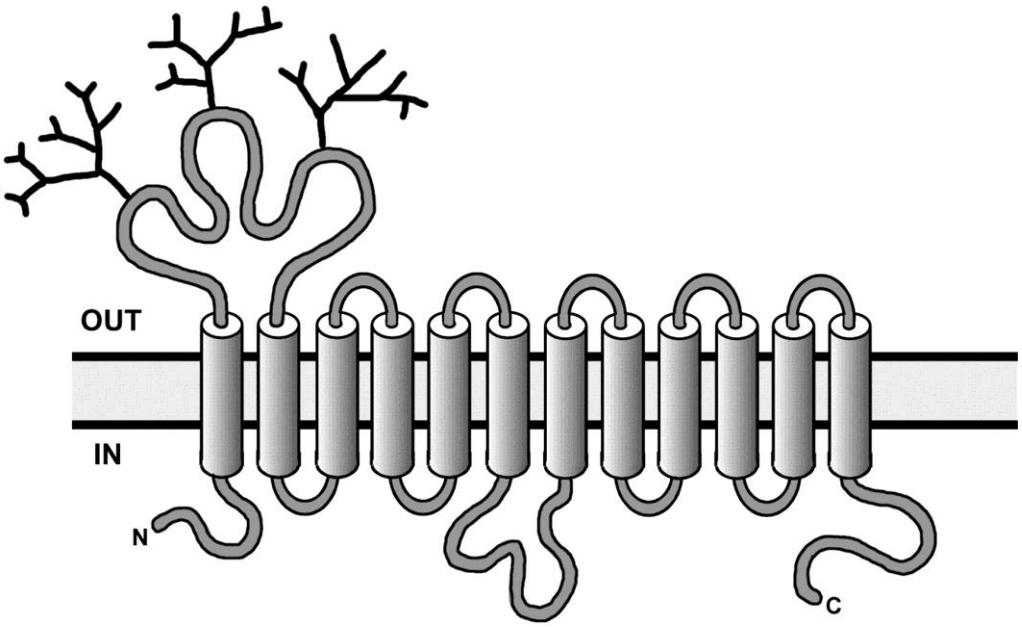

Figure 3. Secondary structure of hOCT1. Both N-terminus and C-terminus are located inside the cell. Taken from: (Jonker and Schinkel, 2004)

3.1 Organic Cation Transporters (OCTs and OCTNs)

3.1.1 OCT1 Transporter (Organic Cation Transporter 1 / SLC22A1)

OCT1 transporter is a member of the SLC22 family and is widely expressed through the body, with significant inter-species and inter-individual differences [32]. Of the three major OCT transporters, OCT1 is the most significantly expressed on the sinusoidal membrane of hepatocytes in human and rat liver. OCT1 is also located on the basolateral membrane of small intestinal enterocytes, renal proximal tubular cell and at lower levels in some neurons, the heart, skeletal muscles, tumor cells and basophilic granulocytes [32, 33].

Function, physiology and clinically significant polymorphisms

OCT1 mediates Na^+-independent transport of Type I organic cations (protonated molecules), such as tetraethylammonium (TEA), 1-methyl-4-phenylpyridinium (MPP+), N1-methylnicotinamide (NMN), dopamine and choline [34], as well as of Type II cations (larger and bulkier molecules) such as methyl-quinine and quinidine. OCT1 mediated organic cation

transport is potential sensitive and electrogenic. The inhibitors of OCT1 with the highest affinity are atropine (IC50 1.2 μM) and prazosin (IC50 1.8 μM) [7, 33].
Knocking out Oct1 from the mouse liver results in a shift in the elimination of Oct1 substrate drugs from the liver to the kidneys, increasing renal excretion of drugs [35]. The tyrosine kinase inhibitors (TKI) imatinib, nilotinib, gefitinib, and erlotinib exert selectively potent inhibitory effects on OCT1, in vitro. There are clinically relevant polymorphisms of OCT1 which are associated with increased metformin exposure, since OCT1 plays important role in metformin transport into hepatocytes [36]. Reduced expression is associated with non synonymous coding variants of OCT1 (rs12208357) [36]. The OCT1 polymorphism, M420del is associated with increased sensitivity to drug inhibition by erlotinib, suggesting the potential of clinical transporter-mediated drug-drug interactions (DDIs) between specific tyrosine kinase inhibitors (TKIs) and OCT1, which may affect the disposition, efficacy, and toxicity of metformin and other drugs that are OCT1 substrates [37]. OCT1 is transcriptionally activated by PXR, PPARγ and HNF1α [38, 39].

Clinical significance

Biguanides (e.g., the OCT1 substrates metformin and phenformin), widely used as oral hypoglycemic agents for the treatment of type II diabetes mellitus [40], can produce lactic acidosis, a lethal side effect. OCT1 transports metformin into hepatocytes and functional loss of variants of the OCT1 transporter is linked to the reduced hepatic uptake of metformin and subsequently, its pharmacodynamic effect by reducing oral glucose tolerance [41]. Individuals carrying alleles including SNPs in positions 420, 401 and 465 display reduced function of OCT1, and seem to have reduced metformin clearance [41]. Phenformin was withdrawn from the market due to altered pharmacokinetics resulting in lactic acidosis.
For several drugs which inhibit OCTs but are not OCT substrates, a higher affinity to OCT1 was observed compared to OCT2 or OCT3 e.g. the glutamate receptor antagonist phencyclidine, the antagonists of histamine receptors diphenylhydramine and ranitidine, the antagonist of the muscarinic acetylcholine receptor atropine, and the antidepressant desipramine.

3.1.2 OCT2 Transporter (Organic Cation Transporter 2 / SLC22A2)

SLC22A2, more commonly referred to as OCT2 (Organic Cation Transporter 2), is a renal uptake transporter that plays a key role in disposition and renal clearance of drugs and endogenous compounds. OCT2 substrate drugs have the potential for drug-drug interactions with co-administered therapeutics that are inhibitors of this transporter.

OCT2 is most strongly expressed in the kidney and is also expressed in the small intestine, lung, skin, placenta, brain and choroid plexus [33, 42]. In humans, OCT2 is expressed in all three segments of renal proximal tubules, in the basolateral membrane of epithelial cells in the small intestine and in the luminal membrane of epithelial cells in trachea and bronchi [7, 32, 33]; in the brain, OCT2 is expressed on the apical (ventricular) membrane in epithelial cells of the choroid plexus [43].

Function, physiology and clinically significant polymorphisms

Since the OCT transporters have overlapping substrates, it is difficult to quantitate the contribution of individual isoforms without knocking out individual isoforms. Oct2 single knockout and Oct1/2 double knockout mice showed that while removal of Oct2 did not have a significant effect on TEA elimination, renal secretion of TEA was completely eliminated and higher plasma levels were observed in the double knock-outs [44].

In the basolateral membrane of the distal tubule in the kidney, OCT2 transporter mediates uptake from the blood to the proximal tubular cells during the renal secretion of organic cations. OCT2 transports many organic cations and plays an important role on the pharmacological, pharmacokinetic and toxicological properties of therapeutics. OCT2 transports monoamine neurotransmitters [43], thereby participating in the regulation of interstitial and intracellular concentrations of monoamine neurotransmitters and cationic drugs.

A single splice variant of OCT2 was identified in kidney, termed OCT2-A, a truncated form of OCT2, appears to have lower Km (or greater affinity) for substrates than OCT2 [45].

Clinical significance

The majority of clinical studies to assess OCT2 transporter activity are conducted using cimetidine as the probe substrate. Drug interactions with procainamide/cimetidine result in a 42% decrease in procainamide renal clearance (CLR), while it results in a 28% decrease in metformin CLR when considering metformin/cimetidine; nephrotoxicity and ototoxicity of cisplatin is decreased after inhibition of OCT2 [7, 32, 46, 47]. Substrates taken up by OCT2 from the systemic circulation may subsequently undergo efflux across the brush-border membrane of the proximal tubule cells by various ABC efflux transporters such as P-gp and BCRP [6]. For example, creatinine is secreted by OCT2-mediated uptake at the basolateral membrane and efflux by MDR1 at the apical membrane.

Few polymorphisms have been reported for this transporter. Genetic polymorphism of OCT2 was evaluated in the Chinese population and the 808G>T polymorphism was attributed to a reduced metformin renal tubular clearance. Furthermore, this mutation correlated with the extent of cimetidine mediated inhibition of metformin renal tubular secretion [48].

3.1.3 OCT3 Transporter (Organic Cation Transporter 3 / SLC22A3)

SLC22A3, more commonly referred to as OCT3 (Organic Cation Transporter 3) or extraneuronal monoamine transporter (EMT), is an uptake transporter that plays a role in the pharmacokinetics and disposition of a variety of cationic drugs [7]. OCT3 is involved in intestinal absorption and hepatic and renal excretion of drugs, and also plays important roles in the function of various physiological systems. OCT3 contributes to neurotransmitter reuptake in the brain, acetylcholine release during extraneuronal cholinergic regulations, as well as to the regulation of histamine release from basophils. Recent studies have also highlighted the potential role of organic cation transporters in various diseases.

OCT3 presents a very broad tissue expression pattern. OCT3 is expressed in epithelial cells, neurons, muscle cells and glial cells [49, 50]. In human, the highest OCT3 mRNA levels are found in the kidney, liver, placenta, heart, and skeletal muscle. OCT3 is also detected, to a lesser extent, in other organs including the lung and brain, as well as in cancer-derived cell lines [23, 51-53]. OCT3 is localized at the basolateral membrane of trophoblasts in the placenta [52], the sinusoidal membrane of hepatocytes, the basolateral membrane of renal proximal tubule epithelial cells, as well as at the luminal membranes of bronchial epithelial cells and small intestinal enterocytes [50, 54]. In rodents, OCT3 is found in various areas of the brain including the hippocampus, hypothalamus, and the ependyma of the third ventricle [55].

Function, physiology and clinically significant polymorphisms

OCT3 participates in the biliary and renal elimination of cationic endobiotics and xenobiotics, and also transports a wide range of monoamine neurotransmitters, hormones, and steroids [53]. In rat and human, OCT3 and OCT1 mediate the first step in biliary excretion of most cationic drugs in the liver. During secretion of organic cations in the kidney proximal tubule, cations are translocated across the basolateral membrane by OCT3 and OCT2 [56]. OCT3 is also involved in renal excretion of epinephrine, histamine, and norepinephrine [7]. In the small intestine, absorption of cationic drugs and xenobiotics from the intestinal lumen is mediated by OCT3 and/or OCTN1-2 in the brush border membrane [33]. In rodents, studies suggest that OCT3 contributes to serotonin uptake in the brain and might play a role in the modulation of behavior

and motor activity [57, 58]. Studies on OCT3 knock-out mice suggest that OCT3 might be involved in the regulation of salt uptake, and highlight that OCT3 is the most important organic cationic transporter in the heart [57, 59].

Five non-synonymous single nucleotide polymorphisms (SNPs) have been identified in the SLC22A3 gene. The mutations caused by three of these polymorphisms (A116S, T400I, and A439V) have been shown to decrease the uptake of both 3H-histamine and 3H-MPP+ in transfected cells [60]. OCT3 polymorphisms may also contribute to inter-individual variations in cationic drug disposition. Comparison of SNPs in the SLC22A3 gene in 213 individuals with methamphetamine use disorder and 443 healthy controls suggested a correlation between some of these SNPs and methamphetamine dependence [61]. However, so far, OCT3 polymorphisms have not been associated with any specific disease pathology.

Clinical significance

Recent findings have shown that the tyrosine kinase inhibitors imatinib, nilotinib, gefitinib, and erlotinib exert selectively potent inhibitory effects on OCT3. Comparison of the IC50 values to the unbound Cmax of these drugs suggests that potential clinically significant drug-drug interactions might take place between specific tyrosine kinase inhibitors and other drugs that are substrates of OCT3 [37]. Furthermore cimetidine, a substrate of OCT3, reduces the renal clearance of procainamide [62], ranitidine [63], dofetilide [64], and varenicline [65]. However, as yet, there is no direct evidence of drug-drug interaction involving OCT3.

3.1.4 OCTN1 (Organic Cation/Carnitine Transporter 1 / SLC22A4)

OCTN1 is a widely expressed organic cation transporter. Alongside OCTN2, it plays a role in L-carnitine tissue distribution and renal reabsorption, although ergothionene appears to be a preferred endogenous substrate. It is polyspecific, and appears to act as both a Na+-dependent and Na+-independent uptake transporter, or exchanger of organic cations, zwitterions and protons. It is implicated in Crohn's disease, the renal secretion of gabapentin, central nervous system penetration of oxaliplatin, as well as in the disposition of cationic respiratory medicines in the lung [7, 30, 66, 67].

OCTN1 is widely expressed in human tissues [68, 69]. It also appears to have higher mRNA expression than OCTN2 in many tissues. It is located on the brush-border membrane (urine-side) of proximal tubule cells, the luminal (air) side of airway epithelial cells [33, 70]. An interesting site of strong expression are CD14+ monocytes [71, 72]. There are reports of OCTN1 localization in mitochondria, as well as significant species differences in both

localization and transport mechanism between human and rat; in particular, high hepatic expression in the rat that is absent in human [28]. Its function in mitochondria requires further investigation, but may be important for carnitine accumulation in this organelle.

Function, physiology and clinically significant polymorphisms

OCTN1 has 11 predicted trans-membrane domains, and can variously function as an organic cation/proton exchanger, a cation exchanger, a Na+-dependent, or Na+-independent zwitterion transporter. Its physiological substrates are carnitine (an important component in transport of fatty acids to the mitochondria) and ergothioneine, although ergothioneine is a superior substrate [73]. In the kidney, it participates in the active secretion and reabsorption of small organic cations and zwitterions, such as carnitine and ergothioneine. OCTN1 was first cloned from a human fetal liver cDNA library [7, 72]. OCTN1 may be important in the reabsorption of zwitterions and the secretion of cations in the proximal tubule. Patients with a point-mutation leading to reduced uptake of gabapentin, have reduced renal secretion of gabapentin [67, 74]. Genetic polymorphisms of OCTN1 and OCTN2 have been linked to Crohn's diseases and colorectal cancer [30, 75]. Variants of the SLC22A4 gene are also associated with susceptibility to rheumatoid arthritis [74].

Clinical significance

At present, there is no direct evidence showing OCTN1 involvement in adverse clinical events, although mechanistic in vitro and in vivo studies suggest a significant role in the disposition of a number of drugs in the central nervous system CNS and the lung. Rat and human OCTN1 transport Oxaliplatin. OCTN1-mediated transport seems to be an important mechanism contributing to the neuronal accumulation and resulting neurotoxicity of oxaliplatin more than that mediated by OCTN2 or OCTs [66]. As OCTN1 is expressed in the apical membrane, it is possible that OCTN1 contributes to the apical transport of gabapentin in the intestine and kidney [67]. OCTN2 and to a lesser extent OCTN1 transport some important respiratory medicines (ipratropium and tiotropium), and due to their expression in the lung, may influence the disposition and absorption of these medicines in this district [76, 77].

3.1.5 OCTN2 (Organic Cation/Carnitine Transporter 2 / SLC22A5)

OCTN2 is a widely expressed organic cation transporter. It plays a key role in L-carnitine oral absorption, tissue distribution and renal reabsorption. It is polyspecific, and appears to act as both a Na^+-dependent and Na^+-independent uptake transporter of organic cations [78]. It is implicated in systemic carnitine deficiency and in Crohn's disease, as well as in the disposition of cationic respiratory medicines in the lung.

OCTN2 is very widely expressed in human tissues (see Table 5.25). In particular, OCTN2 is expressed on the apical membrane (gut-side) of enterocytes, the apical membrane (urine-side) of renal proximal renal tubules, and in skeletal muscle, heart, lung and the eye [31, 33].

Function, physiology and clinically significant polymorphisms

OCTN2 has 12 predicted transmembrane domains and is a high affinity, Na^+-dependent, pH sensitive, co-transporter of L-carnitine, primarily responsible for the uptake of L-carnitine into cells. OCTN2 also operates as a polyspecific Na^+-independent organic cation transporter, and can transport substrates in both direction across the plasma membrane. OCTN2 was first cloned from human kidney and identified as the transporter responsible for systemic carnitine deficiency [79]. OCTN2 has an high degree of sequence homology with OCTN1 [80]. Substrates of OCTN2 include TEA, quinidine, verapamil, pyrilamine, choline, short-chain acyl esters of carnitine, zwitterionic beta-lactam antibiotics, L-lysine and L-methionine [7, 81].

OCTN2 mediates the active absoprtion of L-carnitine in the small intestine and its reabsorption in the proximal tubule. OCTN2 also mediates the uptake of L-carnitine into adipocytes, cardiac myocytes, skeletal muscle cells, neurons, brain, lymphocytes, spermatozoa, and across the blood-retinal barrier [82]. L-Carnitine is an essential component in the mitochondrial oxidation of fatty acids.

In mice containing a missense mutation in Slc22a5, renal excretion of TEA was reduced compared to normal mice, indicating that organic cations are transported in a secretory direction by OCTN2, whereas carnitine is transported in a reabsorptive direction [83].

Over 100 polymorphisms of the SLC22A5 gene are known, and some are implicated in primary systemic carnitine deficiency, a recessive disorder of fatty acid oxidation leading to cardiomyopathy, hepatomegaly and cerebral dysfunction, among other symptoms [84-86].

Polymorphic isoforms of OCTN1 and OCTN2 are also linked to inflammatory bowel diseases [30, 87], although this requires further investigation. PPARγ activators, such as rosiglitazone may up-regulate OCTN2 expression [88].

Clinical significance and Pathophysiology

OCTN2 plays a key role in the absorption, distribution and Na+-dependent renal reabsorption of L-carnitine, which is essential for fatty acid metabolism. Polymorphisms affecting function may lead to primary systemic carnitine deficiency (SCD), which is treated by lifetime dietary supplementation with L-carnitine.
OCTN2 transports some important respiratory medicines (ipratropium and tiotropium), and due to its expression in the lung, may influence the disposition and absorption of these medicines in the lung [76, 77].

4. Aim of the study

Endogenous roles of drug transporters, especially in the transport of physiological compounds, such as metabolites and nutrients, are still not fully investigated. Apart from drug - drug interaction, there is growing interest in determination of other types of interaction with membrane transporters, such as drug – metabolite, drug – nutrient or drug – toxin interactions [8]. Understanding the endogenous functions of membrane transporters will provide new insight into the effects of drugs and other xenobiotic compounds on metabolic and developmental processes [89]. Additionally, to elucidate the impact of membrane transporters on Adsorption, Distribution, Metabolism and Excretion properties of various xeno- and endobiotics, it is necessary to obtain detailed information on transporter expression throughout the organism, especially in primary and toxicologically relevant organs (e.g., liver, kidney, intestine, lungs and blood–brain barrier (BBB)).

In order to expand knowledge about the Organic Cation Transporters (OCTs and OCTNs) and their physiological role, new data have been obtained through the functional and molecular analysis of these transporters in human airway epithelial cells and macrophage.

Further investigation of intracellular localization of different types of transporters is necessary for determination of absorptive or exsorptive function of the transporters. Consecutively, combining gathered information about tissue expression and cell localization, together with well-defined interactions with different types of substrates, will provide new insights and valuable information in physiological, pharmacological and ecotoxicological studies of membrane transporters.

Table 1. Endogeneous Substrates and Inhibitors of Polyspecific Organic Cation Transporters

Class	hOCT1	hOCT2	hOCT3	hOCTN1	hOCTN2
Metabolites					
Acetyl-L-carnitine					**8.5**
Betaine					(<500)
Choline	(16,700)[c]	**210 (381)**	(23,800)[c]	(231)	**(<2,000)**
Creatinine	(>20,000)	**(<2,000)**[c]	(15,700)[c]		
D-Carnitine				(<2,000)	**11, 98**
L-Carnitine	(12,400)[c]	(13,000)[c]	(5,590)[c]	**(24)**	**4.3, 4.8**
Guanidine	**(5,030)**[c]	**(2,300)**[c]	(1,300,6,200)[c]		
Thiamine					
Neurotransmitters					
Acetylcholine	**(580)**	**117 (149)**	(10,490)[c]		
Dopamine	(>20,000)[c]	**390–1,400**	1,200[c]		
Epinephrine	(>30,000)[c]	**400**	**240**		
Histamine	(>20,000)[c]	**940, 13,00**	**180, 220**		
Norepinephrine	(7,100)[c]	**1,500, 1,900**	**510–2,600**		
Serotonin	(>20,000)[c]	**80, 290 (310)**	(1,000)[c]		
Hormones					
Aldosterone					(<500)
Corticosterone	(7, 22)	(34)	(0.12, 0.29)		(<100)
Progesterone	(3.1)	(27)	(4.3)		
Prostaglandin E_2	0.66	0.03			
Prostaglandin $F_{2\alpha}$	0.48	0.33			
Testosterone	(10)[c]	(3)[c]	(44)[c]		
Miscellaneous					
Agmatine	**(24,000)**	**1,400 (3,251)**	**2,500**		
Ergothioneine[d]				**21**	
Stachydrine[d]				**270**	

Km values are expressed in µM. Taken from Koepsell, H., *Polyspecific organic cation transporters: their functions and interactions with drugs.* Trends Pharmacol Sci, 2004. **25**(7): p. 375-81.

Table 2: Tissue distribution of polyspecific transporters

	OCT1		OCT2		OCT3		OCTN1		OCTN2	
	hu	rod	hu	rod	hu	rod	hu	rod	hu	rod
Stomach	+	+	–	–	–	+	∅	+	+	+
Small intestine	+	**+**	+	+	+	+	+	+	+	**+**
Large intestine	+	+	∅	–	∅	+	+	+	+	+
Rectum	–	–	–	–	–	–	∅	–	+	–
Liver	**+**	**+**	∅	**+**	**+**[c]	+	+	+	**+**	+
Pancreas	–	–	–	–	–	–	–	–	+	–
Spleen	+	+	+	–	∅	+	+	+	∅	+
Trachea	+	+	+	+	+	+	**+**	–	+	–
Lung	+	+	+	+	+	+	+	+	+	+
Kidney	+[c]	**+**	**+**	**+**	+[c]	+	**+**	**+**	**+**	**+**
Urinary bladder	+	+	∅	∅	+	+	–	+	–	+
Prostate	–	+	–	–	–	+	+	+	+	+
Testis	–	+	–	∅	–	+	+	+	+	+
Sertoli cells	–	+	–	∅	–	+	–	+	+	+
Sperm	–	–	–	–	–	–	+	–	+	–
Skin	+[b]	+[b]	+[b]	+[b]	+[b]	+[b]	–	+	–	+
Skeletal muscle	+	+	∅	∅	**+**	+	**+**	+	**+**	+
Heart	+	+	–	∅	**+**	**+**	–	+	**+**	+
Blood vessels	–	+	–	∅	+	+	–	–	–	+
Brain	+	+	+	+	+	+	+	+	+	+
Spinal cord	–	–	–	–	–	–	+	–	+	–
Choroid plexus	–	+	–	+	–	+	–	+	–	+
Adrenal gland	–	–	–	+	–	–	–	–	–	–
Mammary gland	+	+	∅	∅	+	+	+	–	+	–
Uterus	–	∅	–	∅	–	**+**	–	+	+	+
Placenta	+	∅	+	∅	**+**	**+**	+	+	**+**	+
Ovary	–	∅	–	∅	–	**+**	–	+	–	+
Thymus	–	+	–	+	∅	+	+	+	+	∅
Bone marrow	–	–	–	–	–	–	**+**	–	∅	–
Epithelial cells	+	+	+	+	+	+	+	+	+	+
Neurons	–	–	+	+	+	+	–	–	–	–
Glial cells	–	–	–	–	+	–	–	∅	–	+
Muscle cells	–	–	∅	∅	+	+	+	+	+	+
Granulocytes	–	+	–	–	–	+	+	–	+	–
Lymphocytes	–	–	–	–	–	–	+	–	+	–
Macrophages	–	–	–	–	–	–	+	–	+	–
Tumor cells	+	–	+	–	+	–	–	–	+	–

The expression was demonstrated by Northern blots, RT–PCR, Western blots or immunohistochemistry. **+** bold face indicates very strong expression, ø no expression detected, - expression has not been investigated.

Taken from Koepsell, H., *Polyspecific organic cation transporters: their functions and interactions with drugs.* Trends Pharmacol Sci, 2004. **25**(7): p. 375-81.

Chapter II – EXPERIMENTAL PROCEDURES

1. Cell cultures and experimental treatments

1.1 Human Airway Epithelial cells

A549, Calu-3, NCl-H441 and BEAS-2B human cell lines were obtained from American Type Culture Collection (ATCC, Rockville, MD, USA). Alveolar carcinoma A549 and normal bronchial epithelial BEAS-2B cells were cultured in Dulbecco's Modified Eagle Medium (DMEM, high glucose) supplemented with sodium pyruvate (1 mM). NCl-H441, obtained from lung papillary adenocarcinoma, were cultured in RPMI-1640 (ATCC) and were used at passages 36-41. Calu-3 cells, obtained from a human lung adenocarcinoma and derived from serous cells of proximal bronchial airways, were cultured in Eagle's Minimum Essential Medium (EMEM) supplemented with sodium pyruvate (1 mM) and were used at passages 45-53. For all cell types, medium was supplemented with 10% fetal bovine serum (FBS) and 1% Penicillin/Streptomycin. Cells were routinely cultured under physiological conditions (37.5°C, 5% CO2, 95% humidity) in 10-cm diameter dishes.

For growth under air-liquid interfaced culture (ALI) conditions, Calu-3 cells were initially seeded on Cell Culture Inserts (12 mm in diameter, pore size 0.4 μm; Falcon) at the density of 75×103 cells/well, with apical and basolateral fluid volumes corresponding to 250 and 700 μl, respectively. After 24 h, the apical fluid was completely removed, and the medium in the basolateral compartment renewed every other day. Cell cultures were employed after 21 days, when the cell monolayers exhibited "tight" barrier properties, as represented by high transepithelial electrical resistance (TEER > 500 Ohm/cm2, measured with an epithelial voltmeter (EVOM, World Precision Instruments, FL, USA)). The integrity of cell monolayers was preserved after the experiments.

Chinese hamster ovary (CHO) cells transfected with OCTN1 (CHO-OCTN1) or OCTN2 (CHO-OCTN2) were kindly provided by Dott. Longo N. Cells were grown in Ham F12 medium supplemented with 6% fetal bovine serum as previously described [90].

1.2 Monocytes and Macrophages

Mononuclear cells were isolated from buffy coats that were obtained from normal healthy donors, provided by the Unit of Immunohematology and Transfusion of the Azienda Ospedaliero-Universitaria of Parma (local Ethics Committee approval # 43899, 03/12/2015). The Buffy coats, that were diluted 1:4 with PBS, were layered on 15 ml of Lympholyte H (Euroclone, Milano, Italy) and centrifuged at 800g for 20 min at 20°C. Peripheral blood mononuclear cells (PBMCs) at the interface were collected, and washed twice in PBS, and centrifuged by centrifugation at 300g for 10 min at 20°C. After the last wash, PMBC were suspended in RPMI containing that contained 10% endotoxin-free fetal bovine serum (FBS) and seeded on plasticware suitable for each determination. After a 30-min incubation at 37°C in an atmosphere at 5% CO2, non-adherent cells were removed with three vigorous washes in pre-warmed sterile Earle's Balanced Salt Solution (EBSS). The purity of adherent monocytes was assessed by staining with anti-CD14 mAb; more than 95% of the isolated cells expressed CD14 (not shown). Adherent monocytes were employed immediately, while whereas monocytes-derived macrophages (MDM) were obtained by incubating monocytes in complete growth medium that was added with 100 ng/ml of recombinant human Granulocyte Macrophage-Colony Stimulating Factor (GM-CSF) for up to 6 d. As previously reported, GM-CSF induced the expression of differentiation markers, such as CD204/SR-A, PPARγ, LPLA2, and PU.1 [91].

2. Uptake studies

For uptake assay, 3×10^4 cells were seeded onto 96-well trays (Falcon) and uptake was measured when the confluence was reached. Activities of OCTs and OCTNs were determined by measuring the uptake of the radiolabeled substrate [^{3}H]1-methyl-4-phenylpyridinium (MPP+) and L-[^{3}H]carnitine or [^{3}H]ergothioneine respectively. After two rapid washes in prewarmed transport buffer (Earle's Balanced Salt Solution (EBSS) containing (in mM) 117 NaCl, 1.8 $CaCl_2$, 5.3 KCl, 0.9 NaH_2PO4, 0.8 $MgSO_4$, 5.5 glucose, 26 TRIS-HCl adjusted to pH 7.4), cells were incubated in transport buffer containing each radiolabeled substrate (2 µCi/ml) for the times detailed in each experiment (see figure legends). For the determination of sodium-independent uptake, a modified EBSS in which NaCl was replaced with equimolar *N*-methylglucamine. Where indicated, the inhibitors were present in the transport buffer at the indicated concentrations. For the determination of L-carnitine intracellular concentration (see figure 11), cell volume was estimated from the distribution space of [^{14}C]urea, as already described [92]. Briefly, [^{14}C]Urea (0.5 mM; 2 µCi/ml) was added to A549 and Calu-3 cells during the last 10 min

of incubation in transport buffer. Calculated cell volumes corresponded to 9.3 ± 0.14 µl/mg of protein and 8.4 ± 0.9 µl/mg of protein for A549 and Calu-3, respectively (not shown).

At the indicated times, transport buffer containing the radiolabeled substrate was removed, and the experiment terminated by two rapid washes (<10 sec) in ice-cold 300 mM urea. Cell monolayers were extracted in ethanol and the radioactivity in cell extracts determined with Wallac Microbeta Trilux^2 liquid scintillation spectrometer (Perkin Elmer, Monza, Italy). Protein content was determined directly in the well using a modified Lowry procedure [93]. The substrate uptake is expressed as nmol or pmol/mg of protein. No relevant difference in transport rates was observed among cells at different passage number.

The apparent kinetic parameters K_m (Michaelis constant) and V_{max} (maximum transport rate) of substrate uptake were calculated by non-linear regression fitting according to the following Michaelis-Menten equations:

$$v = \frac{V_{max} \times [S]}{K_m + [S]} + K_d \times [S] \qquad \text{Equation 1}$$

for a single saturable component plus diffusion, where *v* is the initial influx, V_{max} is the maximal influx, K_m is the Michaelis constant and K_d is the diffusion constant;

$$v = \frac{V_{max1} \times [S]}{K_{m1} + [S]} + \frac{V_{max2} \times [S]}{K_{m2} + [S]} + K_d \times [S] \qquad \text{Equation 2}$$

for two saturable transport components plus diffusion, where the indices 1 and 2 indicate the high- and low-affinity components, respectively.

The following equation was employed to describe the effects of inhibitors on substrate uptake:

$$v = \frac{V_0 - I_{max} \times [I]}{[I]_{0.5} + [I]} \qquad \text{Equation 3}$$

where *v* is the initial influx, v_0 is the uptake in the absence of the inhibitor, I_{max} is the maximal inhibition, and $[I]_{0.5}$ is the inhibitor concentration required for half-maximal inhibition. The Ki value was calculated from $[I]_{0.5}$ employing the following Equation:

$$[I]_{0.5} = \left(1 + \frac{[S]}{Km}\right) \times Ki \qquad \text{Equation 4}$$

2.1 Determination of MPP+ fluxes in polarized Calu-3

Cell monolayers, cultured on permeable supports (Cell Culture Insert, Falcon), were washed once with EBSS. For the determination of apical and basolateral uptake, 50 or 600 µl of EBSS containing [^{3}H]MPP+ (10 µM, 2 µCi) were added to the apical or basolateral compartment, respectively, while the opposite compartment was incubated in EBSS. For the determination of transcellular fluxes, aliquots of the solution in the opposite compartment were collected and the radioactivity was measured with a Wallac Microbeta Trilux2 liquid scintillation spectrometer. To determine the intracellular accumulation of the substrate, the porous membranes were rapidly washed in 300 mM ice-cold urea, then detached from the culture inserts. Cell monolayers were extracted in 0.2 ml ethanol and the radioactivity of cell extracts was measured with Wallac Microbeta Trilux2 liquid scintillation spectrometer. Cell monolayers were then dissolved with 0.5% sodium deoxycholate in 1 M NaOH, and protein content was determined using a modified Lowry procedure, as described previously [93].

3. qRT-Polymerase Chain Reaction

For the analysis of mRNA expression 1 µg of total RNA, extracted with GenElute Mammalian Total RNA Miniprep Kit (Sigma Aldrich, Milano, Italy), was reverse-transcribed and 40 ng of cDNA were amplified as described previously [94], employing the forward and reverse primers shown in Table 3 . The expression of SLC22A4/OCTN1, SLC22A5/OCTN2 and the housekeeping gene RPL15 (ribosomal protein like 15) were monitored employing specific TaqMan® Gene Expression Assays (Life Technologies Italia, Milano, Italy; Cat# Hs00268200_m1, Hs00929869_m1, and Hs03855120_g1, respectively), according to the manufacturer's instructions. The expression of the gene of interest under each experimental condition was normalized to that of the housekeeping gene RPL15 (Ribosomal Protein Like 15), as indicated.

4. Western blot analysis

Western blot analysis was performed as previously described [95]. To evaluate the protein expression, cells were suspended in Laemmli Sample Buffer, briefly sonicated and, after protein quantification [96], boiled for 5 min at 95°C. 50 µg of whole cell lysates were separated through SDS-PAGE (10% acrylamide) and electrophoretically transferred to PVDF membranes (Immobilione-P membrane, Millipore, Milano, Italy). Membranes were incubated for 1 h at RT in blocking solution (Tris-Buffered Saline solution, TBS: 50 mM Tris-HCl pH 7.5, 150 mM NaCl)

added with 5% dried milk, or 1% BSA and 1% casein for OCT3. The incubation with the specific primary antibodies anti-OCTN1, anti-OCTN2 by from Sigma-Aldrich (Milano, Italy; 1:500), anti-ATB0,+ (1:1000; Abcam), anti-SNAT2 by Abcam (BIOTIME SAS, Siena, Italy; 1:500), anti-phospho-mTOR, anti-mTOR and anti-phospho-p70S6K (mTOR Pathway Antibody Sampler Kit, Cell Signalling, Aurogene, Rome, Italy; 1:1000), anti-p70S6K (Cell Signalling; 1:1000), anti-phosphoSTAT3 and anti-STAT3 (Phospho-Stat Antibody Sampler Kit, Cell Signalling; 1:1000) was carried out overnight at 4°C. Blots were then exposed to horseradish peroxidase-conjugated anti-rabbit IgG (1:20.000) for 1 h at RT. Membranes were finally washed and immunoreactivity visualized with enhanced chemiluminescence (Millipore). Actin, detected with a polyclonal antibody (Sigma-Aldrich, 1:1000), was employed for internal standardization.

5. siRNA transfection

Short interfering RNA (siRNA) analysis of SLC22A3/OCT3 was performed employing specific FlexiTube siRNA (Cat.# 1027416) by Qiagen® (Milano, Italy), according to Fast-Forward Transfection protocol provided by the manufacturer. Briefly, cells (1×105/ml) were transfected by adding to 1 ml of cell suspension 200 µl of serum free RPMI containing HiPerFect Transfection Reagent (9 µl) and 100 nM AllStar Negative Control siRNA (Cat.# SI03650318; scrambled) or 25 nM each of 4 different OCT3 siRNA (Cat. # SI00721357, SI04140598, SI04159848, SI04218935). Transfected cells were seeded as required by the experimental plan, and maintained under growing conditions for 96 h. Control, untreated cells were also cultured in parallel.

6. HPLC-MS/MS analysis

For the determination of the intracellular content of L-carnitine, monocytes and MDM, seeded onto 24-well trays, were rapidly washed with PBS and the intracellular pool, extracted through a 10 min-incubation in acetonitrile/methanol (3:1) at 4°C, was analysed by HPLC-ESI-MS/MS. An Agilent 1260 infinity LC (Agilent Technology, Palo Alto, CA, USA) equipped with autosampler injection (Agilent 1260 High performance autosampler) and pump systems (Agilent 1260 Quaternary Pump) was used. Separation was performed by injecting 8 µL of each sample onto an Ascentis Express HILIC column that was equipped with a corresponding pre-column (Supelco, Bellefonte, PA, USA). Two chromatographic eluents were employed, solvent A, acetonitrile/water/100 mM ammonium formate pH 3.2 (90:5:5) and solvent B, acetonitrile/water/100 mM ammonium formate pH 3.2 (50:45:5). Each sample was eluted at a

constant flow rate of 0.45 mL/min under optimized gradient for a total run time of 12 min. Column was maintained at 40 °C. Mass spectrometric analyses were carried out by using an AB SCIEX 4500 Q-TRAP triple quadrupole mass spectrometer that was equipped with a Turbo Ion Spray source (AB Sciex, Foster City, CA). The mass spectrometer was operated in positive electrospray ionization mode. For detection and quantitation, the following ESI inlet conditions were applied: gas 1, air (GS1, 18 psi); gas 2, air (GS2, 20 psi); ion-spray voltage, 5000 V in positive mode; ion-source temperature, 400 °C; curtain gas, nitrogen (CUR, 40 psi); collision gas, nitrogen (CAD, medium). The detection of the ions was performed in the multiple reaction monitoring (MRM) mode. Tuning and optimization of the compound-dependent parameters declustering potential (DP, 141 V), collision energy (CE, 23 V), collision exit potential (CXP, 8 V) were performed by the direct infusion of a standard solution. Entrance potential (EP) was set at 10 V. The monitored transition for L-carnitine was 162.039 m/z (Q1) → 103.010 m/z (Q3). Calibration curve was performed in acetonitrile/methanol (3:1) in parallel. Analyst 1.6.2 software (AB Sciex, Foster City, CA) was used for data acquisition, analyte mass spectrometric parameter optimization and quantitative calculations. Protein content was determined directly in each well using a modified Lowry procedure [93]. L-carnitine content is expressed as nmol/mg of protein.

9. Materials

Fetal bovine serum and lympholyte H were purchased from EuroClone (Milano, Italy). NCl-H441 were purchased from (ATCC, Rockville, MD, USA). Methyl-4-phenylpyridinium iodide, 1-[methyl-^{3}H], 85 Ci/mmol, were from ARC (American Radiolabeled Chemicals, St. Luis, MO, USA) and was obtained from Bcs Biotech (Cagliari, Italy). Carnitine-L-[N-methyl-^{3}H]HCl (80 Ci/mmol) was obtained from Perkin-Elmer (Milano, Italy) and [^{3}H]ergothioneine (0.10 Ci/mmol) from Campro Scientific (Veenendaal, Netherlands). GM-CSF and CSF-1 were purchased from ReliaTech (Wolfenbuttel, Germany). Rabbit monoclonal OCT3 (Abcam) and Alexa-fluor 488 goat anti-rabbit (Abcam) were from Biotime SAS (Siena, Italy); rabbit polyclonal OCT1/2 (Santa Cruz Biotechnology) were obtained from DBA Italia S.R.L (Segrate, MI, Italy) and anti-rabbit IgG, HRP-linked Antibody (Cell Signalling) from EuroClone (Pero, MI, Italy). The antibody against $ATB^{0,+}$ was from BIOTIME SAS (Siena, Italy). Sigma–Aldrich (Milano, Italy)was the source of the inhibitors, as well as of anti-OCTN1, anti-OCTN2, and anti-actin antibodies, and unless otherwise specified, of all other chemicals.

TABLE 3. Primer pairs employed for quantitative RT-PCR chain reaction

Gene ID	Forward Primer	Revers Primer
SLC22A1/OCT1	5′ TGTCACCGAAAAGCTGAGCC 3′	5′ TCCGTGAACCACAGGTACATC 3′
SLC22A2/OCT2	5′ CATCGTCACCGCGTTTAACCTG 3′	5′ AGCCGATACTCATAGAGCCAAT 3′
SLC22A3/OCT3	5′ AGGTATGGCAGGATCGTCATT 3′	5′ GCAGGAAGCGGAAGATCACA 3′
SLC6A14/ATB$^{0,+}$	5′ GCTGCTTGGTTTTGTTTCTTCTTGGTC 3′	5′ GCAATTAAAATGCCCCATCCAGCAC 3′
SLC38A1/SNAT1	5′ CACCACAGGGAAGTTCGTAATC 3′	5′ CGTACCAGGCTGAAAATGTCTC 3′
SLC38A3/SNAT3	5′ ATGAAGAAGGCCGAAATGGGA 3′	5′ TGCTTGGTGGGGTAGGAGTAG 3′
SLC38A4/SNAT4	5′ GAAATTCCAAATACCCTGCCCT 3′	5′ GCGGTGGGTGTAATCCATCA 3′
RPL15	5′ GCAGCCATCAGGTAAGCCAAG 3′	5′ AGCGGACCCTCAGAAGAAAGC 3′

Chapter III – OCTs IN HUMAN AIRWAY EPITHELIAL CELLS

1. INTRODUCTION

Membrane transporters are known to have a significant impact on the absorption and elimination of a large number of drugs, determining their pharmacokinetic profiles, safety and efficacy [97]. A large family of transporters are the Solute Link Carrier, SLC22A, which are often found in epithelial membranes where they mediate uptake and secretion of organic cations [33]. SLC22A gene family includes electrogenic transporters (i.e. OCT1/SLC22A1, OCT2/SLC22A2, and OCT3/SLC22A3) and pH-dependent novel transporters, namely OCTN1/SLC22A4 and OCTN2/SLC22A5 [98]. OCTs are involved in the bidirectional translocation of small (<500 Da) organic cations across the cell membrane. They are endowed with broad, overlapping affinities for a wide range of substrates, including endogenous molecules, such as choline, creatinine and neurotransmitters [99], as well as a variety of xenobiotics [32]. The model substrates for the functional study of OCTs are tetraethylammonium (TEA) and the most specific neurotoxin methyl 4-phenylpiridinium (MPP+) [99, 100]. None of the substrates thus far employed interacts only with a single OCT transporter, as demonstrated employing transfected cell models, such as CHO [101], HEK293 [36, 51] or xenopus oocytes [102, 103]. In non transfected cell models the characterization of OCT transport activity appears further complicated by the lack of specific inhibitors too [99]. The study of OCT transporters has been mainly focused on liver, kidneys, intestine and blood–brain barrier, with the lung remaining largely unchartered terrain, despite its pharmacological relevance [104, 105]. Actually, the lung offers a great potential as a portal into the systemic circulation for drugs endowed with difficult oral pharmacokinetics or stability issue.
Moreover, since several common inhaled drugs, positively charged at physiological pH, have been reported to interact with OCT [106], the role of these transporters in lung epithelium (especially bronchiolar and alveolar systems) deserves particular attention.
Evidence is now emerging that OCTs are involved in transport processes in various cell types of the lung [107, 108], and differential expression of the transporters has been highlighted in cell models from different regions [106]. Thus far, the characterization of OCT-mediated transport in respiratory cell models has been performed employing the fluorescent cation Asp+ as substrate [109, 110]. However, since also the choice of the substrate is known to influence the profile of inhibition of OCT mediated uptake both quantitatively and qualitatively [111], it is conceivable that the use of substrates other than Asp+ may broaden the knowledge about OCT function.

The aim of the first part of this research project has been the identification of optimal cell models for studies concerning cationic drug absorption through OCTs in the airways. In this study we thoroughly characterize OCT transport activity in in vitro models of respiratory epithelium (alveolar A549, bronchial Calu-3, and distal lung NCl-H441 carcinoma cells, as well as in bronchial BEAS-2B cells) by means of an integrated approach combining data of mRNA expression with the kinetic and inhibition analyses of MPP+ transport.

2. RESULTS

2.1 Time-dependent accumulation of MPP+ in A549, Calu-3 and NCl-H441 cells

The uptake of 1-methyl-4-phenylpyridinium (MPP+) by the three cell lines has been preliminary measured at different times, up to 60 min (Figure 4). In A549 MPP+ uptake was linear up to 5 min incubation, while in Calu-3 cells linearity was maintained up to 15 min. MPP+ uptake was completely abolished by an excess of unlabelled substrate, employed to estimate the non-specific binding. This result suggests that, at the concentration of the substrate employed, non saturable uptake in these cells was negligible. Conversely, MPP+ uptake in NCl-H441 cells was very low, although slightly increasing up to 30 min, and hardly inhibited by an excess of the substrate. In light of these results, we can conclude that A549 cells display the highest saturable uptake of MPP+, with Calu-3 following and NCl-H441 endowed with an only modest saturable uptake.

In addition, time-course of MPP+ uptake performed in polarized Calu-3 cells grown under air–liquid interface conditions (Calu-3 ALI), indicated that the accumulation of the substrate was linear up to 30 min and comparable when measured at the apical and basolateral side of the layers (Figure 5, panel A). Under these conditions, the transcellular fluxes of MPP+ were detectable in both directions and quantitatively comparable from apical to basolateral side and vice versa (panel B).

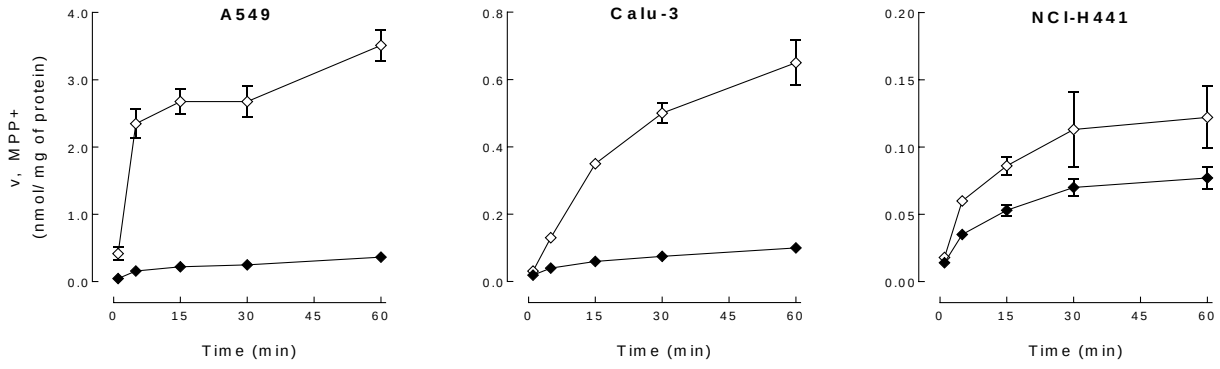

Figure 4. Time-dependent accumulation of MPP+ in A549, Calu-3 and NCl-H441 cells.

Cells were incubated for the indicated times in the transport buffer (see section Material and Methods) containing [^{3}H]MPP+ (10 µM; 2 µCi/ml) (open symbols). Non-specific binding of the substrate was estimated by measuring [^{3}H]MPP+ uptake in the presence of an excess of unlabelled substrate (2 mM) (filled symbols). Each point represents the mean ± S.D. of four independent determinations. The experiments has been repeated three times with comparable results.

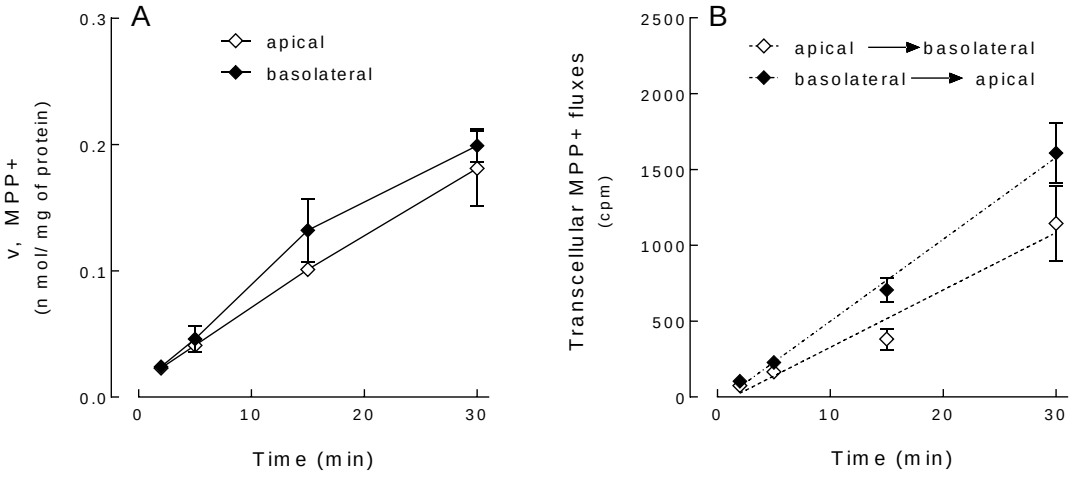

Figure 5. MPP+ fluxes in Calu-3 ALI.

Monolayers of polarized Calu-3 cells grown in air-liquid interface conditions (ALI) were incubated for the indicated time in the transport buffer containing [^{3}H]MPP+ (10 µM; 2 µCi/ml), either added at the apical or at the basolateral side, as indicated. The intracellular MPP+ accumulation (panel A) and the transcellular fluxes of MPP+ (panel B) were determined as described in the section Material and Methods. Each point represents the mean ± S.D. of three independent determinations. The experiments have been repeated twice with comparable results.

2.2 Kinetic analysis of MPP+ uptake

Initial rates of transport were determined in the three cell lines over a wide range of MPP+ concentrations (from 0.8 to 1850 µM), both in the presence and in the absence of sodium (Figure 6). Data obtained under the two experimental conditions were overlapping, thus demonstrating the complete Na+-independence of MPP+ uptake in all cell models. Transport values in A549 cells were best fitted by equation 1 (see section Material and Methods) and the resulting kinetic parameters revealed the presence of an high-affinity transport system plus diffusion (Km about 50 µM with a Vmax of about 1.5 nmol/mg of protein). Consistently, the Eadie-Hofstee plot of the saturable component (insert) was linear, confirming the operation of a single OCT transporter in this model. Also in NCI-H441 cells, transport data were best fitted by equation 1 but in this case the Km values were higher (about 180 µM) and Vmax values about ten times lower than in A549. On the contrary, in Calu-3 cells, MPP+ transport data were best fitted by equation 2, revealing the presence of at least two saturable transport components, one displaying a high-affinity for the substrate (Km ≤ 20 µM) and the other with a low-affinity (Km ≥ 0.6 mM). Accordingly, the regression analysis of the Eadie-Hofstee plot for the saturable MPP+ uptake in these cells (insert) appeared nonlinear, confirming the involvement of at least two different transporters.

A complete description of the apparent kinetic parameters obtained in the cell models is shown in Table 4.

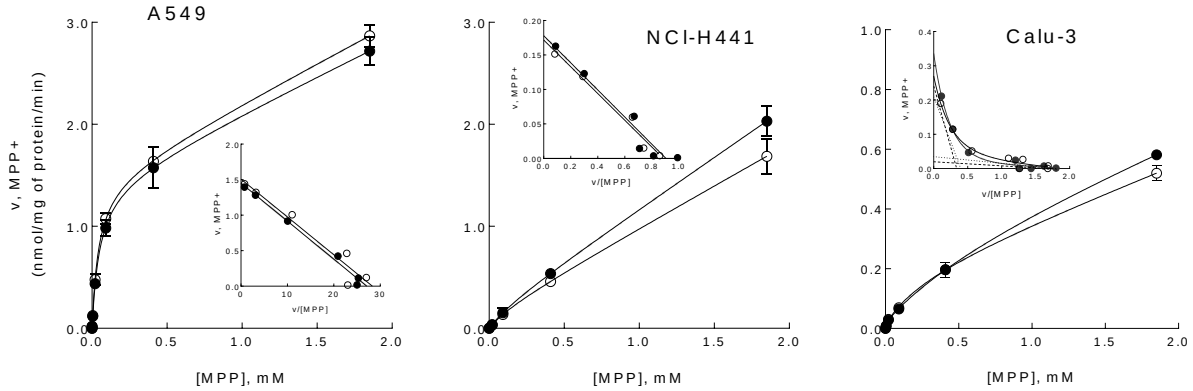

Figure 6. Kinetic analysis of MPP+ uptake.

A549, NCl-H441 and Calu-3 cells were incubated in the presence of the indicated concentrations (from 0.8 to 1850 µM) of [^{3}H]MPP+ (2 µCi/ml) for 5 min (A549), 10 min (Calu-3) or 15 min (NCl-H441), in the absence (open symbols) or in the presence (filled symbols) of Na. Inserts in each graph show the Eadie-Hofstee transformations of the saturable uptake (obtained after subtraction of the diffusive component estimated by the nonlinear fitting). Straight lines are drown employing the values of the kinetic parameters given by nonlinear regression (see Table 4). Curves for Calu-3 represent the nonlinear fitting of the data. Points are mean ± S.D. of three independent determinations. The experiment has been repeated twice with comparable results.

Table 4. Kinetic parameters describing the uptake of MPP+.

Data are estimated from nonlinear regression analysis shown in Figure 6.

		High affinity		Low affinity	
		Km1 mM	Vmax1 nmol/mg of protein/min	Km2 mM	Vmax2 nmol/mg of protein/min
A549	Na^+-present	0.050 ± 0.0015	1.433 ± 0.016		
	Na^+-absent	0.043 ± 0.0019	1.471 ± 0.022		
NCl-H441	Na^+-present	0.184 ± 0.018	0.178 ± 0.009		
	Na^+-absent	0.176 ± 0.0138	0.172 ± 0.007		
Calu-3	Na^+-present	0.014 ± 0.005	0.025 ± 0.005	0.78 ± 0.08	0.269 ± 0.017
	Na^+-absent	0.020 ± 0.004	0.038 ± 0.004	0.60 ± 0.04	0.240 ± 0.023

2.3 Inhibition of MPP+ uptake by OCTs inhibitors

Inibition of MPP^+ uptake in A549 cells

In order to identify the contribution of each OCT to the transport of MPP+ in the three cell models, the uptake of the substrate was measured in the presence of increasing concentrations of the inhibitors quinidine, prostaglandin E2 (PGE2) and corticosterone [99]. In A549 cells both quinidine (Figure 7, panel A), inhibitor of OCT1 [36], and PGE2 (panel B), which preferentially inhibits OCT2 [99], were completely ineffective. On the contrary, the addition of corticosterone (panel C), which can inhibit all OCTs, but has a much higher affinity for OCT3 [99], was able to significantly reduce the uptake of 5 µM MPP+ in a concentration-dependent manner (I0.5 = 1.29 µM; maximal inhibition > 90%). From these data, the calculated Ki was 1.17 µM, a value very close to IC50 of corticosterone for OCT3 [99].

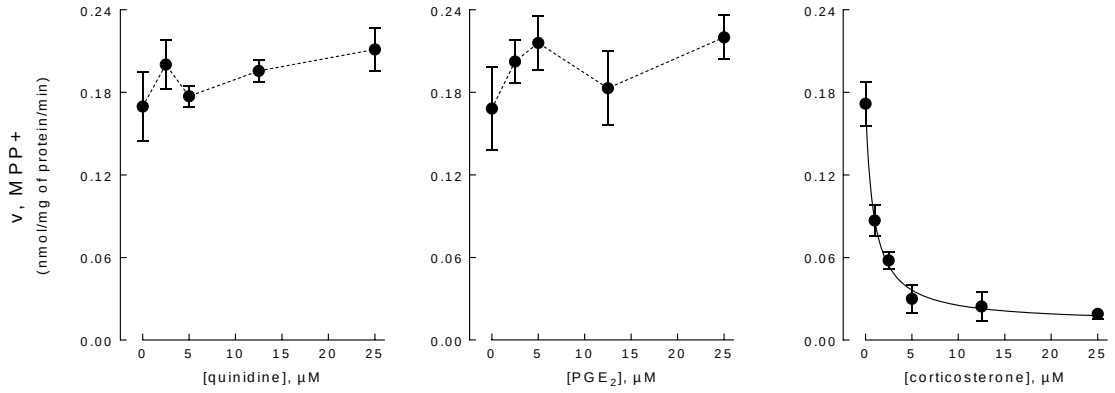

Figure 7. Inhibition of MPP+ uptake in A549 cells.

A549 cells were incubated for 5 min in the transport buffer containing [^{3}H]MPP+ (5 µM; 2 µCi/ml) with the indicated concentrations of inhibitors. Each point represents the mean ± S.D. of four independent determinations. For corticosterone, data were fitted by Equation 3 (see section Material and Methods). The experiment has been repeated three times with comparable results.

Overall these results point to OCT3 as the main transporter for MPP+ in A549 cells, excluding the contribution of OCT1 and OCT2.

Inibition of MPP+ uptake in NCL-H441 cells

In NCl-H441 cells all the inhibitors were ineffective at the concentrations employed for A549 (data not shown). Hence, the inhibition analysis have been performed at a higher concentration of MPP+ (50 µM) with increased concentrations of inhibitors (250 µM). The results, presented in figure 8, demonstrate that only quinidine modestly although significantly inhibited MPP+ uptake, with a maximal inhibition of about 30%. This finding points to OCT1 as the main transporter active in NCl-H441 cells.

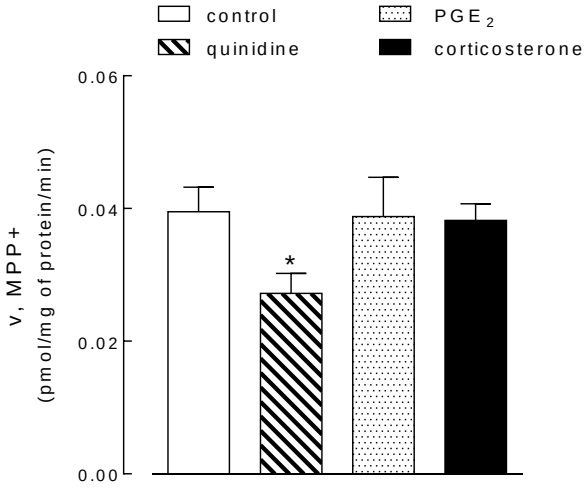

Figure 8. Inhibition of MPP+ uptake in NCl-H441 cells.

NCl-H441 cells were incubated for 15 min in the transport buffer containing [^{3}H]MPP+ (50 µM; 2 µCi/ml) in the absence (control) and in the presence of the indicated inhibitors (250 µM). Bars represent the mean ± S.D. of four independent determinations. The experiments has been repeated three times with comparable results. *p < 0.05 vs control.

Inibition of MPP+ uptake in Calu-3 cells

Due to the operation of different transport components in Calu-3 cells, the inhibition analysis in these cells had to be performed at different concentrations of substrate, so as to properly identify the high and low affinity components. To choose the proper experimental conditions, the relative contribution of the high and low affinity components to total MPP+ uptake has been calculated at different concentrations of substrate, taking advantage of the proper kinetic parameters reported in Table 4. As shown in figure 9 the contribution of the high affinity transporter was prevalent at low concentrations of substrate (up to 10 µM), while the low affinity activity accounted for more than 60% at MPP+ > 100 µM.

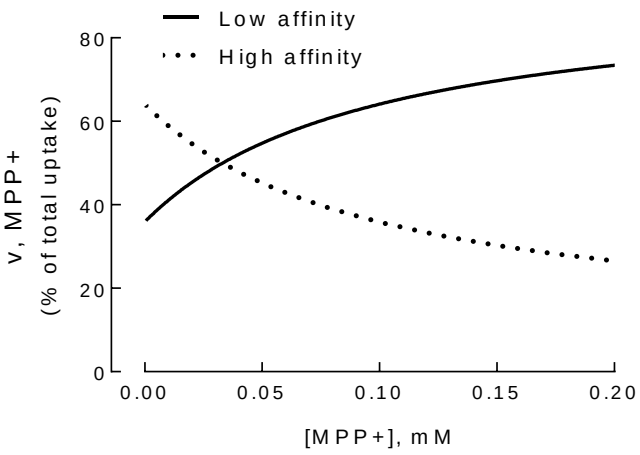

Figure 9. Estimated relative contribution of low and high affinity components to MPP+ transport in Calu-3 cells.

The curves have been calculated on the basis of the kinetic parameters presented in Table 4

The effect of OCT inhibitors in Calu-3 has been hence assessed at both 5 and 100 µM MPP+ (Figure 10). At 5 µM MPP+ (panel A), both corticosterone and quinidine inhibited the uptake, although to a different extent (maximal inhibition of about 80% for corticosterone and 50% for quinidine). I0.5 values were in the order of micromolar (1.038 and 3.98 µM for corticosterone and quinidine, respectively). At 100 µM MPP+ (panel B), a concentration of substrate that better highlights the low affinity transport component, the percent of maximal inhibition obtained by quinidine increased, while that of corticosterone concomitantly decreased. PGE2 was always ineffective.

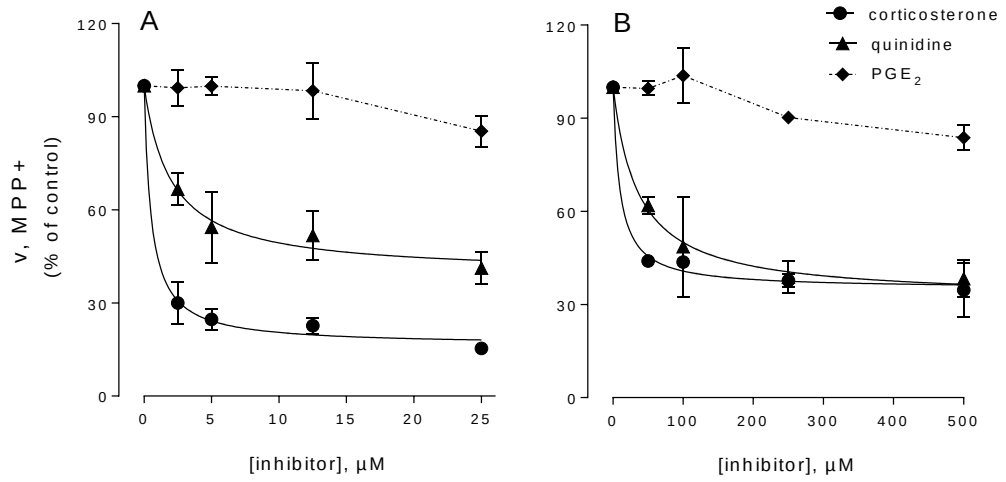

Figure 10. Inhibition of MPP+ uptake in Calu-3 cells.

Cells were incubated for 10 min in the transport buffer containing 5 µM (panel A) or 100 µM (panel B) [^{3}H]MPP+ (2 µCi/ml) in the presence of the indicated concentrations of the inhibitors. Data are expressed as percent of control (absence of inhibitor). Data were fitted by Equation 3 (see section Material and Methods). Each point represents the mean ± S.D. of four independent determinations. The experiment has been repeated three times with comparable results.

The results obtained from the inhibition analysis suggest that both OCT1 and OCT3 are active in Calu-3 cells. In order to exclude the involvement of other transporters such as OCTN1/2 and MATE1, the uptake of MPP+ was measured (Figure 11) at both low (5 µM, panels A and B) and high (100 µM, panels C and D) concentration of substrate, both in the presence and in the absence of sodium, employing transport buffer solutions at different pH (6.4, 7.4 and 8.4). Data obtained show that MPP+ uptake was pH-independent and sodium-independent at any value of pH, both at low and high substrate concentrations, thus excluding the contribution of MATE1, which is pH-dependent [112]. Moreover, carnitine and ergothioneine, the substrates of OCTN2 and OCTN1, respectively [73]and [79], did not inhibit MPP+ uptake (panels B and D). We thus conclude that in Calu-3 cells OCT3 represents the high affinity transporter for MPP+ while OCT1 accounts for the low affinity component.

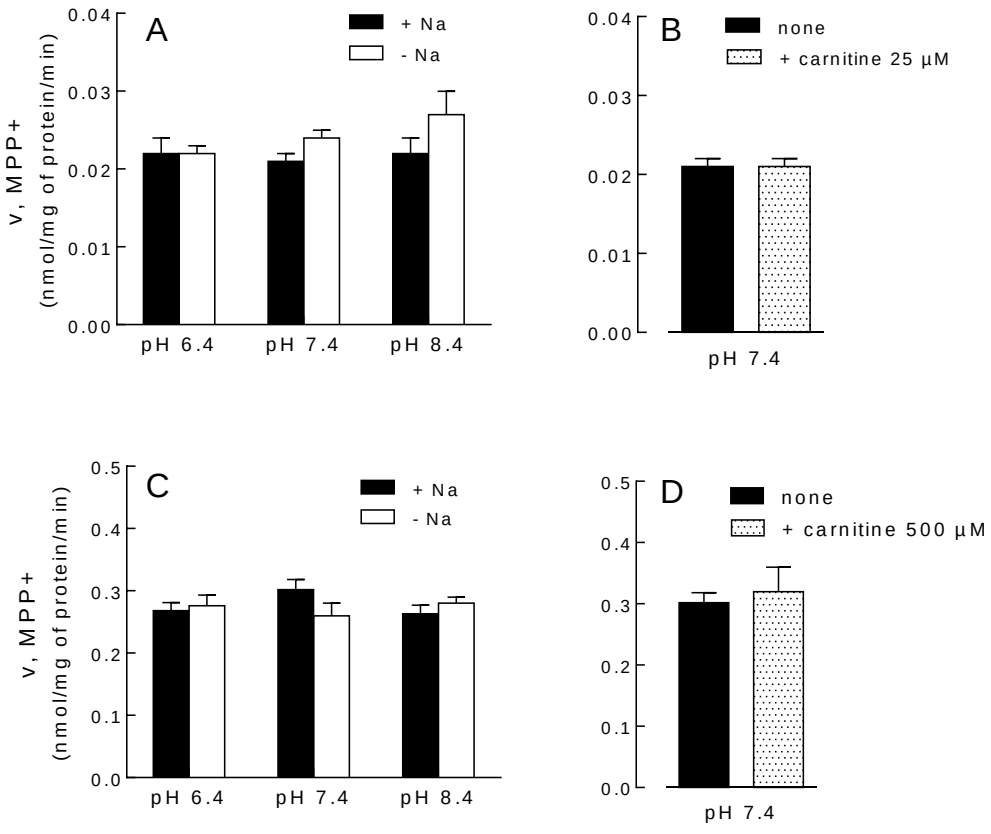

Figure 11. Effect of pH on MPP+ uptake in Calu-3 cells.

Cells were incubated for 10 min in the transport buffer containing 5 µM (panels A and B) or 100 µM (panels C and D) [^{3}H]MPP+ (2 µCi/ml) in the presence or in the absence of sodium (panels A and C) or in the presence of sodium (panels B and D) at the indicated pH. Carnitine was added to the transport buffer as indicated (panels B and D). Each point represents the mean ± S.D. of four independent determinations. The experiment has been repeated twice with comparable results.

Inhibition of MPP^+ uptake in Calu-3 cells grown in Air Liquid Interface condition (ALI)

The inhibition analysis on MPP+ transport has been, in addition, performed in polarized Calu-3 cells maintained under air-liquid interface grown conditions (Calu-3 ALI). The results, presented in figure 12, demonstrate that at 5 µM MPP+ only corticosterone significantly inhibited the uptake at both basolateral and apical sides, while quinidine and PGE2 were ineffective (panels A and B). At 100 µM also quinidine, in addition to corticosterone, significantly inhibited MPP+ uptake at the apical side, while at the basolateral side only the inhibition by corticosterone was significant. In this latter condition PGE2 was completely ineffective and quinidine caused a slight, not significant, inhibition (panels C and D). These results suggest that OCT3 is functional at both the basolateral and apical membranes in polarized Calu-3 cells, while a significant OCT1 activity is observed only at the apical side.

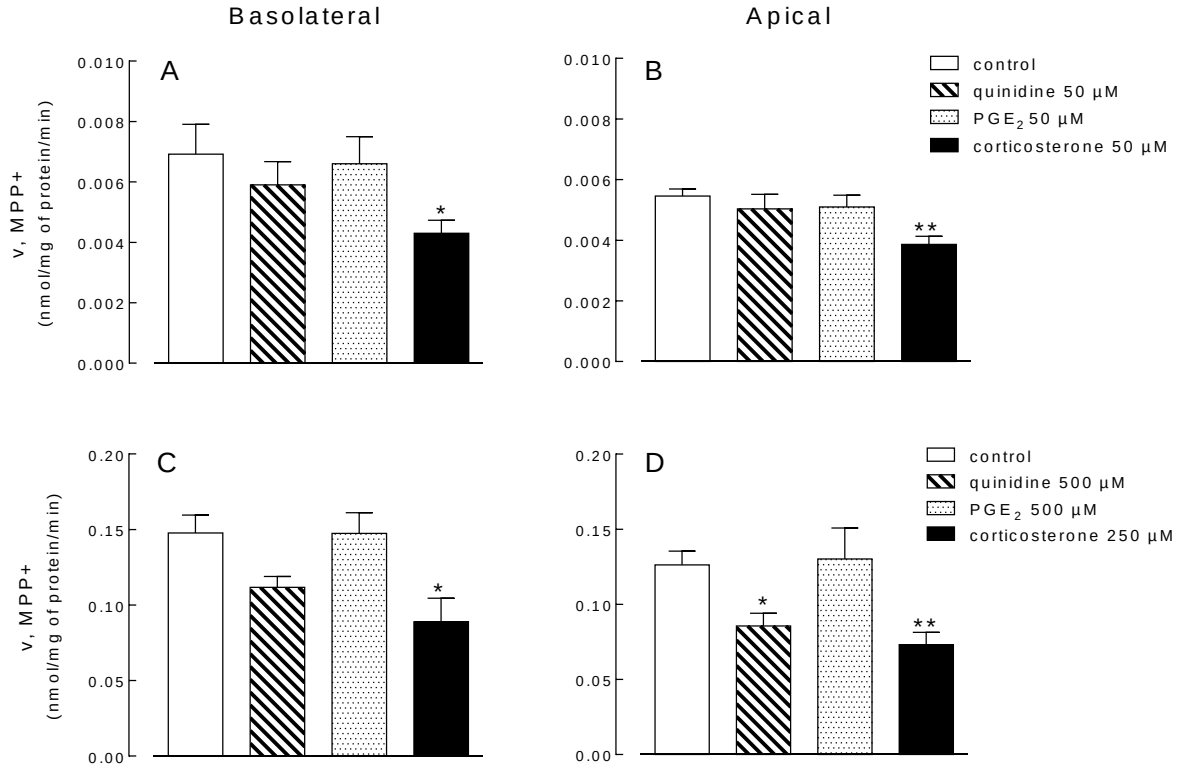

Figure 12. Inhibition of MPP+ uptake in Calu-3 ALI.

Polarized cells were maintained under air-liquid interface growth conditions (21 d). Apical and basolateral side were incubated for 10 min in the transport buffer containing 5 µM (panels A and B) or 100 µM (panels C and D) [^{3}H]MPP+ (2 µCi/ml) in the absence (control) or in the presence of the indicated concentrations of the inhibitors. Bars represent the mean ± S.D. of three independent determinations. The experiment has been repeated twice with comparable results. *$p < 0.05$, **$p < 0.01$ vs control.

2.4 Expression of OCTs and MPP+ transport in silenced cells

Figure 13 shows the expression of OCTs mRNA in A549, NCl-H441 and Calu-3 cells. The level of OCT1was highest in Calu-3,with NCl-H441 following, and only barely detectable in A549. The expression of OCT2 was undetectable in all cell models while OCT3 was clearly evident in both A549 and Calu-3 cells but not in NCl-H441.

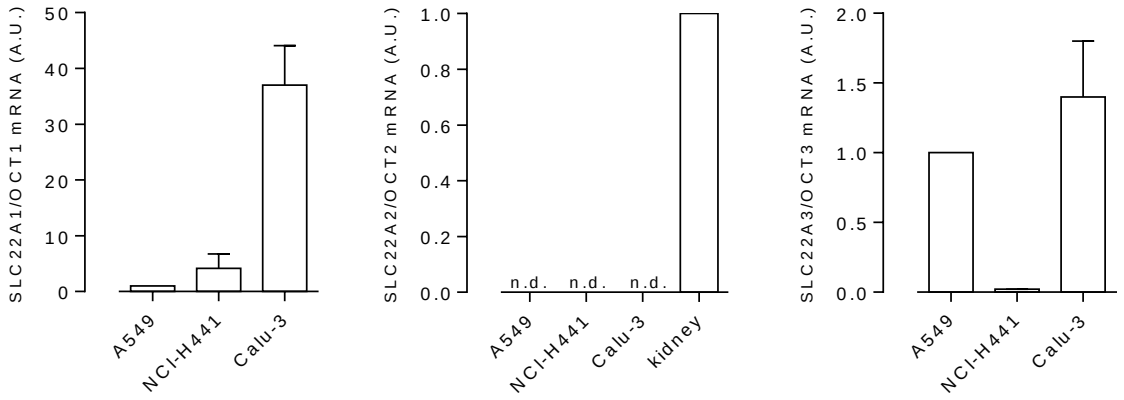

Figure 13. Expression of OCTmRNA.

mRNA levels for OCTs were determined through RT-qPCR analysis. After normalization to RPL-15, the expression of SLC22A1/OCT1, and SLC22A3/OCT3 in the different cell models was expressed relatively to that of A549 (=1). For SLC22A2/OCT2, cDNA obtained from human kidney was employed as positive control and set=1. Data are means ± S.E. of three experiments, each performed in duplicate.

In light of these results, we next employed short interfering RNA (siRNA) to define the operation of OCT1 and OCT3 in A549 and Calu-3 cells. In A549 (Figure 14), a significant, although incomplete, silencing of SLC22A3/OCT3 (about 40% compared with cells transfected with scrambled siRNA) was obtained after 96 h of incubation (panel A). The observed changes of gene expression were associated with a marked reduction of transport activity (>60%, panel B) in SLC22A3/OCT3 siRNA transfected cells. In this latter condition, the corticosterone-inhibitable fraction appeared much smaller compared to that observed in cells transfected with scrambled siRNA (panel C). The silencing of SLC22A1/OCT1 in this cell model was completely ineffective (result not shown). These results, besides confirming the prevalent operation of OCT3 in A549 cells, also validate the efficacy of corticosterone as OCT3 inhibitor.

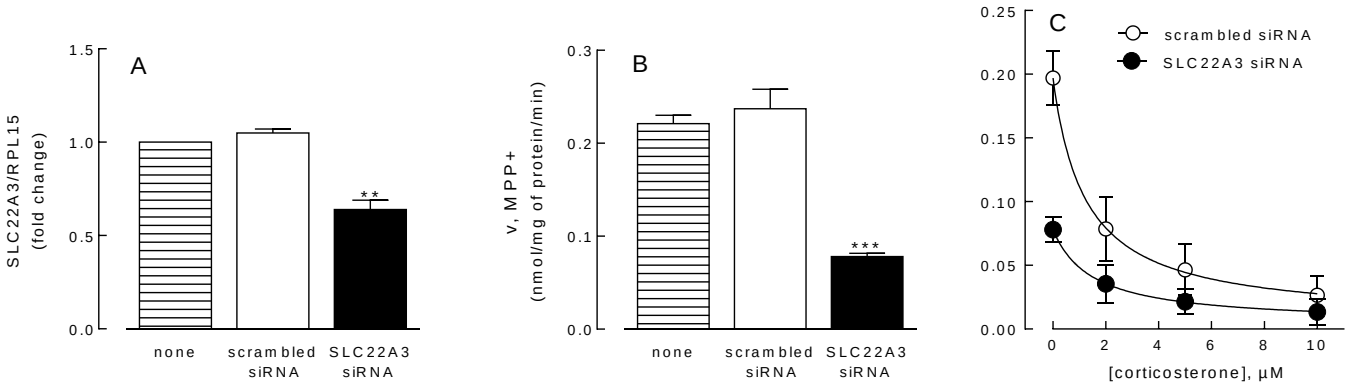

Figure 14. SLC22A3/OCT3 silencing in A549 cells.

A549 cells were transfected with scrambled or SLC22A3/OCT3 siRNA for 96 h, as described in Material and methods. Panel A. The expression of SLC22A3/OCT3 mRNA was assessed by qRT-PCR and shown relatively to that of untransfected cells (none=1). Data are means ± S.E. of three separate determinations, each performed in duplicate. **p b 0.01 vs untransfected cells (none). Panel B. The uptake of [^{3}H]MPP+ (5 µM; 2 µCi/ml; 5 min) was measured in cells untransfected (none) or transfected with scrambled or SLC22A3/OCT3 siRNA. Data are means ± S.E. of three independent experiments, each performed in quadruplicate. ***p b 0.01 vs scrambled siRNA. Panel C. Transfected cells were incubated for 5 min in the transport buffer containing [^{3}H]MPP+ (5 µM; 2 µCi/ml) with the indicated concentrations of corticosterone. Each point represents the mean ± S.D. of four independent determinations. Data were fitted by Eq. (3) (see section Material and methods). The experiment has been repeated twice with comparable results.

Figure 15 shows the effect of SLC22A1/OCT1 and SLC22A3/OCT3 silencing on MPP+ transport activity in Calu-3 cells. As expected, OCT1 and OCT3 siRNA were specifically effective in reducing the expression of SLC22A1 (panel A) and SLC22A3 (panel B), respectively. The reduction was about 50% for both genes. The consequence of gene silencing on MPP+ transport was then evaluated by measuring substrate uptake at 5 µM (panel C) and 100 µM (panel D) MPP+. At 5 µM, only OCT3 silencing caused a significant reduction of MPP+ transport while OCT1 silencing was ineffective. At 100 µM MPP+ both OCT1 and OCT3 siRNA caused a modest (about 30%) although significant inhibition of the transport. These results confirm the contribution of both OCT1 and OCT3 to MPP+ transport in Calu-3 cells.

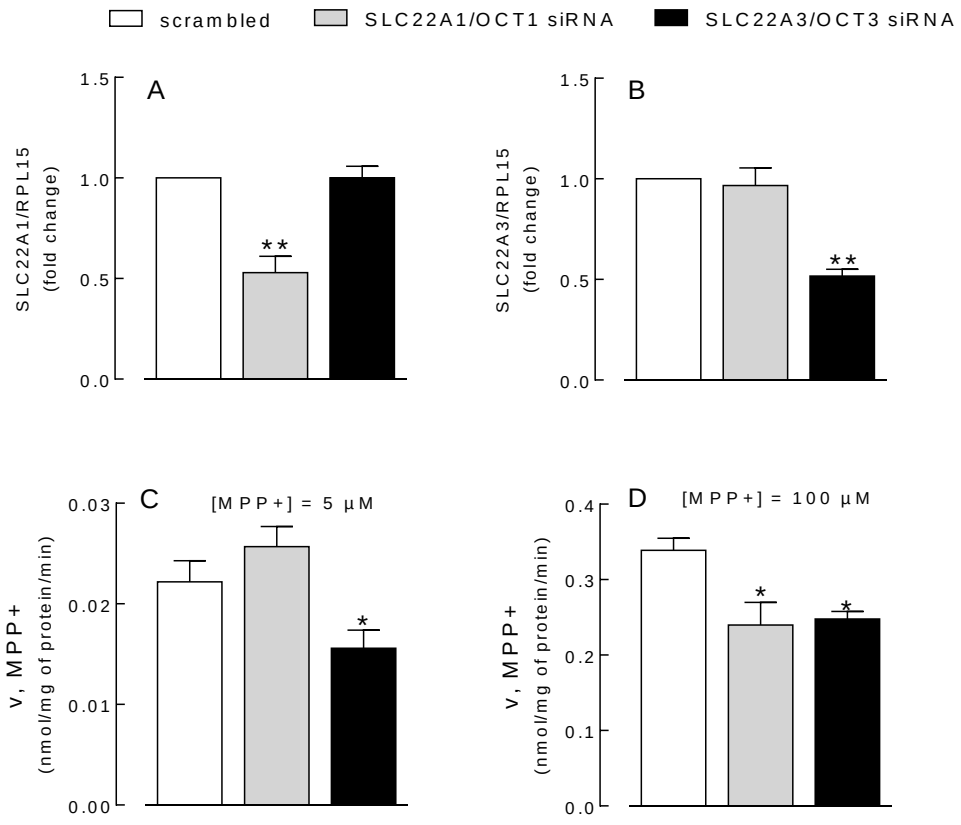

Figure 15. SLC22A1/OCT1 and SLC22A3/OCT3 silencing in Calu-3 cells.

Calu-3 cellswere transfected with scrambled, SLC22A1/OCT1 or SLC22A3/OCT3 siRNA for 96 h, as described inMaterial and methods. Panels A and B. Relative expression of SLC22A1/OCT1 and SLC22A3/OCT3 mRNA assessed by qRT-PCR and shown relatively to that of scrambled transfected cells (=1). Data are means ± S.E. of three separate determinations, each performed in duplicate. **p b 0.01 vs scrambled transfected cells. Panels B and C. The uptake of [3H]MPP+ at 5 µM (panel C) or 100 µM (panel D) was measured. Data are means ± S.E. of two independent experiments, each performed in quadruplicate. *p b 0.05 vs scrambled siRNA.

2.5 Characterization of MPP+ transport in bronchial BEAS-2B epithelial cells

The characterization of MPP+ transport has been performed also in a model of immortalized epithelial cells derived from normal lung (BEAS-2B). Panel A of figure 16 shows that also in these cells MPP+ transport is saturable and almost linear for 60 min. Kinetic analysis performed both in the absence and in the presence of extracellular sodium revealed the presence of at least two saturable transport components, one displaying a very high-affinity for the substrate (Km ≤ 1 µM) and the other with a lower affinity (Km of ~0.1 mM). Both components are endowed with fairly low values of Vmax (0.0025 and 0.045 nmol/mg of protein/min, respectively). The inhibition analysis has been, hence, performed at two different concentration of MPP+, so as to properly identify these components. Both at 1 µM (panel C) and 50 µM (panel D) MPP+ corticosterone and quinidine significantly inhibited MPP+ transport, with a higher effect of corticosterone at the lowest concentration and a predominant effect of

quinidine at 50 μM MPP+. PGE2 was ineffective. These results point to OCT3 and OCT1 as transporters for MPP+ in BEAS-2B cells.

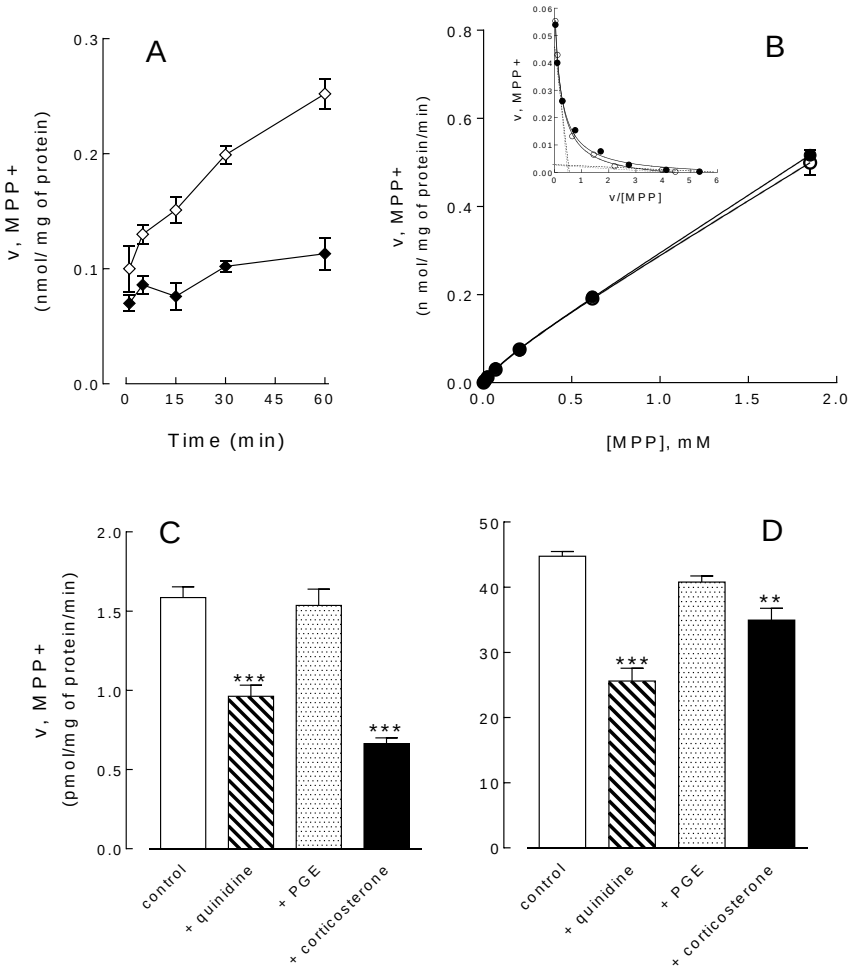

Figure 16. Characterization of MPP+ uptake in BEAS-2B cells.

Panel A. BEAS-2B cells were incubated for the indicated times in the transport buffer (see Material and methods) containing [^{3}H]MPP+ (10 μM; 2 μCi/ml) (open symbols). Non-specific binding of the substrate was estimated by measuring [^{3}H]MPP+ uptake in the presence of an excess of unlabelled substrate (2mM, filled symbols). Each point represents the mean ± S.D. of four independent determinations. Panel B. Cells were incubated in the presence of the indicated concentrations (from0.8 to 1850 μM) of [^{3}H]MPP+ (2 μCi/ml) for 15min in the absence (open symbols) or in the presence (filled symbols) of Na+. Nonlinear fitting of the data was performed employing Eq. (2) (see Material and methods). Insert shows the Eadie–Hofstee transformations of the saturable uptake (obtained after subtraction of the diffusive component estimated by the nonlinear fitting). Curves represent the nonlinear fitting of the data. Straight lines are drawn employing the values of the kinetic parameters given by nonlinear regression. Points are mean ± S.D. of three independent determinations. The experiment has been repeated twice with comparable results. Panels C and D. Cells were incubated for 15 min in the transport buffer containing 1 μM(panel C) or 50 μM (panel D) [^{3}H]MPP+(2 μCi/ml) in the presence of the indicated concentrations of the inhibitors. Each point represents themean±S.D. of four independent determinations. The experiment has been repeated three times with comparable results.

3. DISCUSSION

The aim of the first part of this research project was to define the functional activity and the expression of organic cation transporters (OCTs) in in vitro pulmonary cell models, that could ultimately be employed for studies concerning drug transportation in the lung. In this context, clear-cut differences have been highlighted at functional level among the considered human airway epithelial cell models. In particular, A549 cells appear the ones displaying the more sustained uptake of MPP+, which is mediated by a single high-affinity transporter, as indicated by the results of the kinetic analysis (Figure 6). The inhibition analysis of MPP+ uptake reveals the efficacy of the sole corticosterone, with a Ki value consistent with the affinity of corticosterone for OCT3 [99]. Moreover the use of specific siRNA targeting SLC22A3/OCT3 confirms that this is the transporter functionally operative in MPP+ uptake in A549 cells. In support of functional data, mRNA expression shows that only OCT3 is clearly expressed in these cells. The results are in line with previous findings by other groups [113, 114], while different conclusions have been reached by Salomon et al. when addressing OCT transport activity employing the fluorescent organic cation 4-(4-(dimethylamino)styryl)-N-methylpyridinium iodide (Asp+) as substrate [109]. The authors stated, indeed, that Asp+ uptake was higher in A549 than in other cell types (Calu-3, 16HBE14o- and Caco-2 cells), a result in agreement with our data with MPP+; however, their kinetic analysis indicated the involvement of two different transport components, and both OCT2 and, probably, OCT3 were found active in these cells. We can presume that these discrepancies are likely due to a different specificity of MPP+ and Asp+ towards OCTs, since the first is a specific substrate of OCTs, while different transporters, such as OCTN, may be involved in Asp+ uptake, as demonstrated by the same authors [109].

Data obtained in Calu-3 cells point, instead, to the involvement of more than one transporter in MPP+ uptake. Kinetic analysis indicates the contribution of two saturable components to total uptake, with a high (K_m < 20 μM) and a low (K_m > 0.6 mM) affinity for the substrate. The elaboration of the kinetic parameters allowed us to estimate the relative contribution of the two transport components at any concentration of substrate (Figure 9), that in turn enabled the selection of the optimal discriminating conditions for the inhibition analysis: at low concentrations of MPP+, the contribution of the high affinity component appears largely predominant, and the inhibition by corticosterone identifies OCT3 as the high affinity transporter (Figure 10, left). Conversely, when MPP+ transport is measured at higher concentration (100 μM), where the low affinity component becomes predominant, the inhibition by quinidine increases, pointing to OCT1 as the low affinity transporter (Figure 10, right). The use of specific siRNA confirmed these findings (Figure 15). mRNA expression (Figure 13) excludes the presence of OCT2 in these cells, in line with previous observations by other groups [109, 115, 116]. Moreover, the pH-independency and the lack of inhibition of carnitine and ergothioneine on MPP+ transport, allow excluding the contribution of MATE1 and OCTNs to the transport of

MPP+ in this cell model. We conclude that OCT1 and OCT3 are the ones functionally active in Calu-3, both when unpolarized (i.e. grown on plasticware) and polarized (i.e. grown under air–liquid interface condition, ALI). As far as this latter condition is concerned, we next addressed the cellular localization of the transporters, basolateral rather than apical, an issue, thus far, only roughly defined. To this concern, permeation approaches performed by Mukherjee et al., by employing Asp+ as substrate, suggested the presence of an OCT activity only at the apical side of Calu-3 cells; since the dye was not significantly transported across the monolayers from the apical into the basolateral compartment of the transwell chambers, they excluded OCT activity at the basolateral side of the cells [116]. Conversely, a similar study by MacDonald et al. showed that Asp+ is not only actively taken up at both sides of the cells, but it is also transported across the monolayer with a flux from apical versus basolateral significantly higher than the opposite [115]. Accordingly, our results in Calu-3 ALI indicate a bi-directional transfer of MPP+ into the opposite compartment, which is mediated by both OCT1 and OCT3 at the apical and by OCT3 at the basolateral side of the monolayer.

As far as NCl-H441 cells are concerned, results obtained appear peculiar, since only OCT1 is expressed and a very modest saturable uptake of MPP+ is measurable. Accordingly, results of the kinetic analysis clearly indicate that MPP+ uptake is mediated by a single saturable component endowed with a relatively high affinity (Km =180 μM) and a very low value of Vmax (about ten times lower than that measured in A549 cells). The transport activity could be, hence, ascribed to a non-saturable, rather than to an active component; however, the modest, but significant, inhibitory effect of quinidine and the lack of inhibition by corticosterone and PGE2 confirm that OCT1 is responsible of MPP+ uptake in NCl-H441 cells. Recently, Salomon et al. reported a Km in the similar order of magnitude (881.2 ± 195.3 μM) and a Vmax much higher than our (2.07 ± 0.26 nmol/min/mg protein) for Asp+ uptake [110].Whether these differences could be explained by the involvement of other transporters or by a different specificity of the two substrates employed remains to be established. Finally, we present here for the first time, a functional characterization of MPP+ transport in a model of immortalized human bronchial epithelial cells (BEAS-2B), a line of cells obtained from normal lung.

Overall, these results are of particular relevance for the definition of the operative features of OCT transporters in organotypic in vitro models of human respiratory epithelium. Clear cut differences have been detected among the considered airway epithelial cells as far as OCT expression and activity are concerned. In particular A549 and NCl-H441 cells appear suitable models for the study of drug interaction with the sole OCT3 or OCT1, respectively . Conversely, the simultaneous contribution of OCT1 and OCT3 to cationic drug transport is appreciable in Calu-3 and BEAS-2B cells. All the cell models employed are unusable for studies of drug interaction with OCT2, due to its lack of expression.

These findings are summarized in figure 17, and they can help to identify the proper in vitro model for researches of drug absorption and disposition.

Figure 17. Graphical abstract

Proposed contribution of OCT1-3 for MPP+ uptake in airway epithelial cells (modified from Ingoglia et al. 2015 [117])

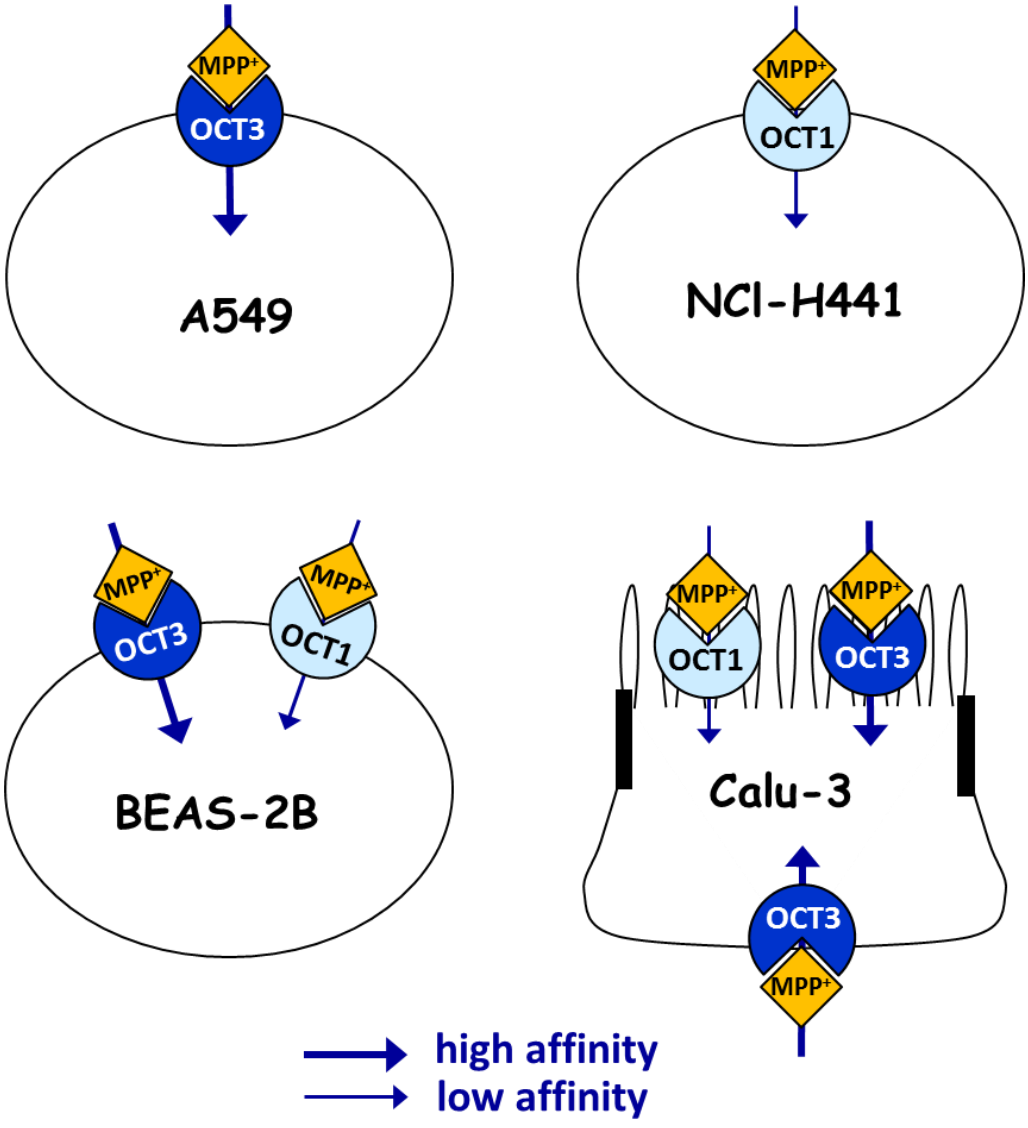

Chapter IV – CARNITINE AND OCTNs IN HUMAN AIRWAY EPITHELIAL CELLS

1. INTRODUCTION

L-Carnitine (3-hydroxy-4-N,N,N-trimethylaminobutyrate) is a quaternary amine synthesized from the essential amino acids lysine and methionine. L-carnitine is intimately involved in the transport of long chain fatty acids across the inner mitochondrial membrane as acyl-carnitine esters, thereby promoting their β-oxidation. Hence, it plays a critical role in the modulation of energy metabolism for tissues that derive a substantial portion of their metabolic energy from fatty acid oxidation, such as the heart, skeletal muscle, liver, placenta.
Inherited defects of all the steps involved in carnitine cycle are transmitted as autosomal recessive traits in humans, confirming the biological relevance of this molecule at both patho- and physiological level [118]. Carnitine cannot be strictly considered an essential nutrient in healthy adults, since it can be both synthesized endogenously by human liver, kidney, and brain [119] and absorbed in the intestinal tract from dietary sources [120].

Appropriate systemic and tissue concentrations of carnitine are mainly maintained by membrane transporters that regulate intestinal absorption, tissue distribution, and renal reabsorption/excretion [121]. Three plasma membrane transporters of carnitine have been identified in human to date, i.e. novel organic cation transporters (OCTNs) OCTN1 (SLC22A4),OCTN2 (SLC22A5), and CT2 (SLC22A16) [99]. In normal tissues, however, only OCTN1 and OCTN2 are ubiquitously expressed, while CT2 is primarily expressed in the testis, kidney, and hematopoietic cells [122].

OCTN1, which is strongly expressed in renal epithelium and, at a lower level, in a wide variety of tissues and cell lines of human origin [72], mediates a bidirectional organic cation transport in a pH-dependent manner [123]. In intact cell systems, it was initially proposed that the model substrate for this transporter is tetraethylamonium (TEA) [70]. More recently, it has been found that, under physiological conditions, OCTN1 is involved in the intracellular accumulation of the mushroom metabolite ergothioneine (ET), an antioxidant which is now considered its specific substrate [73, 124]; it is also involved in the transport of acetylcholine [125] and in the excretion of cationic xenobiotics from renal epithelium [72, 123].

Despite that OCTN1 could transport carnitine [28, 29, 123], the main role in the maintenance of carnitine homeostasis is played by OCTN2 which is involved in intestinal absorption, distribution to tissues, and renal excretion/reabsorption. OCTN2 expression is not limited to polarized cells of intestine, kidney, placenta, and mammary gland but has been found in many other tissues such as liver, heart, testis, skeletal muscle, lung and brain, guaranteeing

carnitine absorption and distribution within the entire organism [126]. OCTN2 catalyzes a Na^+-dependent high-affinity transport with apparent Km ranging between 8 and 80 μM, depending on the tissue [125].

Functional defect of OCTN2 due to genetic mutations causes systemic primary carnitine deficiency (CDSP, MIM 212140), an autosomal recessive disorder characterized by urinary carnitine wasting, that results in low serum carnitine levels and decreased intracellular carnitine accumulation [118, 127], with consequent impairment of fatty acid oxidation. The clinical presentation of the disease may include failure to thrive, respiratory insufficiency, vomiting, progressive cardiomyopathy, skeletal myopathy, hypoglycemia, and hyperammonemia [84]. Since CDSP patients respond to carnitine supplementation, it has been postulated that intracellular carnitine supply in these cases can be performed by transporters other than OCTN2; among them, the amino acid transporter $B^{0,+}$ ($ATB^{0,+}$) has been described to perform a low-affinity transport of L-carnitine (Km ~ 800 μM). This transporter exhibits much higher concentrative capacity than OCTN2 because of its energization by transmembrane gradients of Na^+ and Cl^-, as well as by membrane potential [128]. $ATB^{0,+}$ is principally expressed in intestine, lung, and mammary gland and belongs to the gene family of Na^+- and Cl^-- coupled transporters for a variety of compounds, such as amino acids, neurotransmitters, and osmolytes.

In airways, OCTNs are highly expressed at the apical side of airway epithelial cells in tracheal tissue, as well as in alveolar epithelial cells [72, 79, 129]. In these latter cells, carnitine is involved in the production of pulmonary surfactant [130], the mixture of phospholipids, cholesterol, and proteins that reduces the surface tension at the air–liquid interface of the lung, preventing alveolar collapse and allowing for normal gas exchange. At early stages of life, carnitine biosynthesis is less efficient than in adults and preterm neonates do not synthesize sufficient amounts of carnitine with respect to term infants [131]. Antenatal carnitine administration has been, hence, proven effective in inducing pulmonary surfactant production and lung maturation in both fetal rats and humans [130, 132]; in addition, Ozturk et al. reported that exogenous carnitine supply to mothers who have the risk of premature delivery and to the preterm newborns might prevent or decrease the severity of respiratory distress syndrome (RDS) [133], the most severe complication observed in preterm infants and the most frequent cause of mortality of immature infants.

L-carnitine supplementation can also be important for other lung diseases. In chronic obstructive pulmonary diseases (COPD) patients, L-carnitine administration can improve exercise tolerance and inspiratory muscle strength [134]. It has been also noted that L-carnitine reduces leukotriene synthesis through inhibition of lipoxygenase enzyme [135] and improves the pulmonary function test of children with moderately persistent asthma [136].

Thus far, little is known about the functional operation of carnitine transporters in the airways.

The aim of the second part of this research project is, therefore, to characterize carnitine transport mechanisms in cell models of human airway epithelium, i.e. tracheobronchial Calu-3 and BEAS-2B, bronchiolar-alveolar NCI-H441 and alveolar type II A549 cells.

2. RESULTS

2.1 Time-dependent accumulation of L-carnitine in A549, BEAS-2B, Calu-3 and NCI-H441 cells

The time course analysis of 1 µM L-[^{3}H]carnitine uptake was performed in the four cell lines. As shown in figure 18, substrate uptake increased in a time-dependent manner and was linear up to 3 h in all cell models. Moreover, it appeared strictly Na^+-dependent, being completely abolished by the replacement of extracellular sodium with N-methyl-D-glucamine (NMDG). The rate of L-carnitine transport was maximal in BEAS-2B cells, with A549 and Calu-3 following; NCIH441 cells displayed a modest uptake of L-carnitine, with rate values ten times lower than those observed in BEAS-2B cells. Moreover, in A549 and BEAS-2B an excess of unlabelled carnitine completely suppressed the transport, while a residual activity was still detectable in both Calu-3 and NCI-H441 cells under the same conditions. An incubation time of 30 min was hereafter used for the measurement of L-[^{3}H]carnitine uptake.

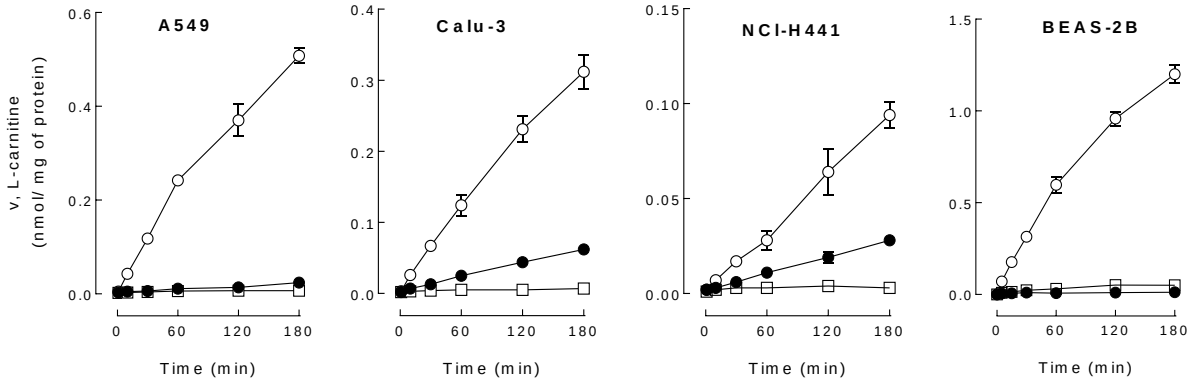

Figure 18. Time-dependent accumulation of L-carnitine in A549, Calu-3, NCI-H441, and BEAS-2B cells. Cells were incubated for the indicated time in transport buffer (see Materials andmethods) containing L-[^{3}H]carnitine (1 µM; 2 µCi/ml), in the presence (open circles) or in the absence of Na+ (open squares). For Na+-free buffer, NaClwas replaced by an equimolar concentration of N-methyl-D-glucamine chloride. Non-specific binding of the substratewas estimated by measuring the uptake of L-carnitine in the presence of an excess of unlabelled substrate (2mM) (filled circles). Each point represents the mean ± S.D. of four independent determinations. The experiment has been repeated three times with comparable results.

2.2 Kinetic analysis of L-carnitine uptake

We next examined the concentration dependent uptake of L-carnitine over a wide range of substrate concentrations (from 0.00049 to 1.85 mM). Results of the Na+-dependent uptake are shown in figure 19. In A549 and BEAS-2B cells the value were best fitted by Equation 1 (see Materials and Methods) and the resulting kinetic parameters revealed the operation of one high-affinity transport system (Km of 1.7 and 3.3 µM, respectively). Consistently, the Eadie-Hofstee plots of the data (inserts) were linear, confirming the operation of a single transporter in both models. On the contrary, in Calu-3 cells L-carnitine transport data were best fitted by Equation 2, revealing the presence of two saturable transport components, one displaying a high-affinity for the substrate (Km = 25 µM) and the other with a low-affinity (Km > 1 mM). Accordingly, the regression analysis of the Eadie-Hofstee plot for carnitine in these cells (insert) appeared nonlinear, confirming the involvement of at least two different transporters. Also in NCl-H441 cells, transport data were best fitted by Equation 2 for an high and a low affinity component. This latter model presented kinetic features very similar to those of Calu-3. A complete description of the apparent kinetic parameters obtained in all cell models is shown in Table 5.

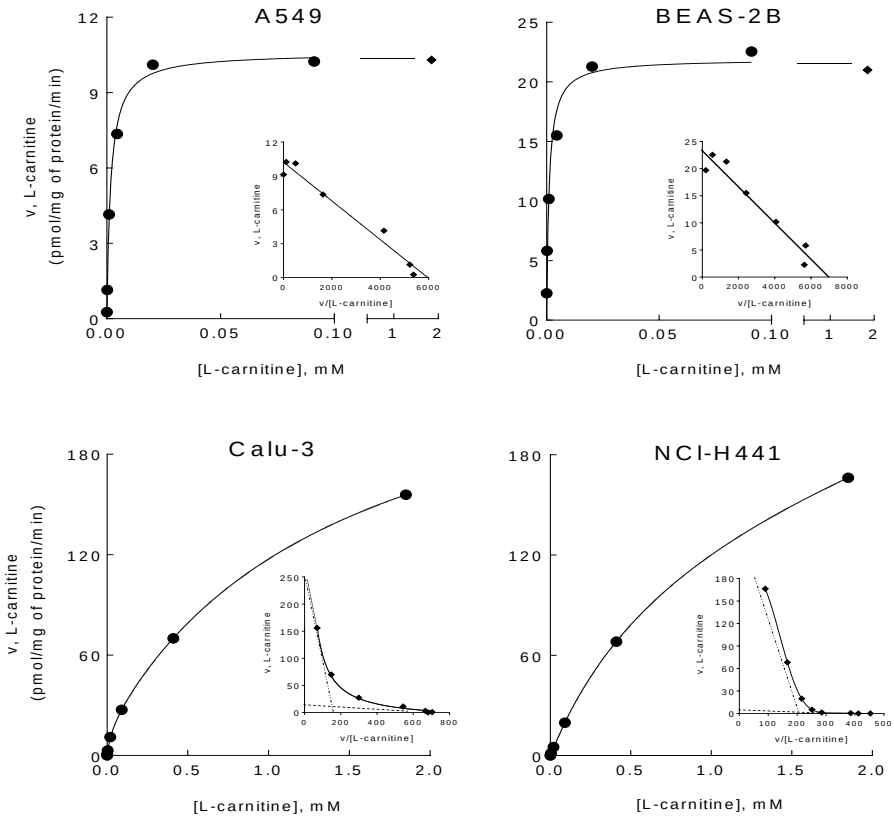

Figure 19. Kinetic analysis of L-carnitine uptake in A549, Calu-3, NCl-H441, and BEAS-2B cells.

Cells were incubated in the presence of the indicated concentrations (from0.49 µM to 1.85mM) of L-[^{3}H]carnitine (2 µCi/ml) for 30min, either in the presence or in the absence of Na+ (not shown). The plot shows the Na+-dependent component, calculated by subtracting transport data obtained in the absence from those in the presence of Na+. Insert in each panel shows the Eadie–Hofstee transformations of the data. Points are mean ±S.D. of three independent determinations. The experiment has been repeated twice with comparable results.

Table 5. Kinetic parameters describing the uptake of carnitine.
Data have been estimated from the nonlinear regression analysis shown in figure 19, employing Equation 1 for A549 and BEAS-2B and Equation 2 for Calu-3 and NCI-H441.

	High affinity		Low affinity	
	K_{m1} μM	V_{max1} pmol/mg of protein/min	K_{m2} μM	V_{max2} pmol/mg of protein/min
A549	1.72 ± 0.3	10.23 ± 0.43		
BEAS-2B	3.2 ± 0.4	23.21 ± 0.68		
Calu-3	25.7 ± 1.4	10.7 ± 0.49	1470 ± 250	251.2 ± 15.6
NCI-H441	12.7 ± 4.1	4.53 ± 0.28	1251 ± 10.8	247.7 ± 5.48

2.3 Expression of carnitine transporters

The expression of SLC22A4/OCTN1, SLC22A5/OCTN2, and SLC6A14/ ATB0,+ has been next evaluated in A549, NCI-H441, Calu-3, and BEAS-2 cells, in terms of both mRNA (Figure 20, panel A) and protein (panel B) level. OCTN1 was expressed in all cell models, although less abundant in NCI-H441; ATB0,+ was maximally expressed in Calu-3 cells with NCI-H441 following and only barely detectable in A549 and BEAS-2B. The expression of OCTN2 was clearly evident in all cell models.

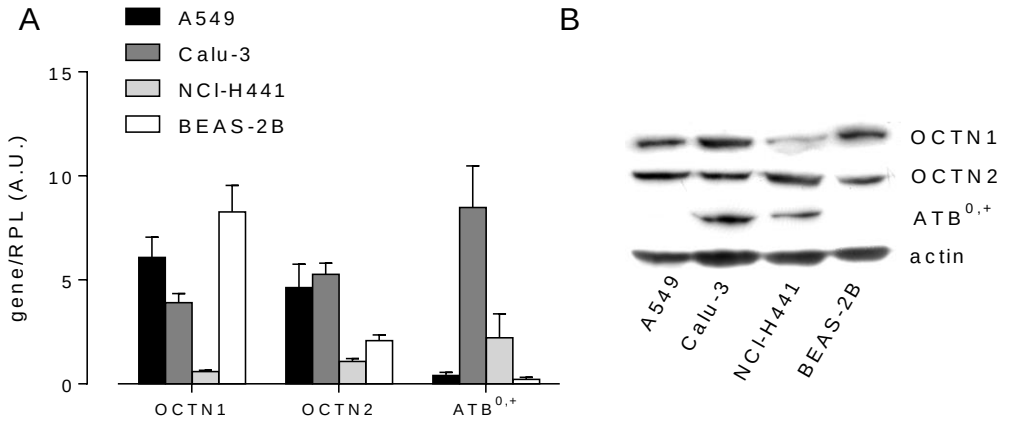

Figure 20. Expression of OCTNs and ATB0,+ in A549, Calu-3, NCI-H441, and BEAS-2B cells.

Panel A. mRNA levels for OCTNs and $ATB^{0,+}$were determined through RT-qPCR analysis. After normalization to RPL-15, the expression of SLC22A4/OCTN1, SLC22A5/OCTN2, and SLC6A14/ATB0,+ was expressed as the ratio between the expression of the gene of interest and that of the housekeeping gene in each cell model. Data are means ± S.E. of three experiments, each performed in duplicate. Panel B. Protein expression was evaluated in total cell lysates, as described in Materials and methods. A representative Western blot is shown. The experiment was repeated twice with comparable results.

2.4 Inhibition analysis of L-carnitine uptake

In order to better address the specific transporters involved in L-carnitine uptake in the different cell models, the uptake of the substrate was measured in the presence of different organic cationic and zwitterionic compounds (Figure 21). In A549 and BEAS-2B, L-carnitine uptake was maximally inhibited by betaine (substrate of OCTN2) and, to a less extent, by TEA (substrate of OCTN1/2). Ergothioneine (ET), the specific high-affinity OCTN1 substrate [73], was ineffective at 100 μM, while, at higher concentrations (1 mM), caused a significant inhibition of carnitine uptake in both cell models; on the contrary, the cationic amino acid arginine, as well as the neutral amino acids leucine and proline, were completely ineffective. The absence of chloride in the transport buffer did not affect carnitine uptake in these cell models, hence excluding the contribution of $ATB^{0,+}$. In Calu-3 cells, leucine showed the strongest inhibitory effect (more than 60%) among the compounds tested, with arginine following; also, betaine produced a significant inhibition of L-carnitine uptake (about 50%), while TEA and ET (at both concentrations) were ineffective. Carnitine transport was significantly inhibited by the use of Cl^-–free buffers. The pattern of inhibition in NCl-H441 cells appeared completely comparable to that of Calu-3 cells, since the effects of the different compounds were overlapping. Overall these results point to the operation of OCTN2 in all cell models and to the further contribution of $ATB^{0,+}$ in Calu-3 and NCl-H441 cells. On the other hand, the inhibitory effect of 1 mM ET in A549 and BEAS-2B cells could suggest the involvement of OCTN1 in carnitine uptake.

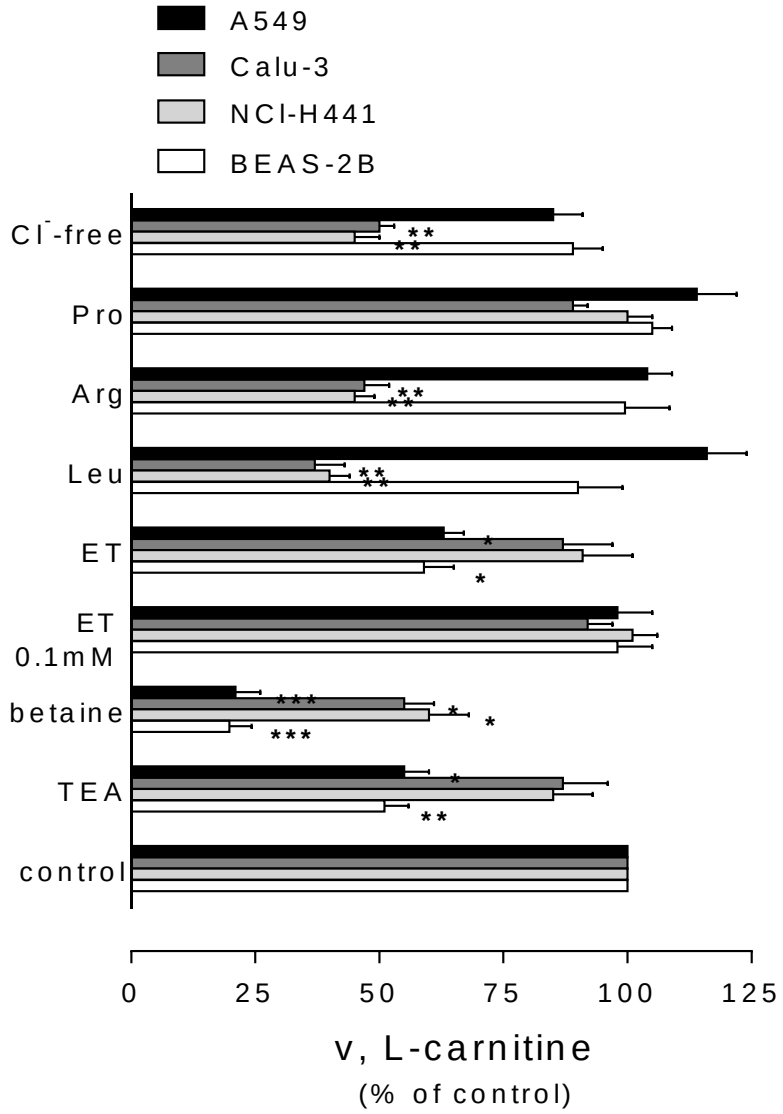

Figure 21. Inhibitory effect of organic cationic and zwitterionic compounds on L-carnitine uptake in A549, Calu-3, NCI-H441, and BEAS-2B cells. The uptake of L-[3H]carnitine (30 min; 1 μM; 2 μCi/ml) was determined in the absence (control) or in the presence of the listed compounds (all tested at the concentration of 1 mM, except for ergothioneine, also used at 0.1 mM). The effect of the Cl-free buffer was evaluated by substituting chloride with gluconate, as described in Materials and methods. The inhibitory effect of each compound is calculated as the residual amount of L-carnitine uptake, expressed as percent of control. Values are mean ± S.E. of three experiments each performed in triplicate.
*p < 0.05, **p < 0.01, ***p < 0.001 versus control with ANOVA.

To verify this hypothesis, an inhibition analysis of L-carnitine uptake by betaine and ET was performed in these cells (Figure 22, panel A). Results obtained indicated that in A549, both compounds inhibited substrate uptake in a dose-dependent manner, with betaine being more effective (Imax=99.6±8%) than ET (Imax=85±15%). The concomitant presence of the two inhibitors, while did not change the maximal inhibition obtained by betaine alone, shifted the inhibition curve towards left. Indeed, the I0.5 value calculated upon simultaneous addition of ET and betaine was the half of that obtained with the sole betaine, (from 0.58±0.1 to 0.27±0.04mM), demonstrating that the two compounds interact with the same transporter, presumably OCTN2. In BEAS-2B, the effect of ET was negligible at low concentrations, while becoming evident at 1mM; also, in these cells, however, the addition of ET to betaine modified only the value of I0.5 (from 0.117mM in the presence of betaine to 0.063mMin the presence of betaine + ET), without affecting the Imax values (84.2% in the presence of betaine and 82.8% in

the presence of betaine + ET). These data suggest that in A549 and BEAS-2B cells, only OCTN2 is operative and point to ergothioneine, when employed at high doses, as a substrate for this transporter. The results shown in figure 22 (panel B) by employing CHO cells transfected with OCTN2 (CHO-OCTN2) confirmed this hypothesis, since 1 mM ET significantly inhibited carnitine transport, confirming that, at high doses, ET also interacts with OCTN2 transporter.

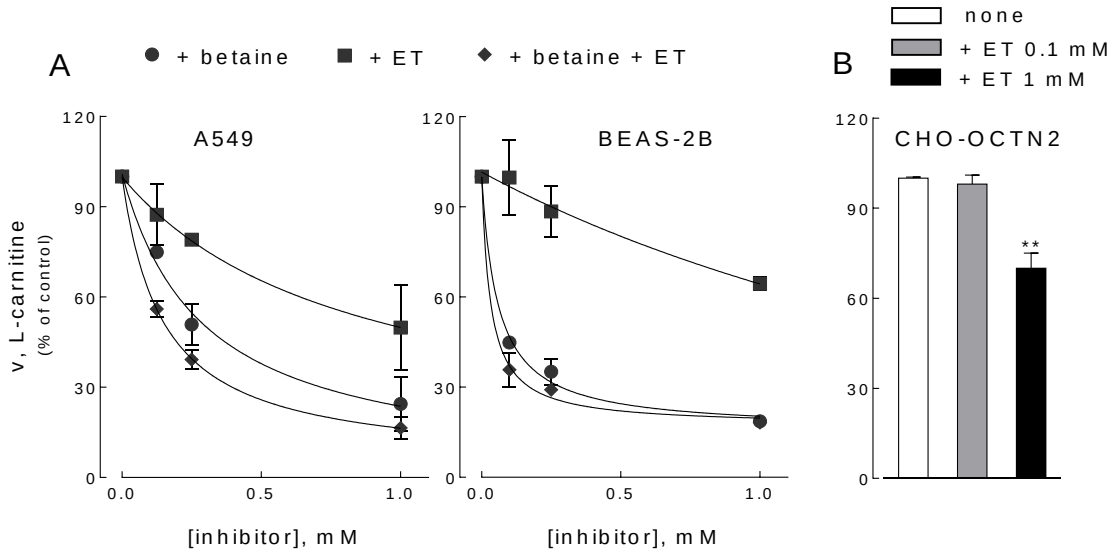

Figure 22. Inhibition of L-carnitine uptake by betaine and ergothioneine.

A549 and BEAS-2B (panel A) and transfected CHO-OCTN2 (panel B) cells were incubated for 30 min in the transport buffer containing L-[^{3}H]carnitine (1 μM; 2 μCi/ml) in the absence (none, control) or in the presence of the indicated concentrations of inhibitor. Each point represents the mean ± S.D. of four independent determinations. Data in panel A were fitted by Eq. (3) (see Materials and methods). The experiment has been repeated three times with comparable results. **p < 0.01 versus control (none).

In Calu-3 and NCI-H441 cells, the inhibition analysis of 1 μM L-carnitine uptake was carried out employing betaine and leucine as inhibitors. Data shown in figure 23 indicate that the inhibitory profile of these compounds is comparable. In Calu-3, the maximal inhibition was 58.4 ± 3.9% and 50.8 ±2.5% for leucine and betaine, respectively, when added individually; when present in combination, the effects of the inhibitors were additive, with a maximal inhibition up to 85.2 ± 1.9%. Comparable effects were observable in NCI-H441. The inhibitory profile obtained suggests that L-carnitine transport in these cell models is mediated by OCTN2 and by $ATB^{0,+}$, a Na^+- and Cl^--coupled transport system for neutral and cationic amino acids; more precisely, it is likely to assume that OCTN2 accounts for the high affinity component,while $ATB^{0,+}$ represents the low-affinity transporter for L-carnitine uptake.

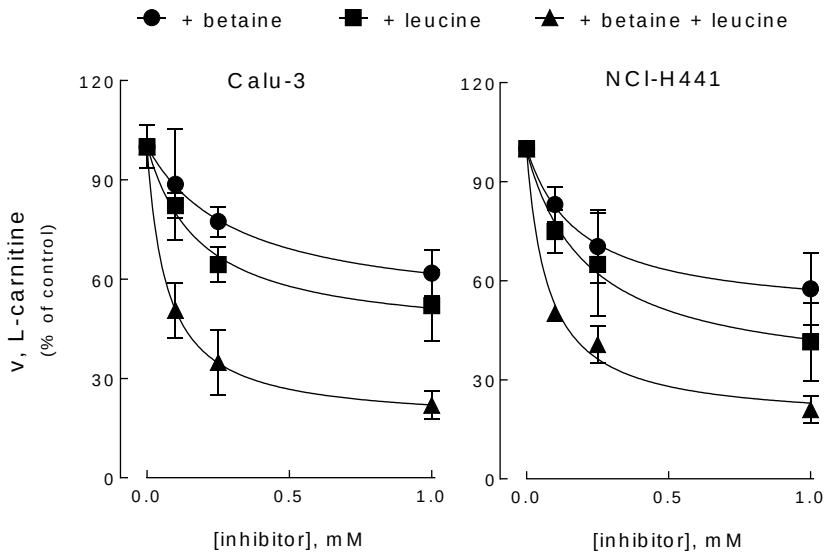

Figure 23. Inhibition of L-carnitine uptake by betaine and leucine in Calu-3 and NCI-H441 cells.

Cellswere incubated for 30min in the transport buffer containing L-[^{3}H]carnitine (1 μM; 2 μCi/ml) with the indicated concentrations of inhibitor. Each point represents the mean ± S.D. of four independent determinations. Data were fitted by Eq. (3) (see Materials and methods). The experiment has been repeated three times with comparable results.

2.5 Carnitine transport in silenced cells

In light of these results, we next employed short interfering RNA (siRNA) to define the operation of the different transporters. In A549 (Figure 24, upper panels), an almost complete suppression of SLC22A5/OCTN2 (80%) was reached after 72 h of incubation (panel A), when a marked reduction of transport activity (>70%) was observed (panel B). Upon SLC22A5/OCTN2 silencing, betaine almost completely lost its inhibitory effect (panel C). Indeed, the inhibition curves obtained in scrambled and SLC22A5 silenced cells were significantly different ($p < 0.01$), with the Imax dropping from 9.8 ± 1 to 2.1 ± 0.2 and I0.5 from 0.55 ± 0.1 to 0.15 ± 0.06, respectively. These results, beside confirming the prevalent operation of OCTN2 in A549 cells, also validate the efficacy of betaine as inhibitor of OCTN2. A less efficient silencing of SLC22A5/OCTN2 (about 40%)was obtained in BEAS-2B (Figure 23, panel D), which caused, however, a significant reduction of carnitine transport referable to a decrease of the betaine-sensitive quote (panel E).

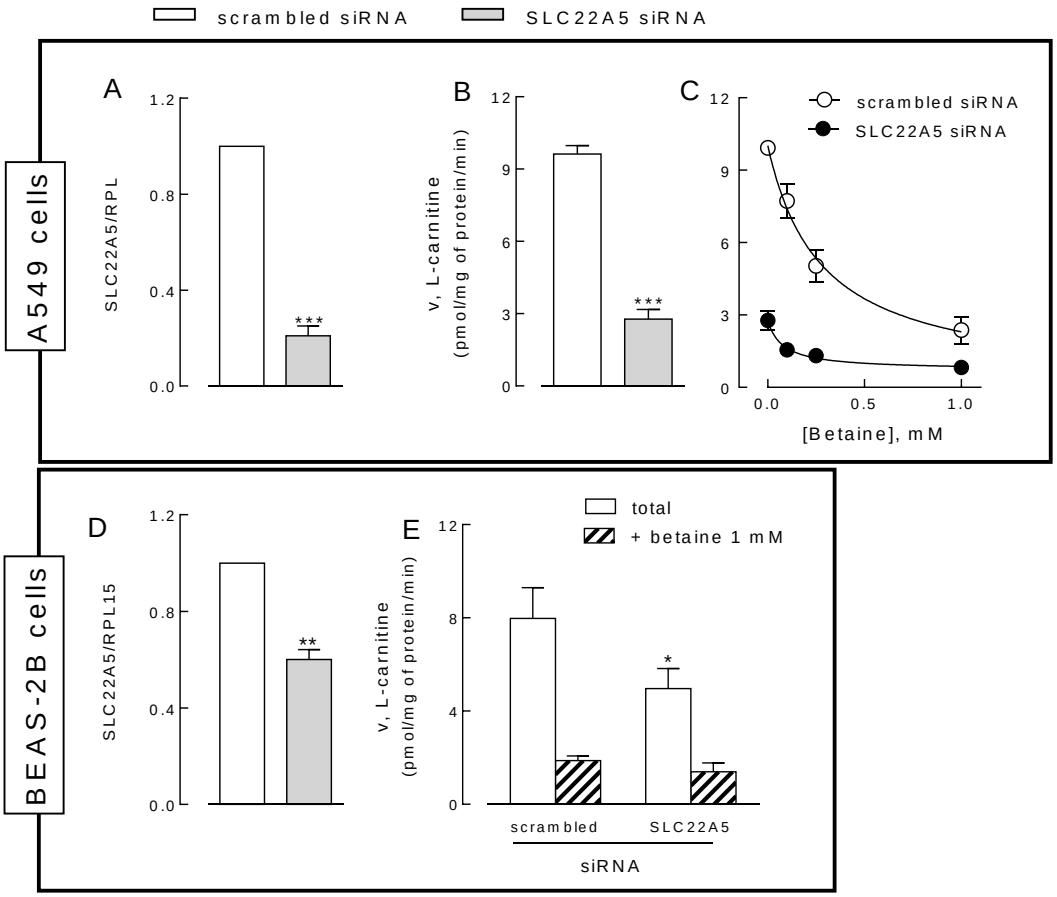

Figure 24. SLC22A5/OCTN2 silencing in A549 and BEAS-2B cells.

A549 (panels A, B, and C) and BEAS-2B (panels D and E) were transfected with scrambled or SLC22A5/OCTN2 siRNA for 72 h, as described in Materials and methods. Panels A and D. The expression of SLC22A5/OCTN2 mRNA in silenced cells was assessed by qRT-PCR and shown relatively to that observed in scrambled transfected cells (=1). Data are means ± S.E. of three separate determinations, each performed in duplicate. Panel B. The uptake of L-[^{3}H]carnitine (30 min; 1 μM; 2 μCi/ml) was measured in cells transfected with scrambled or SLC22A5/OCTN2 siRNA. Data are means ± S.E. of three independent experiments, each performed in quadruplicate. Panels C and E. Transfected cells were incubated for 30 min in the transport buffer containing L-[^{3}H]carnitine (1 μM; 2 μCi/ml) with the indicated concentrations of betaine. Each point represents themean ± S.D. of four independent determinations. The experiments have been repeated twice with comparable results. *p < 0.05, **p < 0.01, ***p < 0.001 vs scrambled transfected cells, with Student's t test. Data in Panel C were fitted by Eq. (3) (see section Materials and methods); differences between curves were statistically significant comparison of fits, seeMaterials and methods; **p < 0.01).

In both Calu-3 and NCl-H441 cells, also SLC6A14/ATB0,+ was silenced beside SLC22A5/OCTN2 (Figure 25). The expression of both genes was markedly reduced (panels A and C) and, consistently, carnitine transport was lowered (panels B and D). In particular, a 60% and 50% reduction of SLC22A5 and SLC6A14, respectively, caused a decrease of about 40% of carnitine transport in Calu-3 cells. In NCl-H441, a 40% reduction of the expression of both genes caused a comparable decrease of transport activity.

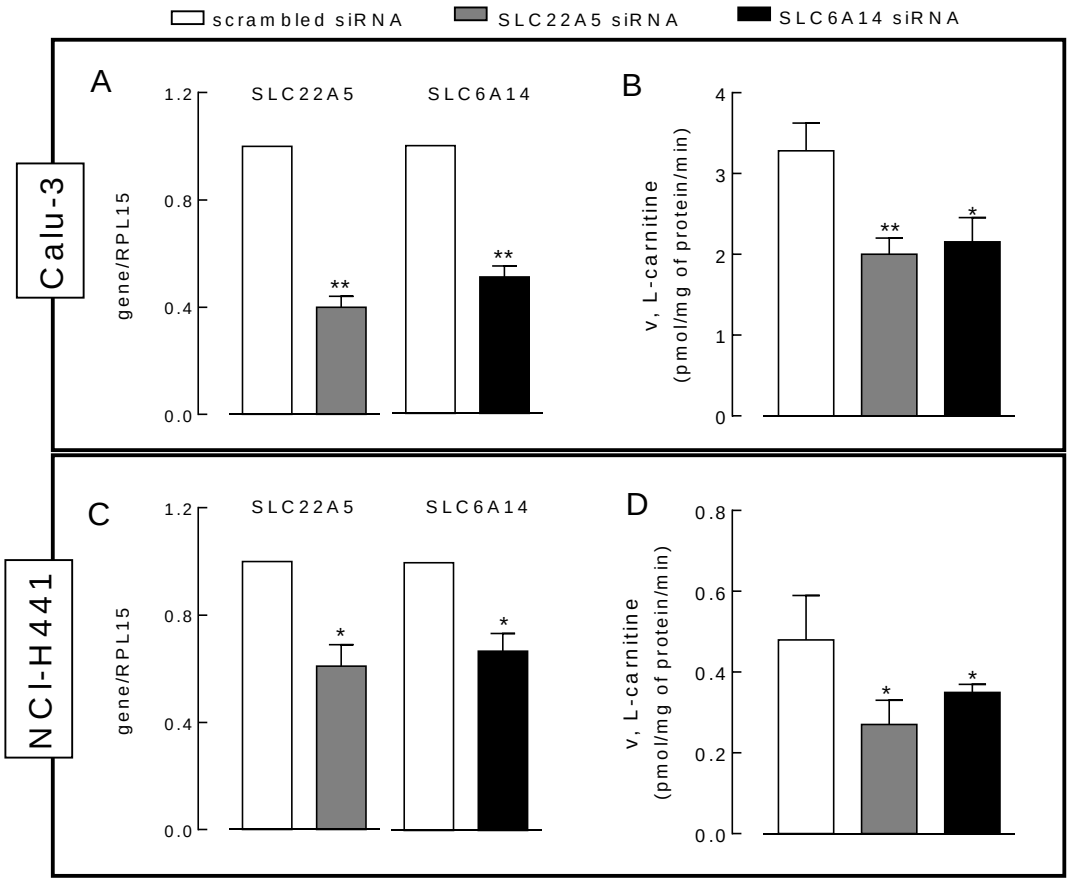

Figure 25. SLC22A5/OCTN2 and SLC6A14/ATB0,+ silencing in Calu-3 and NCl-H441 cells.

Calu-3 cells (panels A and B) and NCl-H441 (panels C and D)were transfectedwith scrambled, SLC22A5/ OCTN2 or SLC6A14/ATB0,+ siRNA for 96 h, as described in Materials and methods. Panels A and C. The expression of SLC22A5/OCTN2 and SLC6A14/ATB0,+ mRNA in silenced cells was assessed by qRT-PCR and shown relatively to that observed in scrambled transfected cells (=1). Data are means ± S.E. of three separate determinations, each performed in duplicate. Panels B and D. The uptake of L-[3H]carnitine in silenced cells was measured at 1 μM substrate. Data are means±S.E. of two independent experiments, each performed in quadruplicate. *p < 0.05, **p < 0.01, with Student's t test.

In order to assess if an impairment of the activity of the high-affinity OCTN2 transporter may differently impact on cell models that express only OCTN2 or both OCTN2 and $ATB^{0,+}$, a time course of 30 μM carnitine uptake (roughly corresponding to the plasma concentration) was performed in A549 and Calu-3 cells silenced with SLC22A5/OCTN2 siRNA (Figure 26). In A549, the intracellular concentration of carnitine was markedly reduced by OCTN2 silencing; on the contrary, in Calu-3 cells, the accumulation of carnitine, much higher than in A549 cells, was not affected by the suppression of OCTN2 transporter. These data suggest that the presence of $ATB^{0,+}$ transporter in Calu-3 cells can compensate for the lack of OCTN2 in supplying cells with extracellular carnitine.

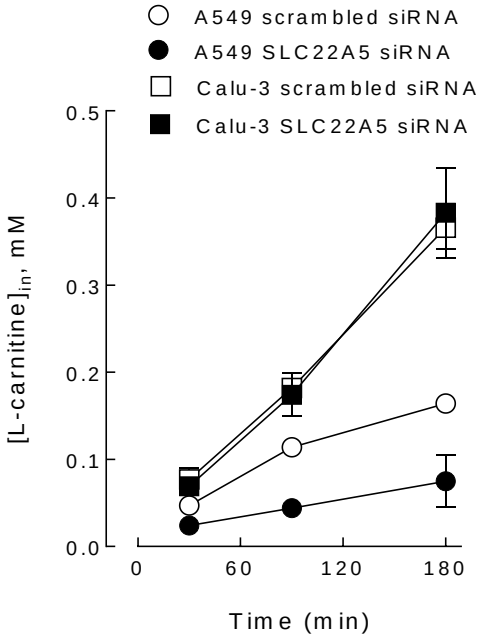

Figure 26. Time-dependent accumulation of L-carnitine in A549 and Calu-3 cells silenced with SLC22A5/OCTN2.

A549 and Calu-3 cells were transfected with scrambled or SLC22A5/ OCTN2 siRNA for 96 h, as described in Materials and methods. Cells were then incubated for the indicated time in the transport buffer (see Materials andmethods) containing L-[3H]carnitine (30 μM; 2 μCi/ml). Each point represents themean±S.D. of four independent determinations. The experiments has been repeated three times with comparable results.

3. DISCUSSION

In the second part of this research project, we performed for the first time a complete characterization of carnitine transport in human airway epithelial Calu-3, A549, NCl-H441, and BEAS-2B cells. Our results indicate that OCTN2 is the major contributor to L-carnitine uptake in A549 and BEAS-2B cells, while $ATB^{0,+}$, beside OCTN2, mediates L-carnitine transport in Calu-3 and NCl-H441 cells. Although many in vitro studies have assessed the expression of OCTN proteins in lung epithelial cell models, investigations into the functional role of these transporters are currently scarce and, in particular, the kinetic properties of carnitine transport has been not fully explored.

Despite some controversial results [137], many studies have thus far shown that OCTN1 and OCTN2 are highly expressed in the respiratory epithelium of human trachea and bronchi [54, 72, 79, 129]. In particular, both transporters have been localized at the apical membrane of differentiated epithelial cells from trachea and lung parenchima, with OCTN2 showing a

relatively stronger expression at the surface of the alveolar type I epithelium [129]. Moreover, the expression of OCTN1/2 proteins has been detected in undifferentiated Calu-3 cells by means of immunocytochemistry and Western blot [109, 115], as well as at the apical surface of Calu-3 grown under air–liquid interface conditions [116]and in NCl-H441 cells [110]. In line with these results, we show here that both OCTN1 and OCTN2 mRNA are expressed in all the cell models employed (Calu-3, A549, NCl-H441, and BEAS-2B cells), and consistently, OCTNs proteins are clearly detectable, although OCTN1 is slightly fainter in NCl-H441 (Figure 20).

Beside the expression of OCTNs, we also provide evidence for the presence of $ATB^{0,+}$ mRNA and protein in Calu-3 cells and, although to a lesser extent, in NCl-H441. This transporter, first described in human epithelial airway cells by Galietta [138], has been reported to be expressed throughout the lung [4]. Conversely, our results clearly indicate that only some airway models (i.e. Calu-3 and NCl-H441) actually express $ATB^{0,+}$, while others, such as A549 and BEAS-2B cells, do not.

In our study, the characterization of the kinetics of L-carnitine transport indicates that A549 and BEAS-2B cells display the most sustained uptake, and that this is mediated by a single high-affinity, sodium dependent transporter (Figure 19). Moreover, in light of the complete inhibition of carnitine uptake by betaine, one of the preferential substrates of OCTN2 [5], we can actually identify the only transporter operative in this model with OCTN2. Conversely, the functional characterization of L-carnitine-mediated transport in Calu-3 and NCl-H441cells reveals that besides OCTN2, also $ATB^{0,+}$ is operative in these two cell models, in line with expression profile. Indeed, the kinetic analysis indicates the involvement of two saturable components, one with a high affinity for the substrate, identifiable with OCTN2 ($Km \leq 25$ μM), and the other with a low affinity ($Km > 1.2$ mM). The marked inhibition of carnitine transport by leucine and arginine, two amino acid substrates of $ATB^{0,+}$, as well as its chloride-dependence, identify the latter component with $ATB^{0,+}$. The Km values for OCTN2 and $ATB^{0,+}$ obtained here are consistent with those reported for the corresponding transporters in other cell models [79, 128]. The estimated kinetic parameters (see Table 5) indicate that the relative contribution of OCTN2 is prevalent at low concentrations of substrate, whereas that of the low-affinity component ($ATB^{0,+}$) becomes prevalent as carnitine concentration increases. In vivo, however, it is presumable that the intracellular content of carnitine is mainly determined by the activity of OCTN2 since $ATB^{0,+}$ activity, under physiological conditions, is likely inhibited by the presence of amino acids (such as leucine, glutamine, arginine), which can compete with carnitine.

The physiological significance of $ATB^{0,+}$ transporter in the lung is to promote an efficient protein clearance through the active reabsorption of amino acids, hence playing a role of critical importance under pathological conditions associated to protein accumulation in the airway spaces, such as acute respiratory distress syndrome (ARDS) or pulmonary alveolar phospholipoproteinosis (PAP) [4]. In our contribution we demonstrate that this transporter can

operate also carnitine uptake, as already suggested by the group of Ganapathy [128]. The presence of this transporter in the cells appears of peculiar relevance in the pharmacological therapy of systemic primary carnitine deficiency (CDSP), an autosomal recessive disorder of carnitine transport caused by mutations in the SLC22A5 gene. In CDSP, functional defect of OCTN2 [118, 127] leads to low serum carnitine levels resulting in defective fatty acid oxidation responsible for the clinical manifestations. Primary therapeutic treatment consists, hence, in the oral supplementation with levocarnitine (L-carnitine) which prevents the metabolic and myopathic manifestations of CDSP by maintaining normal plasma carnitine levels. It has been previously postulated that when OCTN2 is genetically compromised, $ATB^{0,+}$ activity is essential for carnitine absorption [128]. Accordingly, here we find that when OCTN2 activity is impaired by gene silencing, Calu-3 cells, but not A549 that lacks $ATB^{0,+}$, can still accumulate high amounts of carnitine (Figure 26), hence indicating that $ATB^{0,+}$ transporter can compensate for the lack of OCTN2 in supplying cells with extracellular carnitine. This appears to be of peculiar relevance for carnitine homeostasis in patients with genetic defects in OCTN2.

OCTN1 and OCTN2 transporters are highly homologous but have very different specificities [6]. OCTN1 has been reported to mediate carnitine transport even if with a very low affinity [29]. Conversely, the group of Longo N. previously reported that the human OCTN1 failed to cause any significant increase in L-carnitine transport in CHO cells transfected with chimeric OCTN1 transporter [6]. Our results are consistent with this latter finding, since no contribution of a low-affinity component to carnitine transport was detectable in A549 and BEAS-2B cells (Figure 19), despite the evident expression of OCTN1 protein in these cells (Figure 20).

On the other hand, we demonstrate here that the preferential substrate of OCTN1, ergothioneine [73], inhibits carnitine transport in A549 and BEAS-2B cells when employed at high concentrations (1 mM, Figure 21). This effect is clearly due to the inhibitory effect of ET on OCTN2 since, when carnitine uptake was measured in the presence of betaine, the addition of ET halved betaine I0.5 value, without affecting its Imax, hence demonstrating that the two compounds share the same transporter, OCTN2 (Figure 22). This finding is further supported by the results obtained in CHO cells transfected with OCTN2, where ET inhibited carnitine uptake, even if only at the highest concentration (Figure 22, panel B). Our results demonstrate that ET cannot be considered a substrate of the sole OCTN1, since it can also interact with OCTN2, although with a low affinity.

Although the specific physiological role of OCTNs in the lung is not completely understood, the identification of these transporters and the substrates carried are of clinical importance because they can play a significant role in the delivery of cationic drugs such as bronchodilators. The work by Nakamura et al. provided the first evidence that OCTN2 contributes at least in part to the delivery of cationic anti-COPD drugs in BEAS-2B cells [77]; in

the same cell model, Mo et al. reported that L-carnitine ester derivatives of prednisolone (PDSC) are transported by OCTN2 [40]. Moreover, also $ATB^{0,+}$ can be a potential delivery system for a wide variety of drugs: it has been reported that $ATB^{0,+}$ can transport antiviral drugs such as acyclovir and ganciclovir when they are covalently coupled to the side chain of amino acids [43], and recently, the same transporter is under preclinical investigation as a drug target for multiple approach in anticancer therapy. The group of Ganapathy identified this transporter as a novel and effective drug target for the treatment of estrogen receptor (ER)-positive breast cancer [139], and Muller et al. provided evidence for an $ATB^{0,+}$ - selective PET probe which may help in evaluating $ATB^{0,+}$ -targeting drug candidates in vivo in preclinical drug development programs [78].

Thus, since the airway epithelium represents a barrier which inhaled drugs must cross to reach targeted receptors in the underlying airway smooth muscle, a better understanding of the pulmonary transport mechanisms should provide information which can be used to develop more effective inhaled drugs for the treatment of pulmonary diseases. Whether differences among the expression and activity of carnitine transporters here observed in immortal, continuously growing cell lines, are due to the specific district of origin of the cells or to their malignant phenotype deserves to be further addressed. Anyway, it is noteworthy that the results presented here might be useful for the selection of cell models suitable for transport studies.
All the results obtained in this second part of this research project are summarized in the figure 27.

Figure 27. Graphical abstract.
Proposed contribution of L-Carnitine trasnporters in airway epithelial cells (modified from Ingoglia et al [140])

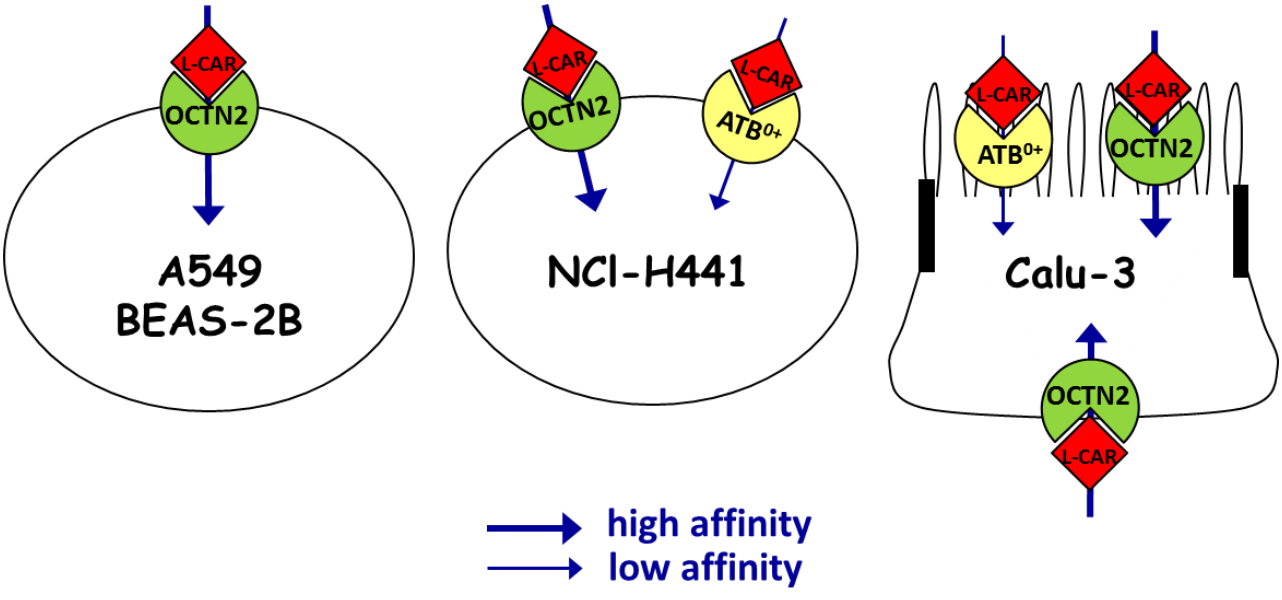

Chapter V – CARNITINE AND OCTNs IN MONOCYTE AND MACROPHAGES

1. INTRODUCTION

Appropriate systemic and tissue concentrations of L-carnitine reflect a balance among intestinal absorption, tissue distribution and renal reabsorption/excretion. These events are mainly mediated by membrane proteins that belong to the SLC22 transporter family, i.e. OCTN1, OCTN2 and OCT6, which are encoded by the genes SLC22A4, SLC22A5 and SLC22A16, respectively [99]; however, also the amino acid transporter $B^{0,+}$ ($ATB^{0,+}$) has also been previously described to perform a low-affinity transport of L-carnitine (Km ~ 800 μM) [128], as recently confirmed by our group in human airway epithelial cells [140].

In the past, the observation that leukocytes, including monocytes and lymphocytes, are enriched in L-carnitine had suggested that the amino acid and its congeners may regulate the immune networks, at least in part by contributing to the maintenance of immune cell membrane structure, viability and function [88]; actually, systemic L-carnitine proved effective in suppressing lipopolysaccharide (LPS)-induced cytokine production and improving murine survival rates during cachexia and septic shock [117], hence displaying immunosuppressive properties. Consistently, results obtained in murine macrophages in vitro showed an inhibitory effect of L-carnitine on iNOS protein, nitric oxide NO production and NF-κB activity confirming which confirm the anti-inflammatory effect of L-carnitine [141].

More recently, the anti-inflammatory role proposed for L-carnitine in the modulation of immune function has been confirmed by many experimental evidences, mainly concerning the gastrointestinal (GI) tract: several publications highlighted , indeed, a link between mutations in genes encoding that encode OCTN1/2 transporters with Crohn's disease (CD) [30], while immunosuppressive and therapeutic properties have been attributed to L-carnitine in gut inflammation[140, 142].

Among immune cells, macrophages act as key players in the normal immune response to pathogens and other relevant stimuli, when monocyte activation and the consequent polarization of macrophages are crucial steps. In the case of injury or infection, monocytes are recruited from the circulation and differentiate into macrophages, with functionally and phenotypically discrete populations [143]. Monocyte/macrophage development is mostly influenced by Monocyte-Colony Stimulating Factor (M-CSF also known as CSF-1) and by Granulocyte/Macrophage-Colony Stimulating Factor (GM-CSF). Depending on the nature of the activation signal, macrophages are, indeed, historically referred to as either classically (M1) or

alternatively (M2) activated macrophages, with the first displaying a microbicidal activity through the release of proinflammatory cytokines and other inflammatory mediators, and the others playing a predominant role in the suppression of immune responses and tissue remodeling [144]. Although it's nowadays widely recognized that macrophage activation exists on a spectrum, and cannot be easily binned into defined groups [145], the M1-like phenotype is expected to be induced in vitro by the treatment with GM-CSF, while macrophages that are grown in the presence of CSF-1 are supposed to be M2-polarized [146, 147]. Regardless of the type of polarization, macrophage differentiation involves changes in gene expression that are driven by multiple transcription factors. Among these, those belonging that belong to the nuclear receptor peroxisome proliferator-activated receptor (PPAR) family are of particular importance due as a result of their roles in regulating lipid metabolism and inflammation [148]. In addition, STAT family members (7 isoforms) are essential for cytokine-regulated processes such as cellular proliferation, differentiation and survival [149].

Nowadays, a tight link between cellular bioenergy/metabolism and the regulation of acute inflammation and immunity has been definitely established [150]. It has been demonstrated, indeed, that the early initiation phase of acute inflammation is mainly anabolic and primarily requires glycolysis for energy, with reduced mitochondrial glucose oxidation; conversely, the later adaptation phase is mostly catabolic and primarily requires fatty acid oxidation for energy. Emerging data support the notion that interactions between inflammation and metabolism play critical roles in chronic inflammatory diseases like such as obesity with diabetes and atherosclerosis, where all these inflammatory and metabolic responses appear seem to be highly heterogeneous and involve cells of both innate and adaptive immunity.

The interplay between immunity, inflammation, and metabolic changes is, today, is a growing field of research; however, the homeostasis of L-carnitine in monocytes/macrophages has not yet been addressed, yet.

The aim of this third part of this research project is to characterize L-carnitine transport during the differentiation of human monocytes to macrophages.

2. RESULTS

2.2 Time-dependent accumulation of L-carnitine in human monocyte and macrophages

The effects of macrophage differentiation on L-carnitine transport were preliminary addressed by performing a time course analysis of 1 mM L-[^{3}H]carnitine uptake, both in freshly isolated monocytes and in MDMs, which were obtained by incubating monocytes for 6 d in the presence of GM-CSF (Figure 28A). Whereas monocytes displayed a modest uptake of L-

carnitine, in MDM the transport of the substrate increased in a time-dependent manner and was linear up to 4 h. This transport activity was completely prevented by an excess of L-carnitine in the extracellular medium, as well as by replacement of extracellular sodium with N-methyl-D-glucamine. In light of these results, we can conclude that L-carnitine enters immune cells through an active, saturable Na^+-dependent transport mechanism whose activity is significantly induced during macrophage differentiation. Consistent with this finding, the determination of the intracellular content of L-carnitine in freshly isolated monocytes and in MDM clearly highlights a higher intracellular content of the molecule in macrophages than in undifferentiated monocytes (Figure 28B).

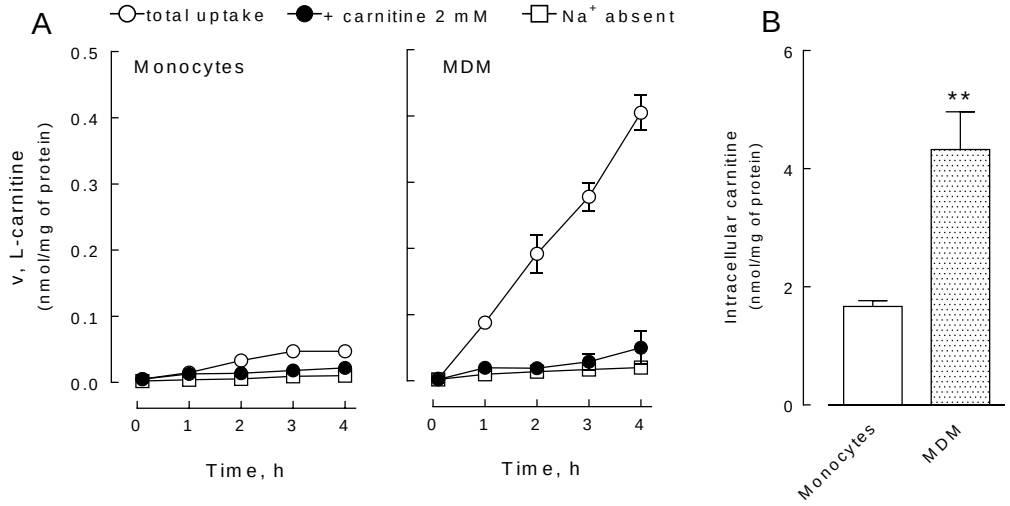

Figure 28. Time-dependent accumulation of L-carnitine in monocytes and MDM.

(A) Freshly isolated monocytes and 6 d-differentiated macrophages (MDM) were incubated for the indicated time in transport buffer that contained L-[^{3}H]carnitine (1 μM; 3 μCi/ml), in the presence (open circles) or absence (open squares) of Na^+. Non-specific binding of the substrate was estimated by measuring the uptake of L-carnitine in the presence of an excess of unlabeled substrate (2 mM) (filled circles). Each point represents the mean ± S.D. of four independent determinations. The experiment has been repeated three times with comparable results. (B) Intracellular content of L-carnitine of freshly isolated monocytes and 6 d-differentiated macrophages was determined by HPLC-tandem mass spectrometry analysis, as described in Materials and Methods. Data are the means of 5 independent determinations, each performed in duplicate. **$p < 0.01$ vs. monocytes.

2.3 Kinetic analysis of L-carnitine uptake in MDM

We next examined the concentration-dependent uptake of L-carnitine over a wide range of substrate concentrations (from 0.001 to 8 mM). Data obtained were best fitted by Eq. 1 (Figure 29A), which revealed the contribution of 2 saturable transport components, one displaying high affinity for the substrate (Km1 = 3.9 ± 2.1 mM) and low capacity (Vmax1 = 3.5 ± 1.2 pmol/mg of protein/min), the other endowed with a very low affinity (Km2 = 10.9 ± 0.5 mM) but high capacity (Vmax2 = 776.7 ± 22.7 pmol/mg of protein/min). Consistently, the Eadie–

Hofstee transformation was nonlinear (Figure 29B). On the basis of these kinetic parameters, the relative contribution of the high- and low-affinity transporters to L-carnitine uptake was extrapolated for substrate concentrations that ranged from 0.001 to 0.1 mM. As shown in figure 29C, the contribution of the high-affinity component was predominant at low concentrations of substrate, whereas the operation of the low-affinity transporter became progressively prevalent as L-carnitine concentration increased.

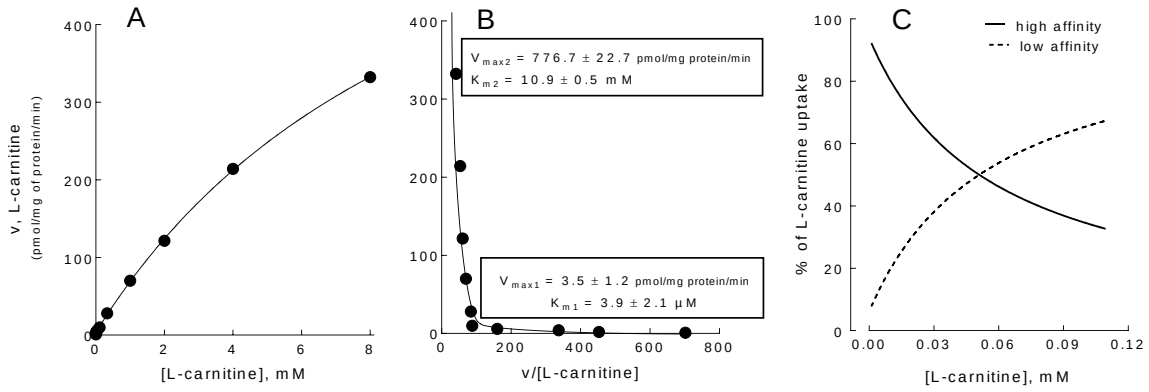

Figure 29. Kinetic analysis of L-carnitine uptake in MDM.

Macrophages were incubated in the presence of the indicated concentrations (from 0.001 to 8 mM) of L-[^{3}H]carnitine (3 µCi/ml) for 30 min, either in the presence or absence of Na^+ (not shown). (A) Plot shows the Na^+-dependent component of carnitine transport, calculated by subtracting transport data obtained in the absence from those in the presence of Na^+. Nonlinear fitting of the data was performed by employing Eqn. 1 (see Materials and methods). (B) Eadie–Hofstee transformation of the data obtained in Panel A, with the curve representing the nonlinear fitting of the data. Points are mean ± S.D. of three independent determinations. Experiment was repeated twice with comparable results. (C) Estimated relative contribution of high and low affinity components to L-carnitine transport in MDM. Curves have been drawn on the basis of the obtained kinetic parameters, shown in panel B.

2.4 Inhibition analysis of L-carnitine uptake in MDM

To identify the transporters that are responsible for L-carnitine uptake in MDM, organic cationic and zwitterionic compounds were employed as inhibitors (Figure 30). In particular, betaine and quinidine were employed as specific substrates of OCTN2, whereas TEA was able to inhibit both OCTN1 and -2. As for ET, it has been thus far considered a specific substrate of OCTN1 [73], although we have recently provided evidence that its specificity is maintained only when it is employed at the proper concentration [82]. Amino acids leucine and arginine have been chosen as inhibitors of $ATB^{0,+}$, a Na^+ and Cl^- dependent transporter for cationic and neutral amino acids whose contribution to L-carnitine transport has been demonstrated in Calu-3 cells [82]. Finally, proline was used to address the involvement of system A, a family of SNATs for small aliphatic amino acids [151]. Results obtained demonstrated that L-carnitine uptake in MDM was significantly inhibited by betaine, quinidine, and TEA, but not by 100 mM

ET, thus excluding a role for OCTN1, while pointing to OCTN2 as one of the transporters involved in L-carnitine transport in this cell model. Cationic amino acid arginine, as well as the neutral amino acid leucine, were completely ineffective, thus excluding the contribution of $ATB^{0,+}$ transporter. Of interest, the presence of proline significantly lowered L-carnitine transport (~30%), which indicated a role for system A transporters in the mediation of L-carnitine uptake in these cells. According to the kinetic features of OCTN2 and SNAT proteins, it is likely that OCTN2 corresponds to the high-affinity transporter, whereas system A accounts for the low-affinity component of L-carnitine uptake in MDM.

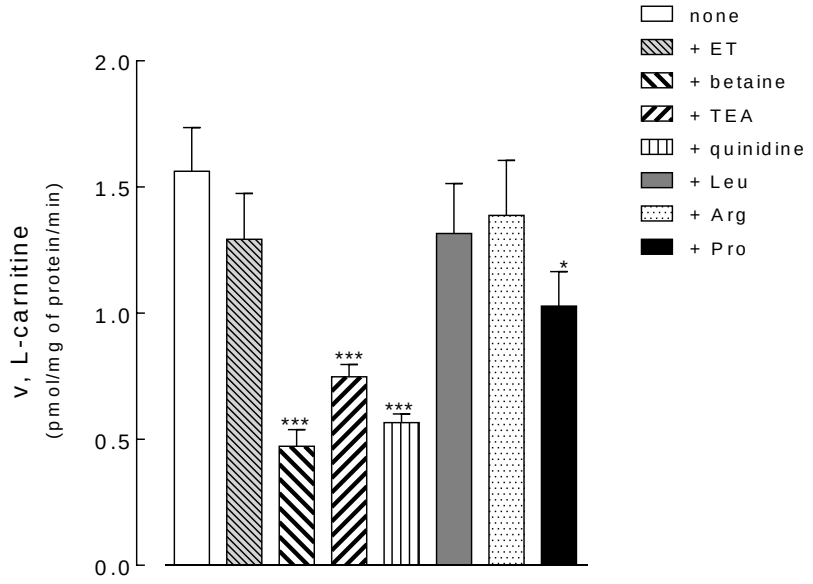

Figure 30. Inhibitory effect of organic cationic and zwitterionic compounds on L-carnitine uptake in MDM.

Uptake of L-[^{3}H]carnitine (30 min; 1 µM; 3 µCi/ml) was determined in MDM in the absence (none) or in the presence of the listed compounds, all tested at the concentration of 1 mM. In particular, betaine and quinidine were employed as specific substrates of OCTN2, while TEA was used to inhibit both OCTN1 and 2. Ergothioneine (ET), which was employed at the proper concentration (100 µM), can be considered a specific substrate of OCTN1. Amino acids leucine (Leu) and arginine (Arg) were chosen as inhibitors of $ATB^{0,+}$, whereas proline (Pro) was used to address the involvement of system A. The inhibitory effect of each compound is calculated as the residual amount of L-carnitine uptake. Values are mean ± S.E. of three experiments each performed in triplicate. *p < 0.05, ***p < 0.001 vs control (none).

2.5 Expression of L-carnitine transporters during the differentiation of monocytes to macrophages

Expression of classic L-carnitine transporters SLC22A4/OCTN1 and SLC22A5/OCTN2, as well as that of system A transporters SLC38A1/SNAT1, SLC38A2/SNAT2, and SLC38A4/SNAT4, was next evaluated, both in freshly isolated monocytes and in MDM, in terms of mRNA (Figure 31A) and protein (Figure 31B). Whereas expression of OCTN1 markedly lowered during monocyte-to-macrophage differentiation, mainly appreciable at protein level, OCTN2 protein, which was undetectable in monocytes, became strongly expressed in MDM,

with a 20-fold increase of the corresponding mRNA. Among the subtypes of system A transporters (SNAT1, SNAT2, and SNAT4), only SNAT2 mRNA increased (4-fold) in MDM, with an evident induction of the corresponding band in Western blot analysis. A time course of OCTN2 expression during GM-CSF treatment, shown in Figure 31C, indicates that a significant induction of mRNA occurred after 6 h and reached maximal levels within 15 h (left), whereas the protein, which was barely detectable after 24 h, became clearly appreciable after 3 d incubation (right).

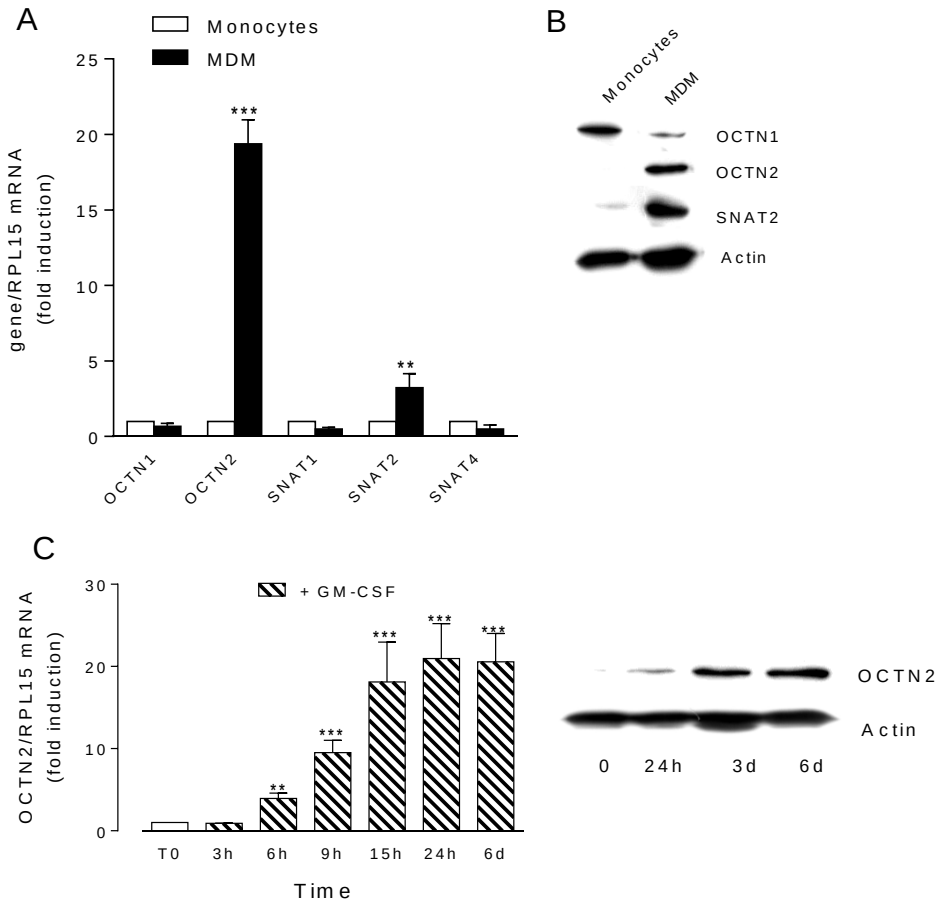

Figure 31. Expression of L-carnitine transporters (OCTN1/2) and of System A transporters (SNAT1/2/4) in MDM.

(A) mRNA levels for SLC22A4/OCTN1, SLC22A5/OCTN2, SLC38A1/SNAT1, SLC38A2/SNAT2 and SLC38A4/SNAT4 were determined in freshly isolated monocytes and in MDM by means of quantitative RT-PCR analysis. After normalization for the housekeeping gene (RPL15), expression of the gene of interest in MDM was shown relatively to its level in freshly isolated monocytes (=1). Data are means ± SEM of three experiments, each performed in duplicate. (B) Protein expression was evaluated in total cell lysates, as described in Materials and methods. A representative Western blot is shown. The experiment was repeated twice with comparable results. (C) Expression of SLC22A5/OCTN2 was measured upon incubation with GM-CSF for the indicated times at both mRNA (left) and protein (right) levels. mRNA data are means ± SEM of three experiments, each performed in duplicate; a representative Western blot, repeated twice with comparable results, is shown. **p < 0.1, ***p < 0.001 vs monocytes (T0).

2.6 Signaling pathway in GM-CSF–mediated OCTN2 induction during macrophage differentiation

Macrophage differentiation involves changes in gene expression that are driven by multiple transcription factors. Among them, evidence suggests that PPARs have a role in the regulation of SLC22A5/OCTN2 expression in different animal and human models [149, 152]. In addition, GM-CSF is known to induce activation of different phosphorylation dependent signaling pathways, including the Jak/Stat pathway [149, 153]. To identify the transcription factor responsible for the GM-CSF–induced OCTN2 transcription, we employed antagonists and agonists of PPARα and PPARγ, as well as of STAT family members. As shown in figure 32, both the synthetic PPARα agonist WY-14643 and, to a lesser extent, the PPARγ agonist rosiglitazone were able to increase the expression of OCTN2 in the absence of GM-CSF, which confirmed that OCTN2 is actually a target of these ligand-activated transcription factors, as previously reported in other models [154]. However, the PPARα antagonist GW6471 only modestly lowered GM-CSF–induced OCTN2 expression, but without reaching statistical significance, whereas PPARγ antagonist GW9662 was completely ineffective, thus indicating that these transcription factors are not involved in the transporter induction by GM-CSF. On the contrary, all the STAT inhibitors employed, i.e., AG490 and nifuroxamide (pan-STAT inhibitors), as well as S3I-201, specific for STAT3, completely suppressed the effect of the cytokine, clearly pointing to the involvement of STAT, in particular STAT3, as the transcription factor responsible for OCTN2 induction by GM-CSF.

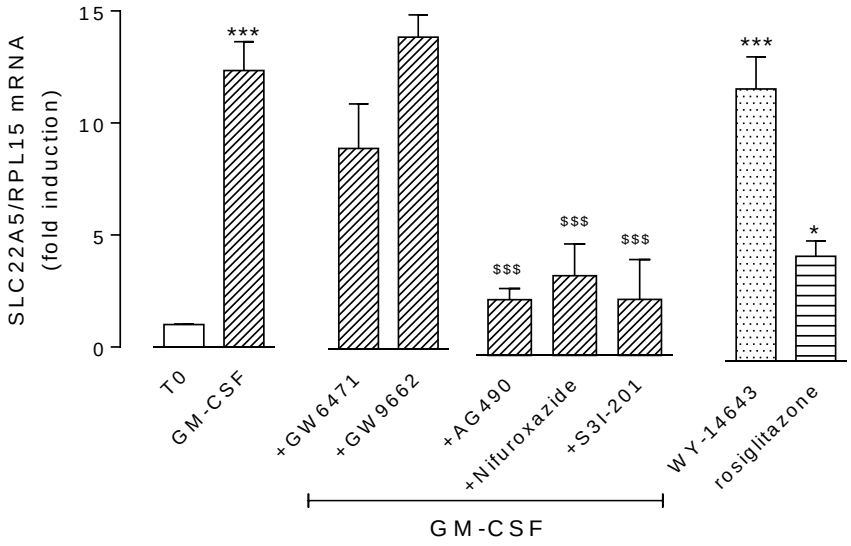

Figure 32. Role of PPARs and STATs transcription factors on the GM-CSF-dependent induction of OCTN2 mRNA. Expression of SLC22A5/OCTN2 mRNA was determined by means of quantitative RT-PCR analysis in freshly isolated monocytes (open bar) and in monocytes that were incubated for 24 h with 50 ng/ml GM-CSF either in the absence or in the presence of the indicated agonists (50 μM WY-14643 for PPARα; 200 nM rosiglitazone for PPARγ) and antagonists (10 μM GW6471 for PPARα; 10 μM GW9662 for PPARγ; 100 μM AG490 and nifuroxamide for STATs; 50 μM S3I-201 for STAT3) of PPARs and STATs transcription factors. After normalization for the housekeeping gene (RPL15), expression of the SLC22A5 in treated monocytes was shown relatively to its level in monocytes (=1). Data are means ± SEM of three experiments, each performed in duplicate. *p < 0.05, ***p < 0.001 vs monocytes; $$$p < 0.001 vs. GM-CSF.

Since accumulating evidence supports a crosstalk between mTOR and STAT3 in the modulation of macrophage development and function [155], we have investigated the involvement of mTOR signaling cascade in the induction of OCTN2 by GM-CSF. As shown in figure 33A, incubation with the cytokine caused a progressive phosphorylation of STAT3, which was detectable after 5 h of treatment and still evident after 24 h, that demonstrates activation of the transcription factor under these conditions. In parallel, a comparable activation of mTOR also occurs at the same experimental times, when a phosphorylation of the kinase in Ser2448 is observed, along with a concomitant increase of phosphorylation of p70S6K, a known target of mTOR. Rapamycin—the specific inhibitor of mTOR—in addition to the expected inhibition of p70S6K phosphorylation, completely prevented GM-CSF–induced phosphorylation of STAT3, which clearly indicated that the differentiation of human monocytes driven by the cytokine requires an mTOR-dependent phosphorylation of STAT3. Consistently, the inhibitor actually reduced the expression of the transporter at both mRNA and protein levels (Figure 33B). We can thus conclude that GM-CSF–mediated induction of L-carnitine transport during macrophage differentiation involves the mTOR-STAT3 molecular axis.

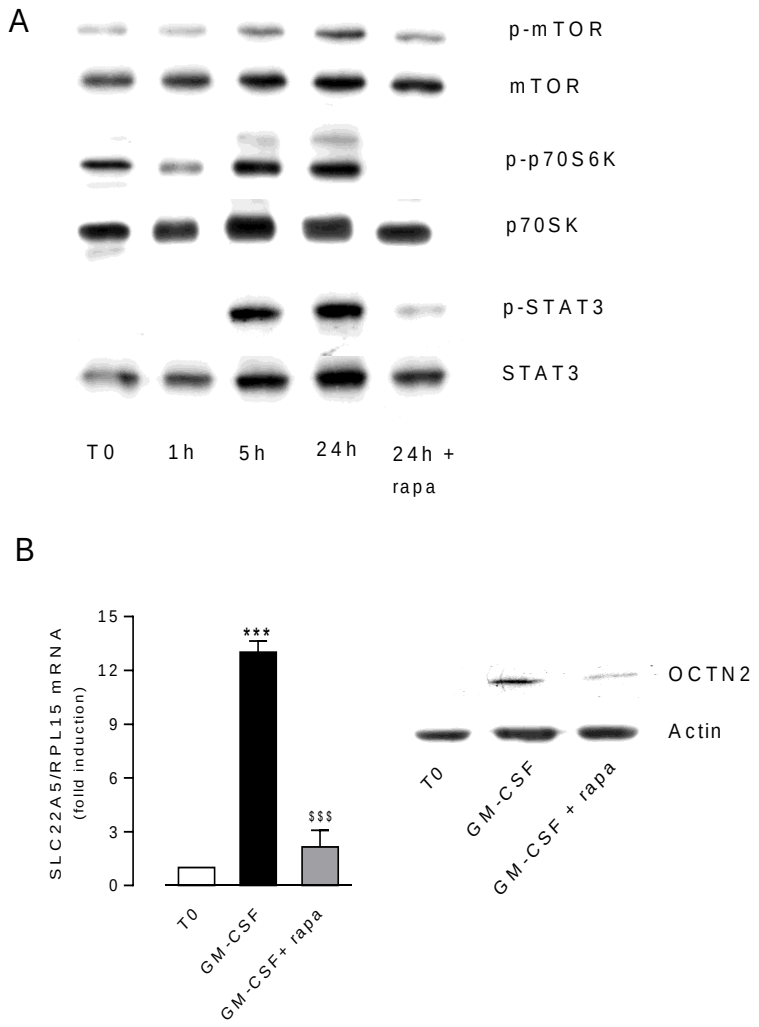

Figure 33. Molecular pathways involved in the GM-CSF-mediated induction of OCTN2.

Protein lysates were obtained from freshly isolated monocytes or from monocytes incubated with GM-CSF for the indicated times, in the absence or in the presence of 100 nM rapamycin (rapa). (A) Representative Western Blots for the indicated proteins are shown. Experiments were repeated three times with comparable results. (B) mRNA (left) and protein (right) level of SLC22A5/OCTN2 was determined in freshly isolated monocytes (T0) and in monocytes incubated with GM-CSF for 24 h in the absence or in the presence of 100 nM rapamycin. mRNA data are means ± SEM of three experiments, each performed in duplicate; a representative Western blot of OCTN2 repeated twice with comparable results is shown. ***p < 0.001 vs T0; $$$p < 0.001 vs GM-CSF.

Involvement of STAT3 was further confirmed by employing other activators of this transcription factor in myeloid cells, in particular IL-6 [30] and CSF-1 [156]. The expected phosphorylation of STAT3 (Figure 34A) was associated with a progressive induction of SLC22A5/OCTN2 mRNA (Figure 34B), which led to a marked increase of OCTN2 protein upon 6-d incubation (Figure 34C).

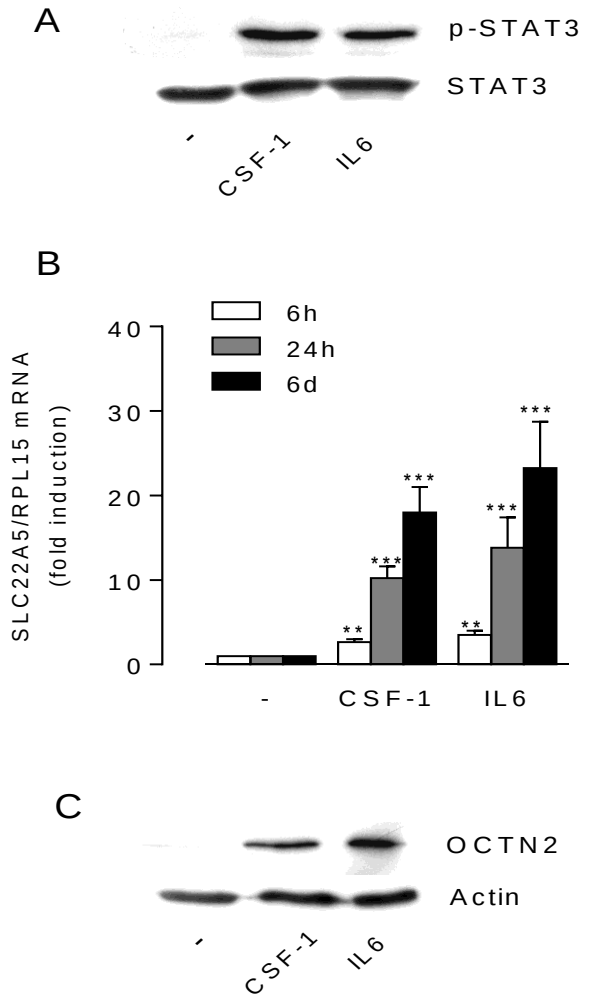

Figure 34. Effect of STAT3 activation on OCTN2 expression

Monocytes were incubated for the indicated times in the presence of CSF-1 (50 ng/ml) or IL6 (20 ng/ml). (A) After 24h protein lysate were analyzed for STAT3 phosphorylation. A representative Western Blot, repeated twice with comparable results, is shown. (B) mRNA level of SLC22A5/OCTN2 was determined by means of quantitative RT-PCR. Data are means ± S.E. of three experiments, each performed in duplicate. Panel C. Expression of OCTN2 was determined after 6 d-treatment. A representative Western Blot, repeated twice with comparable results, is shown. **p < 0.01; ***p < 0.001 vs untreated monocytes (-)

3. DISCUSSION

In this last part of the research project, we demonstrate for the first time to our knowledge that L-carnitine transport increases during the differentiation of human monocytes to macrophages and that this induction is specifically referable to an enhanced expression of OCTN2 transporter at both the gene and protein levels. Moreover, by addressing the molecular pathway that is

driven by GM-CSF in monocytes, we also identify SLC22A5/OCTN2 as a novel target gene of the mTOR-STAT3 axis in human immune cells (Figure 35).

Figure 35. Graphical abstract

Proposed pathway for GM-CSF-dependent induction of OCTN2 transporter in macrophages**.** According to our findings, we propose that GM-CSF signaling activates STAT3 via mTOR which leads to the up-regulation of OCTN2 transporter. Image taken from Ingoglia et al 2016 [141]

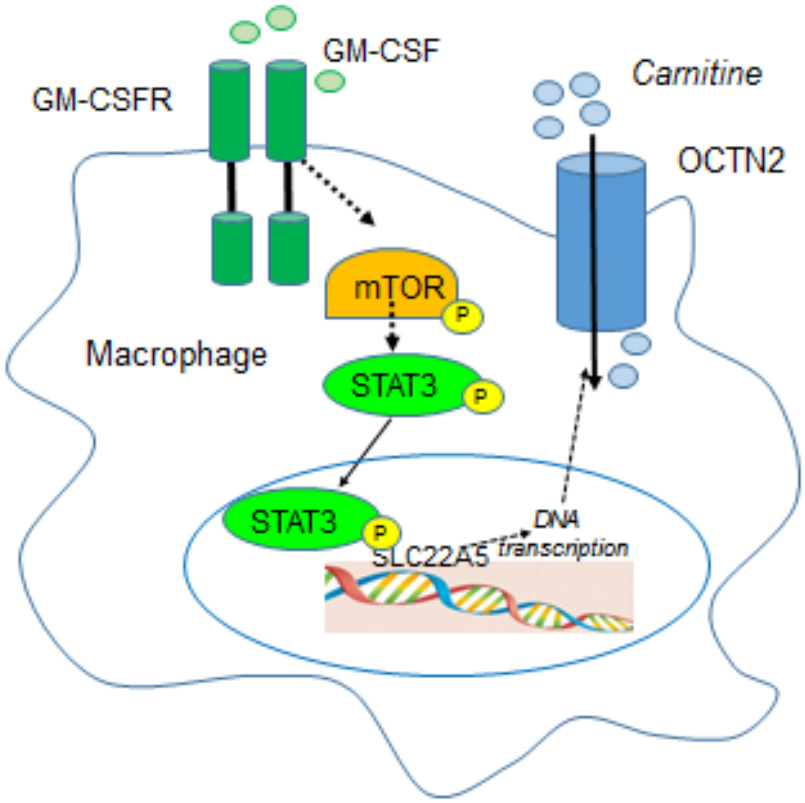

Actually, whereas human monocytes do not exhibit an appreciable transmembrane flux of L-carnitine, a high transport activity is observed in GM-CSF–differentiated macrophages, which ensures a higher intracellular content of the solute (Figure 28). In these cells, kinetic and inhibition analyses (Figures 29 and 30) demonstrate that L-carnitine transport is mediated by 2 saturable components with very different operating features: OCTN2 represents the high-affinity transporter (Km < 4 µM), whereas SNAT2, and thus system A for neutral amino acids, accounts for the low-affinity transporter (Km > 10 mM). Conversely, the ineffectiveness of ET, specific substrate of OCTN1, as well as of leucine and arginine, substrates for the amino acid transporter $B^{0,+}$ ($ATB^{0,+}$), excludes the involvement of these transporters in macrophages. Hence, in macrophages, transport activity of system A seems to replace that of $ATB^{0,+}$ observed in epithelial cells [82]; however, it is important to underline that, despite the coexistence of the 2 transporters, the intracellular content of L-carnitine in macrophages in vivo is expected to be

provided by OCTN2, rather than SNAT2. Indeed, although at 40 μM of extracellular L-carnitine, which roughly corresponds to the plasma concentration [131], the contribution of the two transporters is expected to be equal (Figure 29C), in vivo the presence of neutral amino acids that can interact with higher affinity with SNAT2 likely reduces L-carnitine transport through this transporter. The finding that L-carnitine is a substrate of SNAT2 could be physiologically consistent with the role of L-carnitine as an osmoprotectant that is involved in cell volume and fluid balancing [88]: system A, and in particular the SNAT2 isoform, are known to participate in cell volume regulation under conditions of osmotic stress [92, 157].

At the molecular level, increased activity of L-carnitine transport in GM-SCF–differentiated macrophages results from induction of SLC22A5 and SLC38A2 mRNA levels.
Consistently, the corresponding proteins OCTN2 and SNAT2 are also detectable in macrophages, but not in undifferentiated monocytes. A comparable induction of OCTN2 mRNA and protein is also observed upon differentiation of monocytes with CSF-1, thus pointing to the transporter as a marker of macrophage maturation regardless of M1 or M2 polarization. Similarly, other transport proteins are known to be induced during monocyte-to macrophage differentiation. For example, the treatment of human leukemia THP-1 monocytic cells with PMA has been described to associate with a marked induction of GLUT3 and GLUT5 glucose transporters [158], of the ascorbate transporter SVCT2 [159], and of y+LAT1 arginine transporter [94]; the latter is also induced in human monocytes by incubation with GM-CSF [91]. Conversely, undifferentiated monocytes express high levels of OCTN1 protein that dramatically drop along with the differentiation to macrophages. Our data demonstrate that this transporter is unable to transport L-carnitine, a finding that is consistent with previous results in OCTN1-transfected CHO cells [6], as well as in human airways epithelial cells [82].

Monocyte-to-macrophage differentiation involves changes in gene expression driven by multiple transcription factors. Among these, ligand-activated transcription factors, such as PPARs, are of particular importance for the regulation of lipid metabolism [160, 161]. The PPAR family consists of 3 ligand-activated nuclear receptors (PPARα, -γ, and -δ). In particular, PPARα is predominantly expressed in the liver, but also in macrophages, heart, muscle, and kidneys, where it modulates genes that are involved in long-chain fatty acid oxidation [162]. PPARγ is mainly expressed in adipocytes, where it plays a major role in adipogenesis and triglyceride accumulation and storage. PPARγ signaling is also relevant in myeloid cells for the modulation of immune and inflammatory responses [163]. Previous studies have documented a transcriptional regulation of OCTN2 by PPARα in different animal models [164]. More recently, results of in silico analyses have indicated that in humans OCTN2 is directly regulated by the same transcription factor [165]. In line with these findings, our data show an up-regulation of OCTN2 in human macrophages upon incubation with both PPARα and PPARγ agonists; however, the lack of efficacy of PPARs' inhibitors excludes a role for these transcription factors

in the GM-CSF–dependent induction of OCTN2 expression. On the contrary, we show that GM-CSF induces in monocytes a progressive phosphorylation of STAT3, which is absolutely required for OCTN2 induction (Figures 32 and 33). The role of STATs in influencing the proliferation, differentiation, and survival status of myeloid cells has been the subject of extensive research over the last few years [149]. STAT3 has been demonstrated to be activated by a variety of cytokine receptors, including G-CSF and members of the IL-3/IL-5/ GM-CSF family, as well as by IL-6 [18] and CSF-1 [156]. Here, we show that these 2 latter cytokines both cause phosphorylation of STAT3, as expected, and the induction of SLC22A5/OCTN2 expression (Figure 34B).

Recent studies have demonstrated a close interaction between mTOR and STATs pathways in the control and optimization of immune responses (see [155] for review). In particular, an mTOR-dependent regulation of STAT activation has been described as essential for the proper function of LPS treated dendritic cells [166] and macrophages [167]. In T lymphocytes, the mTOR pathway has been shown to integrate diverse environmental signals by modulating the activation of specific STATs, either involving direct or indirect mTOR dependent phosphorylation of STAT proteins or phosphorylation-independent mechanisms [155]. In macrophages, we demonstrate here that the phosphorylation of STAT3 induced by GM-CSF strictly depends on activation of mTOR, as rapamycin, in addition to abolishing the phosphorylation of p70S6K, as expected, completely suppresses phosphorylation of STAT3, which demonstrates that the GM-CSF–induced differentiation of human monocytes requires the mTOR-STAT axis. Involvement of the kinase in the induction of OCTN2 during macrophage differentiation is consistent with its central role in bolstering intracellular ATP production capacity. Indeed, mTOR has been known for years to serve as a converging point for signals that mediate cellular growth, energy metabolism, and nutrient availability [168]. More recently, a specific role for the kinase as a major regulator of energy production in mitochondria has been also described [152]. In this context, the increase of L-carnitine transport mediated by the GM-CSF-mTOR-STAT axis during macrophage differentiation could serve to provide mature cells with fuel so as to meet the increased demand of energy for exerting their immune functions. In support of this hypothesis, clinical evidence demonstrates that nutritional or pharmacologic supplementation with the amino acid may be beneficial for a number of human disorders [169, 170]. In type II diabetes, for example, dysregulation of immune functions is associated with an impaired fatty acid oxidation [171], the underlying mechanisms of which remain unclear. Results obtained in diabetic rats, however, demonstrated that administration of L-carnitine improved immune function through an enhancement of mitochondrial activity, a decrease of oxidative damage, and delayed cell death in immune organs and blood [172]. Thus, in light of our findings and of evidence in the literature, the definition of the role of L-carnitine transporters under pathologic conditions associated with immune dysfunctions deserves to be further investigated.

CONTRIBUTIONS

ORIGINAL PAPERS:

1. Ingoglia F, Visigalli R., Rotoli BM, Barilli A, Dall'Asta V. (2015) **Functional characterization of the organic cation transporters (OCTs) in human airway pulmonary epithelial cells.** Biochim Biophys Acta Vol. 1848(7): 1563-72. doi: 10.1016/j.bbamem.2015.04.001.

2. Ingoglia F, Visigalli R, Rotoli BM, Barilli A, Riccardi B, Puccini P, Dall'Asta V. **Functional activity of L-carnitine transporters in human airway epithelial cells.** Biochim Biophys Acta. 2016 Feb;1858(2):210-9. doi: 10.1016/j.bbamem.2015.11.013. Epub 2015 Nov 29.

3. Ingoglia F, Visigalli R, Rotoli BM, Barilli A, Riccardi B, Puccini P, Milioli M, Di Lascia M, Bernuzzi G, Dall'Asta V. **Human macrophage differentiation induces OCTN2-mediated L-carnitine transport through stimulation of mTOR-STAT3 axis.** J. Leukoc. Biol. 2016 OCT; 101:000-000; 2017. DOI: 10.1189/jlb.1A0616-254R.

CONGRESS COMMUNICATION:

1. Ingoglia F, Visigalli R., Rotoli BM, Barilli A, Dall'Asta V. "14th International Congresson Amino Acids, Peptides and Proteins". Wien, Austria. 2015. Presentation of the contributions: **"Functional activity of organic cation transporters (OCTs AND OCTNs) in human airway epithelial cells"**

REFERENCES

1. **Singer, S.J. and G.L. Nicolson**, *The fluid mosaic model of the structure of cell membranes.* Science, 1972. 175(4023): p. 720-31.

2. **van Meer, G., D.R. Voelker, and G.W. Feigenson**, *Membrane lipids: where they are and how they behave.* Nat Rev Mol Cell Biol, 2008. 9(2): p. 112-24.

3. **Cho, W. and R.V. Stahelin**, *Membrane-protein interactions in cell signaling and membrane trafficking.* Annu Rev Biophys Biomol Struct, 2005. 34: p. 119-51.

4. **Mansilla, M.C., et al.**, *Control of membrane lipid fluidity by molecular thermosensors.* J Bacteriol, 2004. 186(20): p. 6681-8.

5. **Rees, D.C., L. DeAntonio, and D. Eisenberg**, *Hydrophobic organization of membrane proteins.* Science, 1989. 245(4917): p. 510-3.

6. **Deeley, R.G., C. Westlake, and S.P. Cole**, *Transmembrane transport of endo- and xenobiotics by mammalian ATP-binding cassette multidrug resistance proteins.* Physiol Rev, 2006. 86(3): p. 849-99.

7. **Koepsell, H.**, *Polyspecific organic cation transporters: their functions and interactions with drugs.* Trends Pharmacol Sci, 2004. 25(7): p. 375-81.

8. **Nigam, S.K.**, *What do drug transporters really do?* Nat Rev Drug Discov, 2015. 14(1): p. 29-44.

9. **Catterall, W.A.**, *Ion channel voltage sensors: structure, function, and pathophysiology.* Neuron, 2010. 67(6): p. 915-28.

10. **Ortells, M.O. and G.G. Lunt**, *Evolutionary history of the ligand-gated ion-channel superfamily of receptors.* Trends Neurosci, 1995. 18(3): p. 121-7.

11. **Wickman, K. and D.E. Clapham**, *Ion channel regulation by G proteins.* Physiol Rev, 1995. 75(4): p. 865-85.

12. **Camerino, D.C., et al.**, *Therapeutic approaches to ion channel diseases.* Adv Genet, 2008. 64: p. 81-145.

13. **Benga, G.**, *Water channel proteins (later called aquaporins) and relatives: past, present, and future.* IUBMB Life, 2009. 61(2): p. 112-33.

14. **shin, N.**, *Role of drug transporters: an overview based on knockout animal model studies*, in *Journal of Pharmaceutical Investigation*. 2015. p. 13.

15. **Dean, M., Y. Hamon, and G. Chimini**, *The human ATP-binding cassette (ABC) transporter superfamily.* J Lipid Res, 2001. 42(7): p. 1007-17.

16. **He, L., K. Vasiliou, and D.W. Nebert**, *Analysis and update of the human solute carrier (SLC) gene superfamily.* Hum Genomics, 2009. 3(2): p. 195-206.

17. **Ciarimboli, G.**, *Organic cation transporters.* Xenobiotica, 2008. 38(7-8): p. 936-71.

18. **Kouji, H., et al.**, *Molecular and functional characterization of choline transporter in human colon carcinoma HT-29 cells.* Arch Biochem Biophys, 2009. 483(1): p. 90-8.

19. **Pao, S.S., I.T. Paulsen, and M.H. Saier, Jr.**, *Major facilitator superfamily.* Microbiol Mol Biol Rev, 1998. 62(1): p. 1-34.

20. **Hoglund, P.J., et al.**, *The solute carrier families have a remarkably long evolutionary history with the majority of the human families present before divergence of Bilaterian species.* Mol Biol Evol, 2011. 28(4): p. 1531-41.

21. **Grundemann, D., et al.**, *Drug excretion mediated by a new prototype of polyspecific transporter.* Nature, 1994. 372(6506): p. 549-52.

22. **Koepsell, H., B.M. Schmitt, and V. Gorboulev**, *Organic cation transporters.* Rev Physiol Biochem Pharmacol, 2003. 150: p. 36-90.

23. **Grundemann, D., et al.**, *Molecular identification of the corticosterone-sensitive extraneuronal catecholamine transporter.* Nat Neurosci, 1998. 1(5): p. 349-51.

24. **Koehler, M.R., et al.**, *The two human organic cation transporter genes SLC22A1 and SLC22A2 are located on chromosome 6q26.* Cytogenet Cell Genet, 1997. 79(3-4): p. 198-200.

25. **Grundemann, D. and E. Schomig**, *Gene structures of the human non-neuronal monoamine transporters EMT and OCT2.* Hum Genet, 2000. 106(6): p. 627-35.

26. **Verhaagh, S., et al.**, *Cloning of the mouse and human solute carrier 22a3 (Slc22a3/SLC22A3) identifies a conserved cluster of three organic cation transporters on mouse chromosome 17 and human 6q26-q27.* Genomics, 1999. 55(2): p. 209-18.

27. **Schomig, E., et al.**, *Molecular cloning and characterization of two novel transport proteins from rat kidney.* FEBS Lett, 1998. 425(1): p. 79-86.

28. **Wu, X., et al.**, *Structural and functional characteristics and tissue distribution pattern of rat OCTN1, an organic cation transporter, cloned from placenta.* Biochim Biophys Acta, 2000. 1466(1-2): p. 315-27.

29. **Tamai, I., et al.**, *Molecular and functional characterization of organic cation/carnitine transporter family in mice.* J Biol Chem, 2000. 275(51): p. 40064-72.

30. **Peltekova, V.D., et al.**, *Functional variants of OCTN cation transporter genes are associated with Crohn disease.* Nat Genet, 2004. 36(5): p. 471-5.

31. **Wu, X., et al.**, *cDNA sequence, transport function, and genomic organization of human OCTN2, a new member of the organic cation transporter family.* Biochem Biophys Res Commun, 1998. 246(3): p. 589-95.

32. **Jonker, J.W. and A.H. Schinkel**, *Pharmacological and physiological functions of the polyspecific organic cation transporters: OCT1, 2, and 3 (SLC22A1-3).* J Pharmacol Exp Ther, 2004. 308(1): p. 2-9.

33. **Koepsell, H. and H. Endou**, *The SLC22 drug transporter family.* Pflugers Arch, 2004. 447(5): p. 666-76.

34. **Koepsell, H.**, *Organic cation transporters in intestine, kidney, liver, and brain.* Annu Rev Physiol, 1998. 60: p. 243-66.

35. **Jonker, J.W., et al.**, *Reduced hepatic uptake and intestinal excretion of organic cations in mice with a targeted disruption of the organic cation transporter 1 (Oct1 [Slc22a1]) gene.* Mol Cell Biol, 2001. 21(16): p. 5471-7.

36. **Nies, A.T., et al.**, *Organic cation transporters (OCTs, MATEs), in vitro and in vivo evidence for the importance in drug therapy.* Handb Exp Pharmacol, 2011(201): p. 105-67.

37. **Minematsu, T. and K.M. Giacomini**, *Interactions of tyrosine kinase inhibitors with organic cation transporters and multidrug and toxic compound extrusion proteins.* Mol Cancer Ther, 2011. 10(3): p. 531-9.

38. **Saborowski, M., G.A. Kullak-Ublick, and J.J. Eloranta**, *The human organic cation transporter-1 gene is transactivated by hepatocyte nuclear factor-4alpha.* J Pharmacol Exp Ther, 2006. 317(2): p. 778-85.

39. **Tirona, R.G. and R.B. Kim**, *Nuclear receptors and drug disposition gene regulation.* J Pharm Sci, 2005. 94(6): p. 1169-86.

40. **Bodmer, M., et al.**, *Metformin, sulfonylureas, or other antidiabetes drugs and the risk of lactic acidosis or hypoglycemia: a nested case-control analysis.* Diabetes Care, 2008. 31(11): p. 2086-91.

41. **Shu, Y., et al.**, *Effect of genetic variation in the organic cation transporter 1, OCT1, on metformin pharmacokinetics.* Clin Pharmacol Ther, 2008. 83(2): p. 273-80.

42. **Motohashi, H., et al.**, *Different transport properties between famotidine and cimetidine by human renal organic ion transporters (SLC22A).* Eur J Pharmacol, 2004. 503(1-3): p. 25-30.

43. **Busch, A.E., et al.**, *Human neurons express the polyspecific cation transporter hOCT2, which translocates monoamine neurotransmitters, amantadine, and memantine.* Mol Pharmacol, 1998. 54(2): p. 342-52.

44. **Jonker, J.W., et al.**, *Deficiency in the organic cation transporters 1 and 2 (Oct1/Oct2 [Slc22a1/Slc22a2]) in mice abolishes renal secretion of organic cations.* Mol Cell Biol, 2003. 23(21): p. 7902-8.

45. **Zolk, O., et al.**, *Functional characterization of the human organic cation transporter 2 variant p.270Ala>Ser.* Drug Metab Dispos, 2009. 37(6): p. 1312-8.

46. **Urakami, Y., et al.**, *Creatinine transport by basolateral organic cation transporter hOCT2 in the human kidney.* Pharm Res, 2004. 21(6): p. 976-81.

47. **Dresser, M.J., et al.**, *Interactions of n-tetraalkylammonium compounds and biguanides with a human renal organic cation transporter (hOCT2).* Pharm Res, 2002. 19(8): p. 1244-7.

48. **Wang, Z.J., et al.**, *OCT2 polymorphisms and in-vivo renal functional consequence: studies with metformin and cimetidine.* Pharmacogenet Genomics, 2008. 18(7): p. 637-45.

49. **Inazu, M., H. Takeda, and T. Matsumiya**, *Expression and functional characterization of the extraneuronal monoamine transporter in normal human astrocytes.* J Neurochem, 2003. 84(1): p. 43-52.

50. **Muller, J., et al.**, *Drug specificity and intestinal membrane localization of human organic cation transporters (OCT).* Biochem Pharmacol, 2005. 70(12): p. 1851-60.

51. **Hayer-Zillgen, M., M. Bruss, and H. Bonisch**, *Expression and pharmacological profile of the human organic cation transporters hOCT1, hOCT2 and hOCT3.* Br J Pharmacol, 2002. 136(6): p. 829-36.

52. **Sata, R., et al.**, *Functional analysis of organic cation transporter 3 expressed in human placenta.* J Pharmacol Exp Ther, 2005. 315(2): p. 888-95.

53. **Wu, X., et al.**, *Identity of the organic cation transporter OCT3 as the extraneuronal monoamine transporter (uptake2) and evidence for the expression of the transporter in the brain.* J Biol Chem, 1998. 273(49): p. 32776-86.

54. **Lips, K.S., et al.**, *Polyspecific cation transporters mediate luminal release of acetylcholine from bronchial epithelium.* Am J Respir Cell Mol Biol, 2005. 33(1): p. 79-88.

55. **Schmitt, A., et al.**, *Organic cation transporter capable of transporting serotonin is up-regulated in serotonin transporter-deficient mice.* J Neurosci Res, 2003. 71(5): p. 701-9.

56. **Motohashi, H., et al.**, *Gene expression levels and immunolocalization of organic ion transporters in the human kidney.* J Am Soc Nephrol, 2002. 13(4): p. 866-74.

57. **Feng, N., et al.**, *Local inhibition of organic cation transporters increases extracellular serotonin in the medial hypothalamus.* Brain Res, 2005. 1063(1): p. 69-76.

58. **Kitaichi, K., et al.**, *Behavioral changes following antisense oligonucleotide-induced reduction of organic cation transporter-3 in mice.* Neurosci Lett, 2005. 382(1-2): p. 195-200.

59. **Zwart, R., et al.**, *Impaired activity of the extraneuronal monoamine transporter system known as uptake-2 in Orct3/Slc22a3-deficient mice.* Mol Cell Biol, 2001. 21(13): p. 4188-96.

60. **Sakata, T., et al.**, *Functional analysis of human organic cation transporter OCT3 (SLC22A3) polymorphisms.* J Pharmacol Sci, 2010. 113(3): p. 263-6.

61. **Aoyama, N., et al.**, *Association between gene polymorphisms of SLC22A3 and methamphetamine use disorder.* Alcohol Clin Exp Res, 2006. 30(10): p. 1644-9.

62. **Somogyi, A., A. McLean, and B. Heinzow**, *Cimetidine-procainamide pharmacokinetic interaction in man: evidence of competition for tubular secretion of basic drugs.* Eur J Clin Pharmacol, 1983. 25(3): p. 339-45.

63. **van Crugten, J., et al.**, *Selectivity of the cimetidine-induced alterations in the renal handling of organic substrates in humans. Studies with anionic, cationic and zwitterionic drugs.* J Pharmacol Exp Ther, 1986. 236(2): p. 481-7.

64. **Abel, S., et al.**, *Effect of cimetidine and ranitidine on pharmacokinetics and pharmacodynamics of a single dose of dofetilide.* Br J Clin Pharmacol, 2000. 49(1): p. 64-71.

65. **Feng, B., et al.**, *Effect of human renal cationic transporter inhibition on the pharmacokinetics of varenicline, a new therapy for smoking cessation: an in vitro-in vivo study.* Clin Pharmacol Ther, 2008. 83(4): p. 567-76.

66. **Jong, N.N., et al.**, *Oxaliplatin transport mediated by organic cation/carnitine transporters OCTN1 and OCTN2 in overexpressing human embryonic kidney 293 cells and rat dorsal root ganglion neurons.* J Pharmacol Exp Ther, 2011. 338(2): p. 537-47.

67. **Urban, T.J., et al.**, *Effects of genetic variation in the novel organic cation transporter, OCTN1, on the renal clearance of gabapentin.* Clin Pharmacol Ther, 2008. 83(3): p. 416-21.

68. **Garrett, Q., et al.**, *Expression and localization of carnitine/organic cation transporter OCTN1 and OCTN2 in ocular epithelium.* Invest Ophthalmol Vis Sci, 2008. 49(11): p. 4844-9.

69. **Wu, X., et al.**, *Functional characteristics and tissue distribution pattern of organic cation transporter 2 (OCTN2), an organic cation/carnitine transporter.* J Pharmacol Exp Ther, 1999. 290(3): p. 1482-92.

70. **Tamai, I., et al.**, *Involvement of OCTN1 (SLC22A4) in pH-dependent transport of organic cations.* Mol Pharm, 2004. 1(1): p. 57-66.

71. **Grundemann, D.**, *The ergothioneine transporter controls and indicates ergothioneine activity--a review.* Prev Med, 2012. 54 Suppl: p. S71-4.

72. **Tamai, I., et al.**, *Cloning and characterization of a novel human pH-dependent organic cation transporter, OCTN1.* FEBS Lett, 1997. 419(1): p. 107-11.

73. **Grundemann, D., et al.**, *Discovery of the ergothioneine transporter.* Proc Natl Acad Sci U S A, 2005. 102(14): p. 5256-61.

74. **Tokuhiro, S., et al.**, *An intronic SNP in a RUNX1 binding site of SLC22A4, encoding an organic cation transporter, is associated with rheumatoid arthritis.* Nat Genet, 2003. 35(4): p. 341-8.

75. **Martini, M., et al.**, *Association of the OCTN1/1672T variant with increased risk for colorectal cancer in young individuals and ulcerative colitis patients.* Inflamm Bowel Dis, 2012. 18(3): p. 439-48.

76. **Mukherjee, M., et al.**, *In-cell Western detection of organic cation transporters in bronchial epithelial cell layers cultured at an air-liquid interface on Transwell((R)) inserts.* J Pharmacol Toxicol Methods, 2013. 68(2): p. 184-9.

77. **Nakamura, T., et al.**, *Transport of ipratropium, an anti-chronic obstructive pulmonary disease drug, is mediated by organic cation/carnitine transporters in human bronchial epithelial cells: implications for carrier-mediated pulmonary absorption.* Mol Pharm, 2010. 7(1): p. 187-95.

78. **Tein, I.**, *Carnitine transport: pathophysiology and metabolism of known molecular defects.* J Inherit Metab Dis, 2003. 26(2-3): p. 147-69.

79. **Tamai, I., et al.**, *Molecular and functional identification of sodium ion-dependent, high affinity human carnitine transporter OCTN2.* J Biol Chem, 1998. 273(32): p. 20378-82.

80. **Grigat, S., et al.**, *The carnitine transporter SLC22A5 is not a general drug transporter, but it efficiently translocates mildronate.* Drug Metab Dispos, 2009. 37(2): p. 330-7.

81. **Ohashi, R., et al.**, *Na(+)-dependent carnitine transport by organic cation transporter (OCTN2): its pharmacological and toxicological relevance.* J Pharmacol Exp Ther, 1999. 291(2): p. 778-84.

82. **Liang, Y., S. Li, and L. Chen**, *The physiological role of drug transporters.* Protein Cell, 2015. 6(5): p. 334-50.

83. **Ohashi, R., et al.**, *Molecular and physiological evidence for multifunctionality of carnitine/organic cation transporter OCTN2.* Mol Pharmacol, 2001. 59(2): p. 358-66.

84. **Nezu, J., et al.**, *Primary systemic carnitine deficiency is caused by mutations in a gene encoding sodium ion-dependent carnitine transporter.* Nat Genet, 1999. 21(1): p. 91-4.

85. **Tang, N.L., et al.**, *Mutations of OCTN2, an organic cation/carnitine transporter, lead to deficient cellular carnitine uptake in primary carnitine deficiency.* Hum Mol Genet, 1999. 8(4): p. 655-60.

86. **Wang, Y., et al.**, *Phenotype and genotype variation in primary carnitine deficiency.* Genet Med, 2001. 3(6): p. 387-92.

87. **Waller, S., et al.**, *Evidence for association of OCTN genes and IBD5 with ulcerative colitis.* Gut, 2006. 55(6): p. 809-14.

88. **D'Argenio, G., et al.**, *Colon OCTN2 gene expression is up-regulated by peroxisome proliferator-activated receptor gamma in humans and mice and contributes to local and systemic carnitine homeostasis.* J Biol Chem, 2010. 285(35): p. 27078-87.

89. **Nigam, S.K. and V. Bhatnagar**, *How much do we know about drug handling by SLC and ABC drug transporters in children?* Clin Pharmacol Ther, 2013. 94(1): p. 27-9.

90. **Amat di San Filippo, C. and N. Longo**, *Tyrosine residues affecting sodium stimulation of carnitine transport in the OCTN2 carnitine/organic cation transporter.* J Biol Chem, 2004. 279(8): p. 7247-53.

91. **Barilli, A., et al.**, *In Lysinuric Protein Intolerance system y+L activity is defective in monocytes and in GM-CSF-differentiated macrophages.* Orphanet J Rare Dis, 2010. 5: p. 32.

92. **Dall'Asta, V., et al.**, *Amino acids are compatible osmolytes for volume recovery after hypertonic shrinkage in vascular endothelial cells.* Am J Physiol, 1999. 276(4 Pt 1): p. C865-72.

93. **Gazzola, G.C., et al.**, *The cluster-tray method for rapid measurement of solute fluxes in adherent cultured cells.* Anal Biochem, 1981. 115(2): p. 368-74.

94. **Barilli, A., et al.**, *Arginine transport in human monocytic leukemia THP-1 cells during macrophage differentiation.* J Leukoc Biol, 2011. 90(2): p. 293-303.

95. **Visigalli, R., et al.**, *Rapamycin stimulates arginine influx through CAT2 transporters in human endothelial cells.* Biochim Biophys Acta, 2007. 1768(6): p. 1479-87.

96. **Farinha, C.M., et al.**, *Biochemical methods to assess CFTR expression and membrane localization.* J Cyst Fibros, 2004. 3 Suppl 2: p. 73-7.

97. **Ayrton, A. and P. Morgan**, *Role of transport proteins in drug discovery and development: a pharmaceutical perspective.* Xenobiotica, 2008. 38(7-8): p. 676-708.

98. **Koepsell, H.**, *The SLC22 family with transporters of organic cations, anions and zwitterions.* Mol Aspects Med, 2013. 34(2-3): p. 413-35.

99. **Koepsell, H., K. Lips, and C. Volk**, *Polyspecific organic cation transporters: structure, function, physiological roles, and biopharmaceutical implications.* Pharm Res, 2007. 24(7): p. 1227-51.

100. **Wright, S.H.**, *Role of organic cation transporters in the renal handling of therapeutic agents and xenobiotics.* Toxicol Appl Pharmacol, 2005. 204(3): p. 309-19.

101. **Suhre, W.M., et al.**, *Molecular determinants of substrate/inhibitor binding to the human and rabbit renal organic cation transporters hOCT2 and rbOCT2.* Mol Pharmacol, 2005. 67(4): p. 1067-77.

102. **Gorboulev, V., et al.**, *Cloning and characterization of two human polyspecific organic cation transporters.* DNA Cell Biol, 1997. 16(7): p. 871-81.

103. **Zhang, L., et al.**, *Cloning and functional expression of a human liver organic cation transporter.* Mol Pharmacol, 1997. 51(6): p. 913-21.

104. **Bosquillon, C.**, *Drug transporters in the lung--do they play a role in the biopharmaceutics of inhaled drugs?* J Pharm Sci, 2010. 99(5): p. 2240-55.

105. **Gumbleton, M., et al.**, *Spatial expression and functionality of drug transporters in the intact lung: objectives for further research.* Adv Drug Deliv Rev, 2011. 63(1-2): p. 110-8.

106. **Salomon, J.J. and C. Ehrhardt**, *Organic cation transporters in the blood-air barrier: expression and implications for pulmonary drug delivery.* Ther Deliv, 2012. 3(6): p. 735-47.

107. **Bleasby, K., et al.**, *Expression profiles of 50 xenobiotic transporter genes in humans and pre-clinical species: a resource for investigations into drug disposition.* Xenobiotica, 2006. 36(10-11): p. 963-88.

108. **Endter, S., et al.**, *RT-PCR analysis of ABC, SLC and SLCO drug transporters in human lung epithelial cell models.* J Pharm Pharmacol, 2009. 61(5): p. 583-91.

109. **Salomon, J.J., et al.**, *Transport of the fluorescent organic cation 4-(4-(dimethylamino)styryl)-N-methylpyridinium iodide (ASP+) in human respiratory epithelial cells.* Eur J Pharm Biopharm, 2012. 81(2): p. 351-9.

110. **Salomon, J.J., et al.**, *The cell line NCI-H441 is a useful in vitro model for transport studies of human distal lung epithelial barrier.* Mol Pharm, 2014. 11(3): p. 995-1006.

111. **Belzer, M., et al.**, *Substrate-dependent ligand inhibition of the human organic cation transporter OCT2.* J Pharmacol Exp Ther, 2013. 346(2): p. 300-10.

112. **Otsuka, M., et al.**, *A human transporter protein that mediates the final excretion step for toxic organic cations.* Proc Natl Acad Sci U S A, 2005. 102(50): p. 17923-8.

113. **Ishiguro, N., et al.**, *Decreased biosynthesis of lung surfactant constituent phosphatidylcholine due to inhibition of choline transporter by gefitinib in lung alveolar cells.* Pharm Res, 2008. 25(2): p. 417-27.

114. **Wang, T., et al.**, *Choline transporters in human lung adenocarcinoma: expression and functional implications.* Acta Biochim Biophys Sin (Shanghai), 2007. 39(9): p. 668-74.

115. **Macdonald, C., et al.**, *Characterization of Calu-3 cell monolayers as a model of bronchial epithelial transport: organic cation interaction studies.* J Drug Target, 2013. 21(1): p. 97-106.

116. **Mukherjee, M., D.I. Pritchard, and C. Bosquillon**, *Evaluation of air-interfaced Calu-3 cell layers for investigation of inhaled drug interactions with organic cation transporters in vitro.* Int J Pharm, 2012. 426(1-2): p. 7-14.

117. **Ingoglia, F., et al.**, *Functional characterization of the organic cation transporters (OCTs) in human airway pulmonary epithelial cells.* Biochim Biophys Acta, 2015. 1848(7): p. 1563-72.

118. **Longo, N., C. Amat di San Filippo, and M. Pasquali**, *Disorders of carnitine transport and the carnitine cycle.* Am J Med Genet C Semin Med Genet, 2006. 142C(2): p. 77-85.

119. **Carter, A.L., T.O. Abney, and D.F. Lapp**, *Biosynthesis and metabolism of carnitine.* J Child Neurol, 1995. 10 Suppl 2: p. S3-7.

120. **Rebouche, C.J.**, *Carnitine function and requirements during the life cycle.* FASEB J, 1992. 6(15): p. 3379-86.

121. **Tamai, I.**, *Pharmacological and pathophysiological roles of carnitine/organic cation transporters (OCTNs: SLC22A4, SLC22A5 and Slc22a21).* Biopharm Drug Dispos, 2013. 34(1): p. 29-44.

122. **Wu, Y., et al.**, *Carnitine transporter CT2 (SLC22A16) is over-expressed in acute myeloid leukemia (AML) and target knockdown reduces growth and viability of AML cells.* Apoptosis, 2015. 20(8): p. 1099-108.

123. **Yabuuchi, H., et al.**, *Novel membrane transporter OCTN1 mediates multispecific, bidirectional, and pH-dependent transport of organic cations.* J Pharmacol Exp Ther, 1999. 289(2): p. 768-73.

124. **Kato, Y., et al.**, *Gene knockout and metabolome analysis of carnitine/organic cation transporter OCTN1.* Pharm Res, 2010. 27(5): p. 832-40.

125. **Pochini, L., et al.**, *OCTN cation transporters in health and disease: role as drug targets and assay development.* J Biomol Screen, 2013. 18(8): p. 851-67.

126. **Wagner, C.A., et al.**, *Functional and pharmacological characterization of human Na(+)-carnitine cotransporter hOCTN2.* Am J Physiol Renal Physiol, 2000. 279(3): p. F584-91.

127. **Scaglia, F., Y. Wang, and N. Longo**, *Functional characterization of the carnitine transporter defective in primary carnitine deficiency.* Arch Biochem Biophys, 1999. 364(1): p. 99-106.

128. **Nakanishi, T., et al.**, *Na+- and Cl--coupled active transport of carnitine by the amino acid transporter ATB(0,+) from mouse colon expressed in HRPE cells and Xenopus oocytes.* J Physiol, 2001. 532(Pt 2): p. 297-304.

129. **Horvath, G., et al.**, *Epithelial organic cation transporters ensure pH-dependent drug absorption in the airway.* Am J Respir Cell Mol Biol, 2007. 36(1): p. 53-60.

130. **Lohninger, A., et al.**, *Effect of carnitine on foetal rat lung dipalmitoyl phosphatidylcholine content and lung morphology. Carnitine and lung surfactant, I.* J Clin Chem Clin Biochem, 1990. 28(5): p. 313-8.

131. **Kepka, A., et al.**, *The role of carnitine in the perinatal period.* Dev Period Med, 2014. 18(4): p. 417-25.

132. **Lohninger, A., et al.**, *Effects of prenatal treatment with betamethasone, L-carnitine, or betamethasone-L-carnitine combinations on the phosphatidylcholine content and composition of the foetal and maternal rat lung.* Eur J Clin Chem Clin Biochem, 1996. 34(5): p. 387-91.

133. **Ozturk, M.A., et al.**, *Free carnitine levels in respiratory distress syndrome during the first week of life.* Am J Perinatol, 2006. 23(7): p. 445-9.

134. **Borghi-Silva, A., et al.**, *L-carnitine as an ergogenic aid for patients with chronic obstructive pulmonary disease submitted to whole-body and respiratory muscle training programs.* Braz J Med Biol Res, 2006. 39(4): p. 465-74.

135. **Kavukcu, S., et al.**, *The effects of L-carnitine on respiratory function tests in children undergoing chronic hemodialysis.* Turk J Pediatr, 1998. 40(1): p. 79-84.

136. **Al-Biltagi, M., et al.**, *L-carnitine improves the asthma control in children with moderate persistent asthma.* J Allergy (Cairo), 2012. 2012: p. 509730.

137. **Sakamoto, A., et al.**, *Quantitative expression of human drug transporter proteins in lung tissues: analysis of regional, gender, and interindividual differences by liquid chromatography-tandem mass spectrometry.* J Pharm Sci, 2013. 102(9): p. 3395-406.

138. **Marguet, D., et al.**, *Dynamics in the plasma membrane: how to combine fluidity and order.* EMBO J, 2006. 25(15): p. 3446-57.

139. **Karunakaran, S., et al.**, *SLC6A14 (ATB0,+) protein, a highly concentrative and broad specific amino acid transporter, is a novel and effective drug target for treatment of estrogen receptor-positive breast cancer.* J Biol Chem, 2011. 286(36): p. 31830-8.

140. **Ingoglia, F., et al.**, *Functional activity of L-carnitine transporters in human airway epithelial cells.* Biochim Biophys Acta, 2016. 1858(2): p. 210-9.

141. **Ingoglia, F., et al.**, *Human macrophage differentiation induces OCTN2-mediated L-carnitine transport through stimulation of mTOR-STAT3 axis.* J Leukoc Biol, 2016.

142. **Sonne, S., et al.**, *Carnitine deficiency in OCTN2-/- newborn mice leads to a severe gut and immune phenotype with widespread atrophy, apoptosis and a pro-inflammatory response.* PLoS One, 2012. 7(10): p. e47729.

143. **Gordon, S. and P.R. Taylor**, *Monocyte and macrophage heterogeneity.* Nat Rev Immunol, 2005. 5(12): p. 953-64.

144. **Martinez, F.O., et al.**, *Macrophage activation and polarization.* Front Biosci, 2008. 13: p. 453-61.

145. **Murray, P.J., et al.**, *Macrophage activation and polarization: nomenclature and experimental guidelines.* Immunity, 2014. 41(1): p. 14-20.

146. **Hamilton, J.A.**, *Colony-stimulating factors in inflammation and autoimmunity.* Nat Rev Immunol, 2008. 8(7): p. 533-44.

147. **Kittan, N.A., et al.**, *Cytokine induced phenotypic and epigenetic signatures are key to establishing specific macrophage phenotypes.* PLoS One, 2013. 8(10): p. e78045.

148. **Wahli, W. and L. Michalik**, *PPARs at the crossroads of lipid signaling and inflammation.* Trends Endocrinol Metab, 2012. 23(7): p. 351-63.

149. **Coffer, P.J., L. Koenderman, and R.P. de Groot**, *The role of STATs in myeloid differentiation and leukemia.* Oncogene, 2000. 19(21): p. 2511-22.

150. **Liu, T.F., et al.**, *NAD+-dependent sirtuin 1 and 6 proteins coordinate a switch from glucose to fatty acid oxidation during the acute inflammatory response.* J Biol Chem, 2012. 287(31): p. 25758-69.

151. **Mackenzie, B. and J.D. Erickson**, *Sodium-coupled neutral amino acid (System N/A) transporters of the SLC38 gene family.* Pflugers Arch, 2004. 447(5): p. 784-95.

152. **Morita, M., et al.**, *mTORC1 controls mitochondrial activity and biogenesis through 4E-BP-dependent translational regulation.* Cell Metab, 2013. 18(5): p. 698-711.

153. **Lehtonen, A., et al.**, *Granulocyte-macrophage colony-stimulating factor (GM-CSF)-induced STAT5 activation and target-gene expression during human monocyte/macrophage differentiation.* J Leukoc Biol, 2002. 71(3): p. 511-9.

154. **Luci, S., et al.**, *PPARalpha agonists up-regulate organic cation transporters in rat liver cells.* Biochem Biophys Res Commun, 2006. 350(3): p. 704-8.

155. **Saleiro, D. and L.C. Platanias**, *Intersection of mTOR and STAT signaling in immunity.* Trends Immunol, 2015. 36(1): p. 21-9.

156. **Huynh, J., et al.**, *CSF-1 receptor signalling from endosomes mediates the sustained activation of Erk1/2 and Akt in macrophages.* Cell Signal, 2012. 24(9): p. 1753-61.

157. **Franchi-Gazzola, R., et al.**, *The role of the neutral amino acid transporter SNAT2 in cell volume regulation.* Acta Physiol (Oxf), 2006. 187(1-2): p. 273-83.

158. **Fu, Y., et al.**, *Facilitative glucose transporter gene expression in human lymphocytes, monocytes, and macrophages: a role for GLUT isoforms 1, 3, and 5 in the immune response and foam cell formation.* Blood Cells Mol Dis, 2004. 32(1): p. 182-90.

159. **Qiao, H. and J.M. May**, *Macrophage differentiation increases expression of the ascorbate transporter (SVCT2).* Free Radic Biol Med, 2009. 46(8): p. 1221-32.

160. **Chawla, A.**, *Control of macrophage activation and function by PPARs.* Circ Res, 2010. 106(10): p. 1559-69.

161. **Varga, T., Z. Czimmerer, and L. Nagy**, *PPARs are a unique set of fatty acid regulated transcription factors controlling both lipid metabolism and inflammation.* Biochim Biophys Acta, 2011. 1812(8): p. 1007-22.

162. **Rigamonti, E., G. Chinetti-Gbaguidi, and B. Staels**, *Regulation of macrophage functions by PPAR-alpha, PPAR-gamma, and LXRs in mice and men.* Arterioscler Thromb Vasc Biol, 2008. 28(6): p. 1050-9.

163. **Tontonoz, P. and B.M. Spiegelman**, *Fat and beyond: the diverse biology of PPARgamma.* Annu Rev Biochem, 2008. 77: p. 289-312.

164. **Ringseis, R., G. Wen, and K. Eder**, *Regulation of Genes Involved in Carnitine Homeostasis by PPARalpha across Different Species (Rat, Mouse, Pig, Cattle, Chicken, and Human).* PPAR Res, 2012. 2012: p. 868317.

165. **Luo, H., et al.**, *Transcriptional regulation of the human, porcine and bovine OCTN2 gene by PPARalpha via a conserved PPRE located in intron 1.* BMC Genet, 2014. 15: p. 90.

166. **Haidinger, M., et al.**, *A versatile role of mammalian target of rapamycin in human dendritic cell function and differentiation.* J Immunol, 2010. 185(7): p. 3919-31.

167. **Weichhart, T., et al.**, *The TSC-mTOR signaling pathway regulates the innate inflammatory response.* Immunity, 2008. 29(4): p. 565-77.

168. **Sarbassov, D.D., S.M. Ali, and D.M. Sabatini**, *Growing roles for the mTOR pathway.* Curr Opin Cell Biol, 2005. 17(6): p. 596-603.

169. **De Simone, C., et al.**, *Carnitine depletion in peripheral blood mononuclear cells from patients with AIDS: effect of oral L-carnitine.* AIDS, 1994. 8(5): p. 655-60.

170. **Flanagan, J.L., et al.**, *Role of carnitine in disease.* Nutr Metab (Lond), 2010. 7: p. 30.

171. **Chawla, A., K.D. Nguyen, and Y.P. Goh**, *Macrophage-mediated inflammation in metabolic disease.* Nat Rev Immunol, 2011. 11(11): p. 738-49.

172. **Hao, J., et al.**, *Mitochondrial nutrients improve immune dysfunction in the type 2 diabetic Goto-Kakizaki rats.* J Cell Mol Med, 2009. 13(4): p. 701-11.